FEMFLOW3D Version 2.0
A Finite-Element Program for the Simulation of Three-Dimensional Groundwater Systems

Presentation to the Office of the Nevada State Engineer

Prepared for

SOUTHERN NEVADA
WATER AUTHORITY

June 2006

Timothy J. Durbin, a consultant to the Southern Nevada Water Authority (SNWA) prepared this report entitled *"FEMFLOW3D Version 2.0 - A Finite-Element Program for the Simulation of Three-Dimensional Groundwater Systems"*, June, 2006. This report is one of several reports prepared in support of SNWA groundwater applications 54003 through 54021 in Spring Valley (Hydrographic Area 184).

Timothy J. Durbin

Timothy J. Durbin, Consulting Hydrologist
Timothy J. Durbin, Inc.

6/22/06

Date

TABLE OF CONTENTS

TABLE OF CONTENTS (CONTINUED)

TABLE OF CONTENTS (CONTINUED)

This Page Intentionally Left Blank

LIST OF FIGURES

LIST OF FIGURES (CONTINUED)

LIST OF TABLES

LIST OF TABLES (CONTINUED)

1.0 INTRODUCTION

1.1 General Description

FEMFLOW3D is a computer program that simulates flow and transport in three-dimensional groundwater systems using the finite-element method (Durbin and Bond, 1998; Durbin and Berenbrock, 1985). However, this document describes only the groundwater-flow component of FEMFLOW3D. The document is divided into three principal sections. Section 2.0 describes the program and its mathematical basis. Section 3.0 describes how the input files to the program should be formatted. Section 4.0 describes test cases in which FEMFLOW3D was used to simulate problems with known analytical solutions, and the FEMFLOW3D results were compared with these solutions. Appendix A is a CD that contains the FORTRAN source code for FEMFLOW3D and the input and output files for the test cases. The mathematical descriptions in Section 2.0 are more detailed than some readers may require, but these descriptions are necessary for the complete documentation of FEMFLOW3D. Most readers can skip Section 2.0 and can proceed directly to Section 3.0, which describes how to prepare input files for FEMFLOW3D.

This document describes Version 2.0 of FEMFLOW3D, which represents a number of changes from Version 1.0 (Durbin and Bond, 1998) and earlier versions (Durbin and Berenbrock, 1985). The principal modifications are to simulate groundwater flow in fault planes such that faults can be conduits and barriers to groundwater flow, and to input the finite-element mesh in terms of hydrogeologic compartments. Another change is to associate each program module with separate input and output files.

FEMFLOW3D can be used to simulate both regional and small-scale groundwater systems. It can be used to simulate confined and unconfined groundwater systems based on an adjustable mesh that follows the water table movement. It can be used to simulate groundwater systems containing hydrogeologic units that pinchout or are offset by faults. Finally, it can simulate longitudinal flow along fault planes in addition to transverse flow across faults. FEMFLOW3D includes provisions for simulating specified-head boundaries, including drainage nodes; specified fluxes, including pumping from wells completed in multiple layers; groundwater evapotranspiration by phreatophytes; and stream-aquifer interactions.

FEMFLOW3D includes three alternative solvers for solving the system of linear equations generated by the finite-element method at each time-step iteration. The solver SRELAX uses the point overrelaxation method. The solver SITPACK uses a conjugate-gradient method. The solver SAMG uses the algebraic multigrid method. SRELAX is the slowest but most robust of the solvers. SIPACK usually is the fastest for mid-sized problems (10,000 or fewer nodes). SAMG usually is the fastest for large problems (50,000 or more nodes).

The structure of the FEMFLOW3D computer program consists of a main program and a set of subroutines (Table 1-1 and Figure 1-1). The main program – designated FEMFLOW3D – is a simple driver that allows various calculations to be iteratively performed over a user-defined series of time steps. The main program sequentially calls two blocks of subroutines. The first block controls which input files are read (subroutine SETFILES), sets the time-stepping scheme, solution parameters, and the output controls (subroutine BASIC), and reads in the finite-element mesh previously created by the user (subroutines NODES and ELEMS). The second block marches the simulation through the time-stepping scheme, performing the necessary calculations to solve the various relevant groundwater equations based upon the user-defined parameters for the groundwater system. The second block of subroutines generally handles: (1) a set of mathematical calculations related to the finite-element method; (2) a specific feature of the hydrologic system; and/or (3) special features related to the management of input or output data.

FEMFLOW3D is based on the finite-element solution of the three-dimensional equation of groundwater flow in the form

$$\frac{\partial}{\partial x_i}\left(K_{ij}\frac{\partial h}{\partial x_j}\right) + W = S\frac{\partial h}{\partial t} \qquad (1\text{-}1)$$

for

i = 1,2,3 and
j = 1,2,3, and

where

h = the hydraulic head [L],
K_{ij} = a component of the hydraulic conductivity tensor [Lt^{-1}],
S = the specific storage [L^{-1}],
W = the source injection rate per unit volume [t^{-1}],
x_i = the spatial coordinate in x_i direction in a right-hand Cartesian coordinate system [L],
t = time [t].

The form of the governing equation makes no assumption about the alignment of the coordinate system with respect to the alignment of the principal components of the hydraulic conductivity tensor.

The governing equation is subject to the water table boundary condition in the form

$$K_{ij}\frac{\partial h}{\partial x_j}n_i = -S_y\frac{\partial h_f}{\partial t}n_3 \qquad (1\text{-}2)$$

for

i = 1,2,3 and
j = 1,2,3

Table 1-1
Subroutine and Function Calls Within FEMFLOW3D
(Page 1 of 2)

Subroutine or Function	Subroutine Purpose	Calls Within	Called By
FEMFLOW3D	Main program marches simulation through time steps	SETFILES BASIC NODES ELEMS WFLOW STEPS SYSTEM_CLOCK	NONE
SETFILES	Identifies input files	OPENFILES	FEMFLOW3D
OPENFILES	Opens input files; creates and opens output files	None	SETFILES BASIC NODES ELEMS WPARAMS WSTART WOUTPUT WCHEAD WFLUX WEVAP WRIVER WFAULT
BASIC	Inputs simulation controls	OPENFILES STEPS SRELAX SITPACK SAMG	FEMFLOW3D
NODES	Inputs node coordinates, controls mesh expansion and contraction	OPENFILES	FEMFLOW3D
ELEMS	Inputs element incidences	OPENFILES	FEMFLOW3D
WFLOW	Controls groundwater-flow calculations	WPARAMS WSTART WOUTPUT WCHEAD WFLUX WEVAP WRIVER WFAULT	FEMFLOW3D
WPARAMS	Inputs aquifer parameters	OPENFILES WSHAPE	WFLOW
WSTART	Inputs initial heads	OPENFILES	WFLOW
WOUTPUT	Outputs computed heads	OPENFILES	WFLOW
WCHEAD	Inputs and implements specified head nodes	OPENFILES TABLE	WFLOW
WFLUX	Inputs and implements specified-flux nodes	OPENFILES TABLES	WFLOW

Table 1-1
Subroutine and Function Calls Within FEMFLOW3D
(Page 2 of 2)

Subroutine or Function	Subroutine Purpose	Calls Within	Called By
WEVAP	Inputs and implements groundwater - evapotranspiration nodes	OPENFILES TABLE	WFLOW
WRIVER	Inputs and implements river nodes	OPENFILES TABLE	WFLOW
WFAULT	Inputs and implements faults	OPENFILES	WFLOW
SRELAX	Solves system of equations by over-relaxation method	None	BASIC WFLOW
SITPACK	Solves system of equations by conjugate-gradient method	ITPACK solver package	BASIC WFLOW
SAMG	Solves system of equations by algebraic multigrid method	AMG solver package	BASIC WFLOW
WSHAPE	Performs volume and area integrations	None	WPARAMS
PACK	Creates conductance and storage matrices	None	WFLOW WPARAMS WCHEAD WFLUX WEVAP WRIVER WFAULT
TABLE	Interpolates from table of values	INTERP	WCHEAD WFLUX WEVAP WRIVER
INTERP	Interpolates between two points in table	None	TABLE

where

n_i = a component of the outward normal vector on the water table surface [L^0],
K_{ij} = a component of the hydraulic conductivity tensor [Lt^{-1}],
h = the hydraulic head [L],
h_f = the elevation of the water table [L],
x_j = the spatial coordinate in the j direction,
S_y = the specific yield.

The application of the finite-element method to Equation 1-1 yields, at each time step, the system of linear equation in the form (Pinder and Gray, 1977; Hayakorn and Pinder, 1983; Zienkiewicz, 1988)

$$\left([A] + \frac{1}{\Delta t}[B]\right)\{H^{(t)}\} = \frac{1}{\Delta t}[B]\{H^{(t-\Delta t)}\} + \{F\} \quad (1\text{-}3)$$

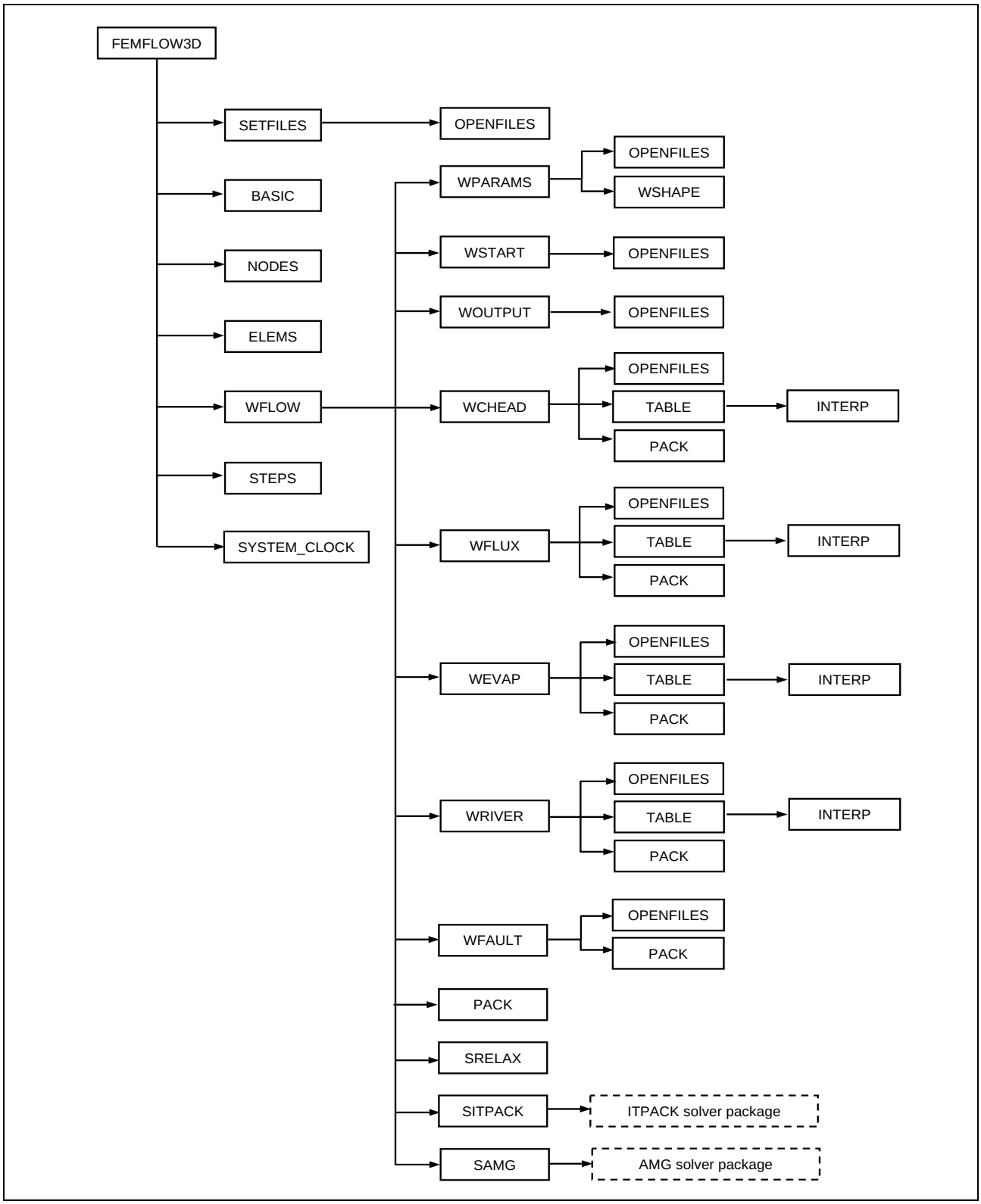

Figure 1-1
Subroutines and Functions Used in FEMFLOW3D

where

$[A]$	=	a matrix that represents the geometry of the groundwater system and the hydraulic conductivity of the system,
$[B]$	=	a matrix that represents the geometry of the groundwater system and the storativity of the system,
$\{H^{(t)}\}$	=	a vector of computed heads at the current time step,
$\{H^{(t-\Delta t)}\}$	=	a vector of computed heads at the previous time step, and
$\{F\}$	=	a vector of sources and sinks.

Various subroutines within FEMFLOW3D create the matrices $[A]$ and $[B]$ and the vector $\{F\}$ at each time step (and time step iteration) and solve the resulting system of equations.

FEMFLOW3D performs its flow simulations by solving the governing equations of groundwater flow using the finite-element method. The finite-element method involves designing three-dimensional geometric grids – or meshes – that represent the physical dimensions of an aquifer system. A mesh is comprised of three-dimensional tetrahedral elements. However, a mesh is input to FEMFLOW3D as wedge-shape elements that subsequently are disaggregated into tetrahedral elements. The finite-element method allows features, such as irregular and/or random geographic features and irregular boundaries, to be accurately represented by a finite-element mesh. This method also permits increased detail within localized areas of particular interest within the study area. Hydrologic features that FEMFLOW3D can simulate include the following.

Representation of Groundwater System as Three-Dimensional Continuum

A groundwater system is represented in FEMFLOW3D as a three-dimensional continuum comprising hydrogeologic features such as aquifers and aquitards. This approach accounts for conductive and storage properties of both aquifers and aquitards. Where the vertical propagation of pressure is important to the simulation of storage effects in aquitards, the aquitard may need to be represented in the finite-element mesh by multiple element layers. Figure 1-2 shows an oblique view of a mesh constructed to represent two hydrogeologic units partially separated locally by an intervening aquitard.

Aquifers and other three-dimensional features of a groundwater system are represented in FEMFLOW3D with wedge, pyramid, or tetrahedral elements. The basic building block is a six-node wedge-shaped element, although the internal model calculations are performed using tetrahedral elements. Internally within FEMFLOW3D, wedge and pyramid elements are separated into corresponding tetrahedral elements. The wedge-shaped elements are oriented spatially, as shown on Figure 1-3, wherein the triangular faces are sub-horizontal and the quadrilateral faces are sub-vertical. Wedge elements with one or two zero-height sub-vertical edges can be used to represent particular hydrogeologic units that pinchout, or to make geographic changes in the vertical discretization of the grid. As shown on Figures 1-4 and 1-5, a wedge-shaped element with one zero-height reduces to a five-node pyramid, and a wedge-shaped element with two zero-height edges reduces to a tetrahedron.

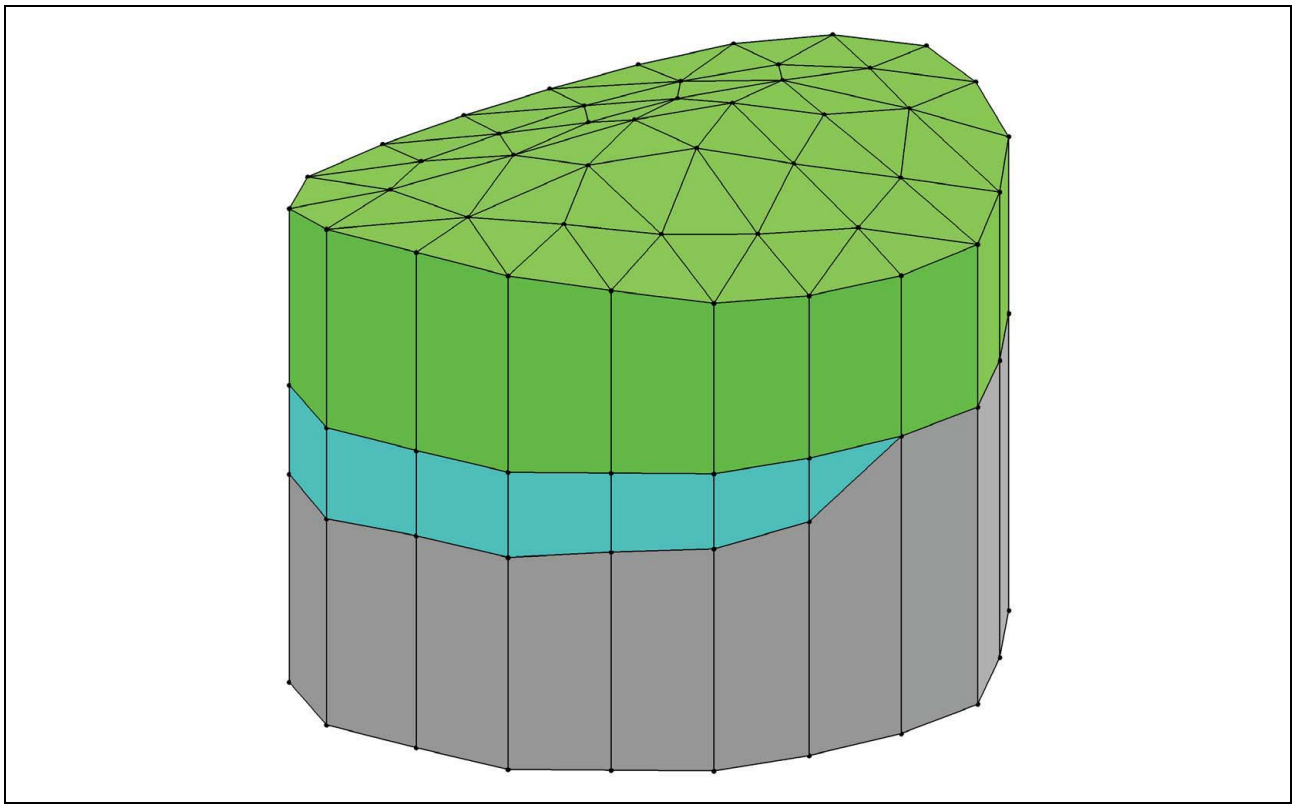

Figure 1-2
Oblique View of Finite-Element Mesh With Embedded Aquitard

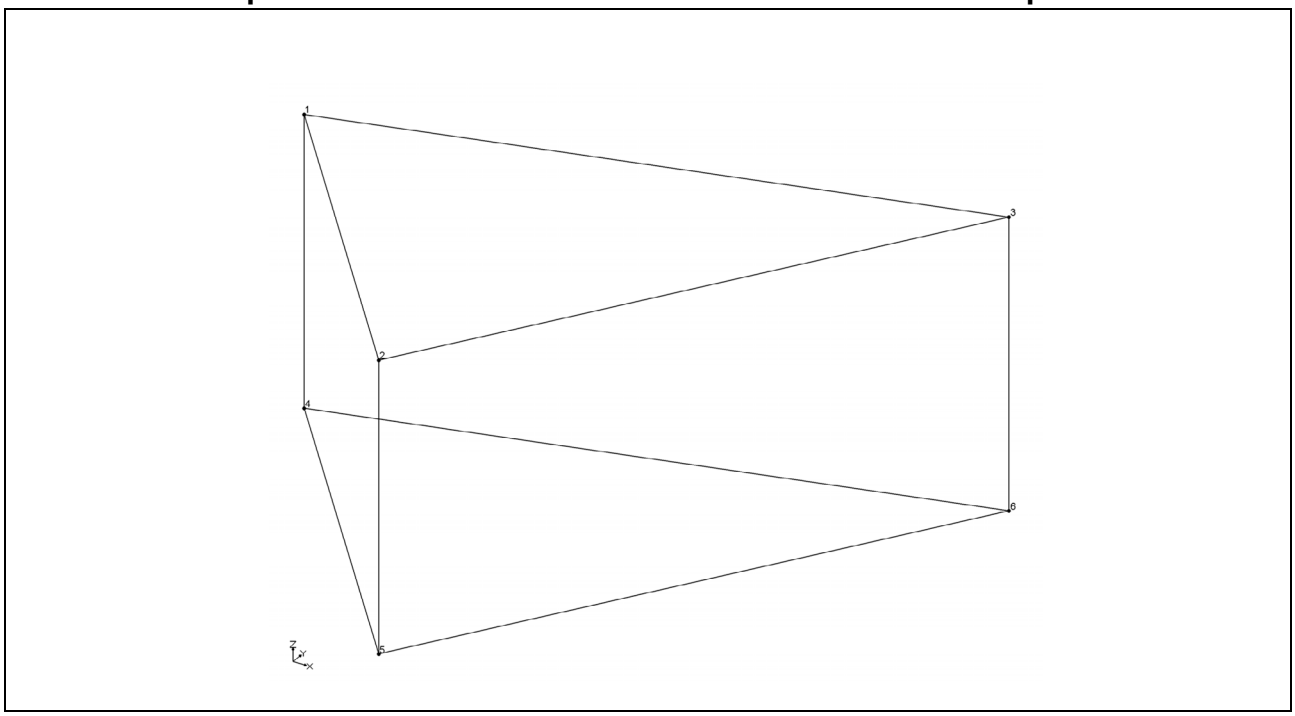

Figure 1-3
Orientation of Wedge-Shaped Elements With Respect to X-Y-Z Coordinate Axes

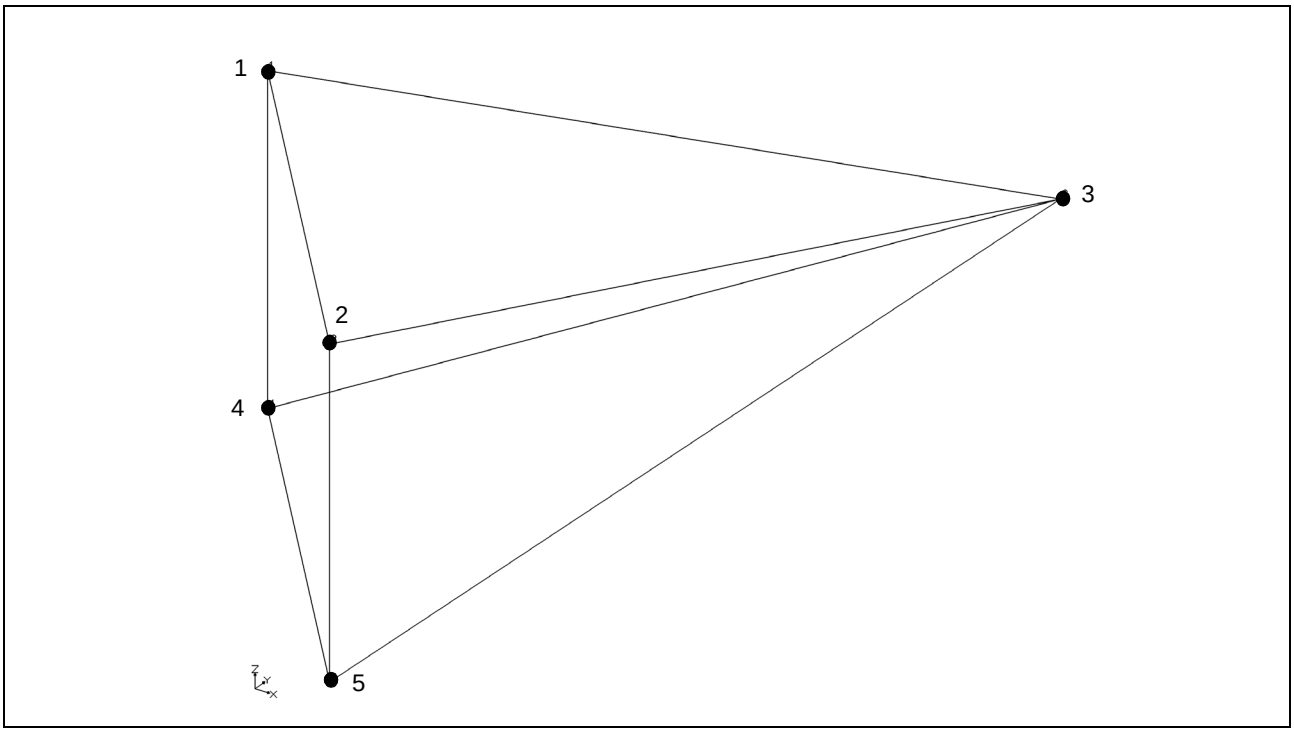

Figure 1-4
Wedge-Shaped Element With One Zero-Height Edge

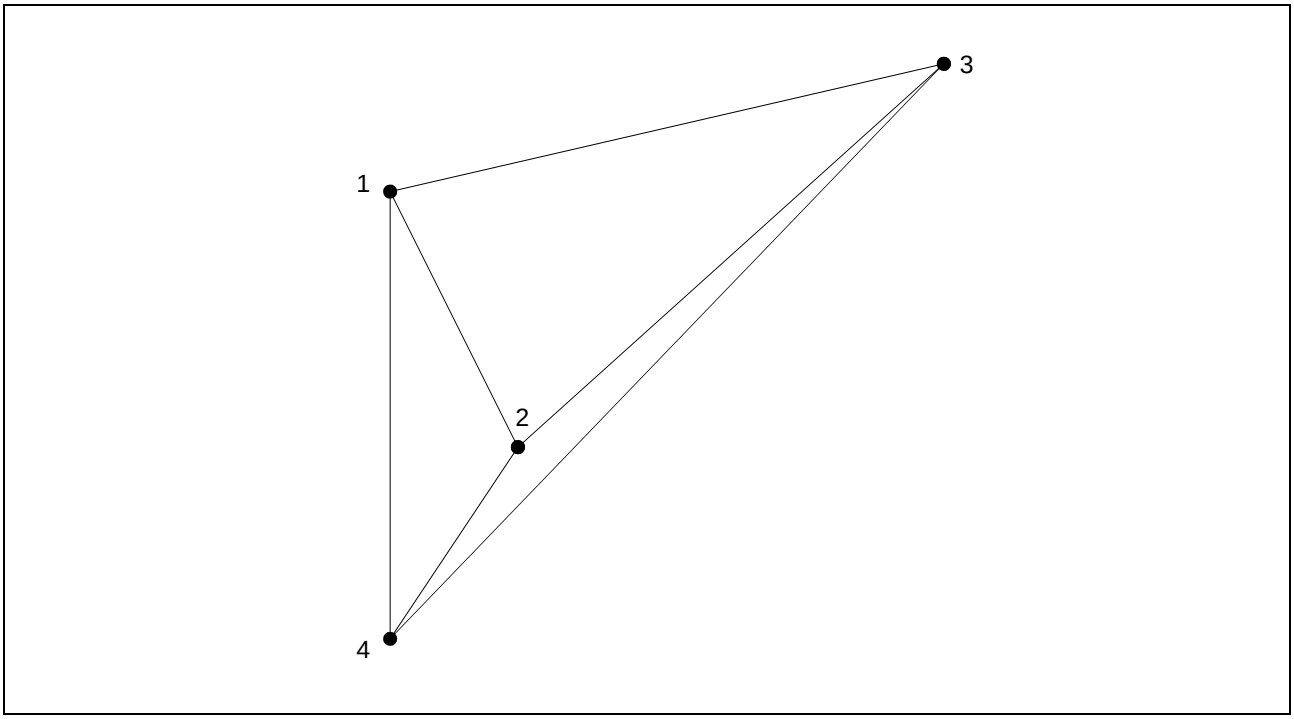

Figure 1-5
Wedge-Shaped Element With Two Zero-Height Edges

Representation of Faults as Two-Dimensional Features

Faults are represented in FEMFLOW3D as two-dimensional vertical or sloping features – or fault planes – comprised of three-node triangular elements oriented in three-dimensional space. A fault plane possesses both conductive and storage properties along the plane. A fault also possesses conductive properties transverse to the fault, which represents resistance to flow from or into the adjacent aquifer into or from the fault. The groundwater within a well is always lower than the average groundwater level within the vicinity of the well because of the local radial flow to the well. The well features within FEMFLOW3d can be used to simulate that effect. Figure 1-6 shows an oblique view of two offset hydrogeologic structural blocks separated by a fault.

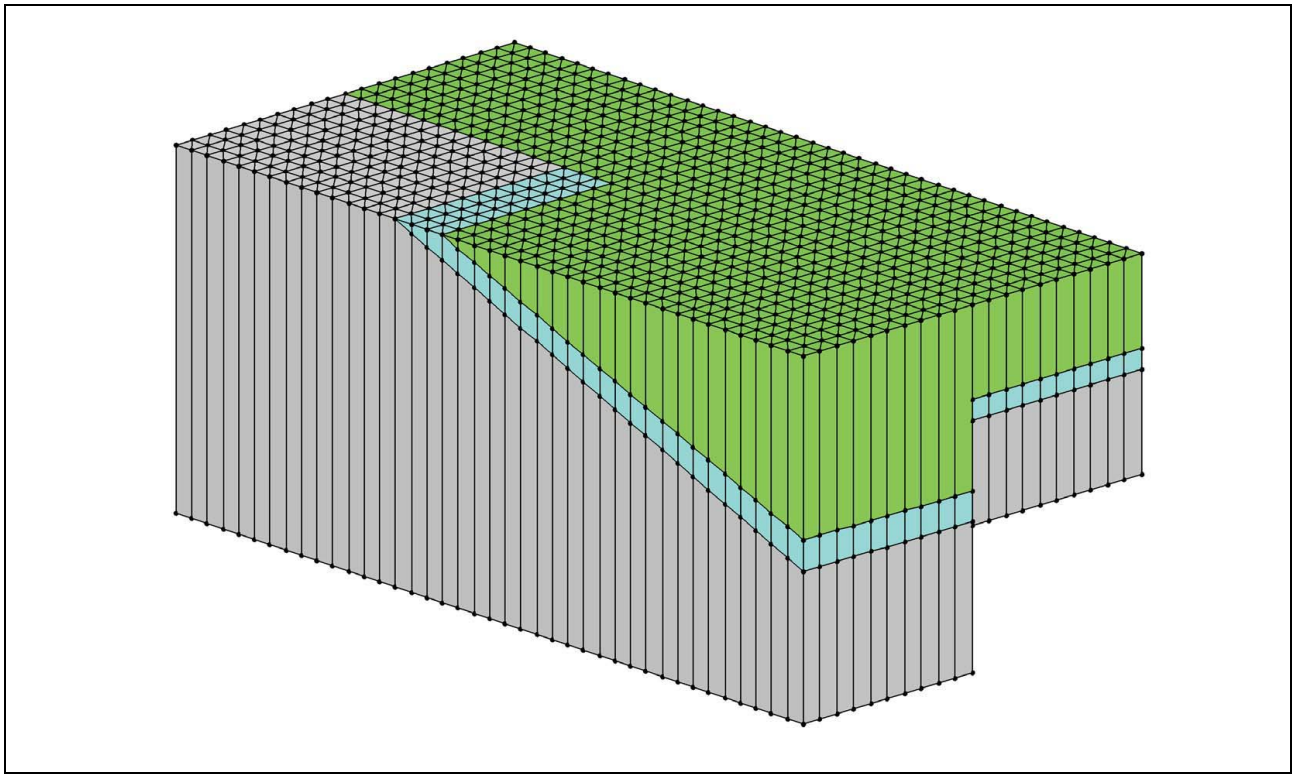

Figure 1-6
Two Structural Blocks Offset by a Fault

Compartmentalization of Aquifer Features

A three-dimensional mesh constructed in FEMFLOW3D can contain one or more hydrogeologic compartments. Typically, a compartment represents a hydrogeologic structural block that has been offset by faults. Figures 1-7 and 1-8 show examples of multi-compartment meshes. Figure 1-7 illustrates a mesh for two geologic blocks that have been offset by a reverse fault. In this case, FEMFLOW3D permits the blocks to be defined separately and then to be connected hydraulically through the FEMFLOW3D representation of faults. Figure 1-8 illustrates a mesh for five compartments with intervening vertical faults.

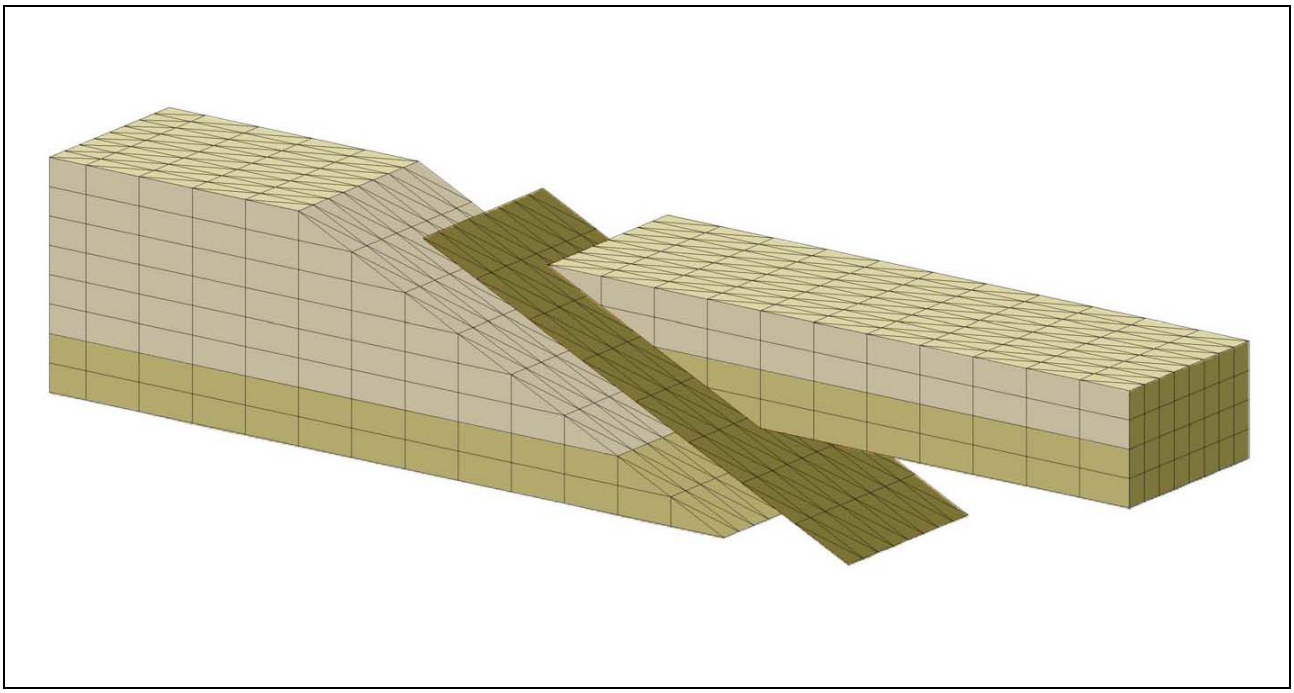

Figure 1-7
Two Hydrogeologic Compartments Offset by a Sloping Fault

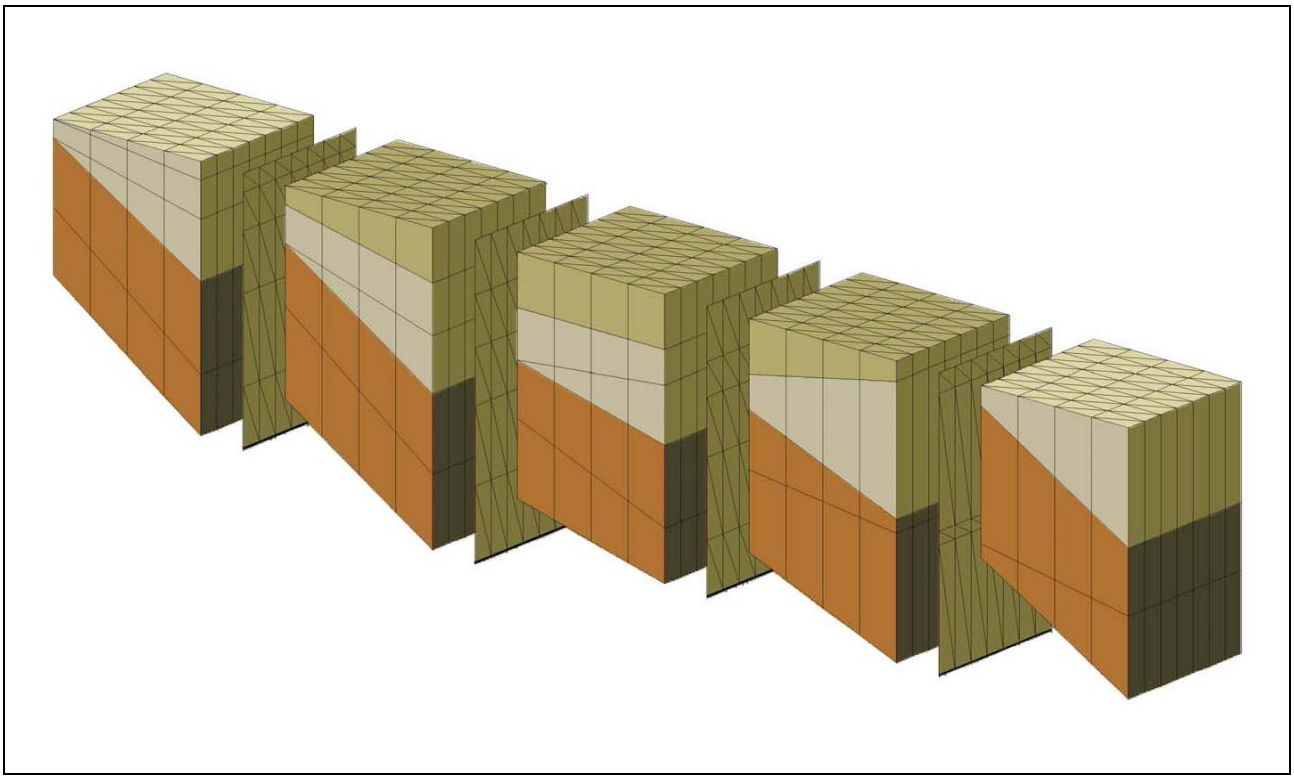

Figure 1-8
Five Hydrogeologic Compartments Offset by Vertical Faults

Specified-Head Boundaries

Specified-head boundary conditions can be imposed by assigning boundary heads to the corresponding nodes in the finite-element mesh. The boundary heads can be constant or vary with time. Time-varying boundary heads are specified using a table representing the hydrograph of the boundary heads, and the head at a particular time is interpolated from the table. Additionally, drainage nodes can be specified that allow discharge from the modeled flow domain, but do not allow flow into the domain. The drainage nodes could be used to simulate features such as subsurface agricultural drains.

Specified-Flux Boundaries and Internal Source-Sink Terms

As with specified-head boundary conditions, constant or time-varying specified-flux boundary conditions can be assigned to specific nodes in the model mesh. Time-varying specified-flux boundary conditions are represented by a table representing the hydrograph of the fluxes, and the flux at a particular time is interpolated from the table. Internal source-sink terms can also be defined in the same manner. FEMFLOW3D also can represent pumping, injection, or observation wells screened over multiple layers of the finite-element mesh. This feature of FEMFLOW3D also can be used to make the translation from groundwater levels at the mesh scale to groundwater levels within a well.

Groundwater Evapotranspiration

The depth-dependent evapotranspiration of groundwater from a shallow water table due to phreatophytes can be simulated by specifying the maximum evapotranspiration rate and an extinction depth. Evapotranspiration rates are defined for specific nodes in the model mesh, and, as with fluxes and specified-heads, can be defined as varying with time by employing a table. FEMFLOW3D can represent overlapping coverages of vegetation with different extinction depths and maximum evapotranspiration rates.

Stream-Aquifer Interactions

To simulate river-aquifer interactions, river flow is routed through a main channel and its tributaries. The exchange of water between the local river-channel reach and the groundwater system depends on the wetted width of the reach, flow depth, river-bed elevation, river-bed thickness, and river-bed hydraulic conductivity. Additionally, when water seeps from the river reach into the groundwater system, the simulation allows for a break in the hydraulic connection between the river and the groundwater system. At the break, the rate of groundwater recharge from the river is essentially independent of the depth to the groundwater table. This condition is assumed in FEMFLOW3D to occur when the hydraulic gradient from the river to the water table reaches unity in the vertical direction. FEMFLOW3D simulates the break based on the groundwater head beneath the river channel.

1.2 Measurement Units

Input parameters in FEMFLOW3D can be specified in any units, as long as the units are consistent throughout the input files. That is, if the thickness of a particular layer of the finite-element mesh is specified in meters, then all length units should be specified in meters, areas should be specified in meters squared, and volumes should be specified in meters cubed. Likewise, if time steps are specified in the unit of days, then the hydraulic conductivity must be specified with a unit of days. In other words FEMFLOW3D imbeds no specific system of units.

1.3 Array Dimensions

The array dimensions for FEMFLOW3D are specified in PARAMETER statements contained in the source code file DIMEN.INC (Appendix A). The array dimensions can be changed for a particular usage by editing the PARAMETER statements and recompiling the source code.

1.4 Model Building and View Tools

FEMFLOW3D can be used with GMS (Groundwater Modeling System), which was developed for the U.S. Army Corps of Engineers. FEMFLOW3D creates output files for viewing the finite-element meshes with GMS. For the aggregated compartment mesh, FEMFLOW3D outputs a file with the extension .3dm, which can be input to GMS for viewing the mesh. For the fault mesh, FEMFLOW3D outputs a file with the extension .2dm. Correspondingly, FEMFLOW3D outputs files with computed heads for viewing in GMS. For the aggregated compartment mesh, the file has the extension .HED.PLT. For the fault mesh, the file has the extension .FLT.PLT.

2.0 PROGRAM DETAILS

2.1 General Description

FEMFLOW3D is organized into a set of subroutines that construct Equation 1-3, solve the corresponding system of equations, or perform various utility functions. The subroutines and their linkages are listed in Table 1-1, and they are described below.

2.2 Subroutine SETFILES

Subroutine SETFILES identifies the files to be used in a simulation. SETFILES has two entry points. Entry point SETFILES1 identifies the files relating to groundwater flow. Entry point SETFILES2 identifies files relating to solute transport, but those files are not addressed in this document.

The inputs to FEMFLOW3D occur in separate files for each of the major subroutines. A super file contains the name of the particular simulation and the names of the individual input files that apply to the simulation. Subroutine SETFILES1 is the first subroutine called by the main subroutine FEMFLOW3D, and it reads the super file. SETFILES1 then automatically creates corresponding names for the output files based in part on the simulation name. SETFILES1 also confirms the mandatory files have been included in the simulation and that all of the specified files actually exist. Furthermore, for the optional features of FEMFLOW3D, the occurrence of the corresponding file name in the super file invokes the feature in the simulation. For example, if an input file occurs in the super file for the simulation of specified heads, that occurrence sets the switch in FEMFLOW3D for the simulation of specified heads.

2.3 Subroutine BASIC

2.3.1 Background

Subroutine BASIC reads in the simulation parameters, including the compartment names, the within-time-step iteration parameters, the solution method for the system of linear equations, the parameters for the solution method, the stress-period configuration, the time-step scheme within each stress period, and output controls. BASIC calls subroutine STEPS, which sets up the stress-period configuration and time-step scheme for the simulation. BASIC also calls one of three subroutines that set up the inputs for the solver to be used for the system of linear equations that is generated at each within-time-step iteration. Either subroutine SRELAX, subroutine SITPACK, or SAMG is called. As will be explained in detail in the documentation associated with these subroutines, these subroutines represent one of three alternative methods of solving a system of linear equations: the

point over-relaxation method, the conjugate-gradient method, or the algebraic multigrid method. Only one of these three subroutines will be called, based on the selection of a particular solver method by the user.

2.3.2 Mathematical Basis

As part of the input to subroutine BASIC, the user must define the simulation in terms of one or more stress periods. Each stress period is then divided into a specified number of time steps. The time steps can be uniform in duration, or can increase geometrically over the stress period. Correspondingly, the simulation period is defined in terms of the number of stress periods, the duration of each stress period, the number of time steps within each stress period, and the geometric factor for increasing the duration of successive time steps within each stress period.

At each time step, one or more iterations are required to solve the system of equations generated by the finite-element method (which is described in more detail in Section 2.9). Although the system of equations is basically linear, some groundwater fluxes are nonlinearly head-dependent. This nonlinearity occurs in the simulation of specified-head drainage nodes, groundwater evapotranspiration, and stream-aquifer interactions. For each of these cases, the corresponding fluxes are non-linearly head dependent.

FEMFLOW3D uses Picard iterations to address nonlinearity, which entails evaluating the system parameters based on the heads at the last iteration. Based on these parameter values, new heads are computed. This cycle is repeated within a time step until the change in heads between two iterations is less than a specified value (called the convergence criterion). In particular, the convergence criterion is defined as follows:

$$\max_{I} \left(\left| H_{I,t}^{(k+1)} - H_{I,t}^{(k)} \right| \right) \leq \varepsilon \qquad \text{for } I = 1,2,3,\ldots,n \tag{2-1}$$

where

k = the iteration within the time step,

t = the time at the current time step [t],

I = the node number in the finite-element mesh for which heads are being computed,

$H_{I,t}^{(k+1)}$ = the computed head at node I at the iteration k+1 at t [L],

$H_{I,t}^{(k)}$ = the computed head at node I at the iteration k at t [L],

n = the number of equations, which corresponds to the number of nodes in the finite-element mesh, and

ε = the convergence criterion [L].

The within-time-step iterations should not be confused with the solver iterations. The over-relaxation method, conjugate-gradient method, and multigrid method involve iterations to solve a system of linear equations. The within-time-step iterations involve solving different systems of equations,

where the systems differ by the iterative improvement of the head-dependent coefficients of the matrices [*A*] and [*B*] and the vector {*F*}. The within-time-step iterations are the Picard iterations used to solve the system of non-linear equations, while the solver iterations are those used to solve the system of linearized equations generated at each Picard iteration.

For particularly non-linear simulations, the Picard iterations will not converge because of oscillations. To address these cases, FEMFLOW3D provides for the under-relaxation of the iterations based on a scheme using an under-relaxation factor, which is defined by the user. Using this under-relaxation factor, the head $H_{I,t}^{(k+1)}$ at a given iteration is decelerated by a weighted difference between what the head $\tilde{H}_{I,t}^{(k+1)}$ would have been without any under-relaxation and the last computed head value $H_{I,t}^{(k)}$. This is mathematically expressed as by the relation

$$H_{I,t}^{(k+1)} = H_{I,t}^{(k)} + \gamma(\tilde{H}_{I,t}^{(k+1)} - H_{I,t}^{(k)}) \qquad (2\text{-}2)$$

where

$\tilde{H}_{I,t}^{(k+1)}$ = what the head would have been without any under-relaxation [L], and
γ = the under-relaxation factor wherein $\gamma_{\min} \le \gamma \le 1$ [L^0].

The value of γ is dependent on the progress of the iterative scheme. As the iterations converge, γ approaches unity. The relation between γ and convergence is given by the relation

$$\delta = \gamma_{min} + (1 - \gamma_{min})e^{-\alpha(\delta - \varepsilon)} \quad \text{for } \delta > \varepsilon \qquad (2\text{-}3)$$

and

$$\gamma = 1 \quad \text{for } \delta \le \varepsilon \qquad (2\text{-}4)$$

where

$$\delta = \max_I(\left| H_{I,t}^{(k+1)} - H_{I,t}^{(k)} \right|) \quad \text{for } I = 1, 2, \ldots, n \qquad (2\text{-}5)$$

and where

γ = the under-relaxation factor [L^0],
γ_{min} = the minimum value of the under-relaxation factor [L^0],
ε = the convergence criterion described in Equation 2-1, and
α = a shape factor that controls the rate of increase in γ with decreased δ.

The relation for the under-relaxation factor is shown in Figure 2-1 for $\gamma_{\min} = 0.1$, $\varepsilon = 0.01$, and $\alpha = 5$.

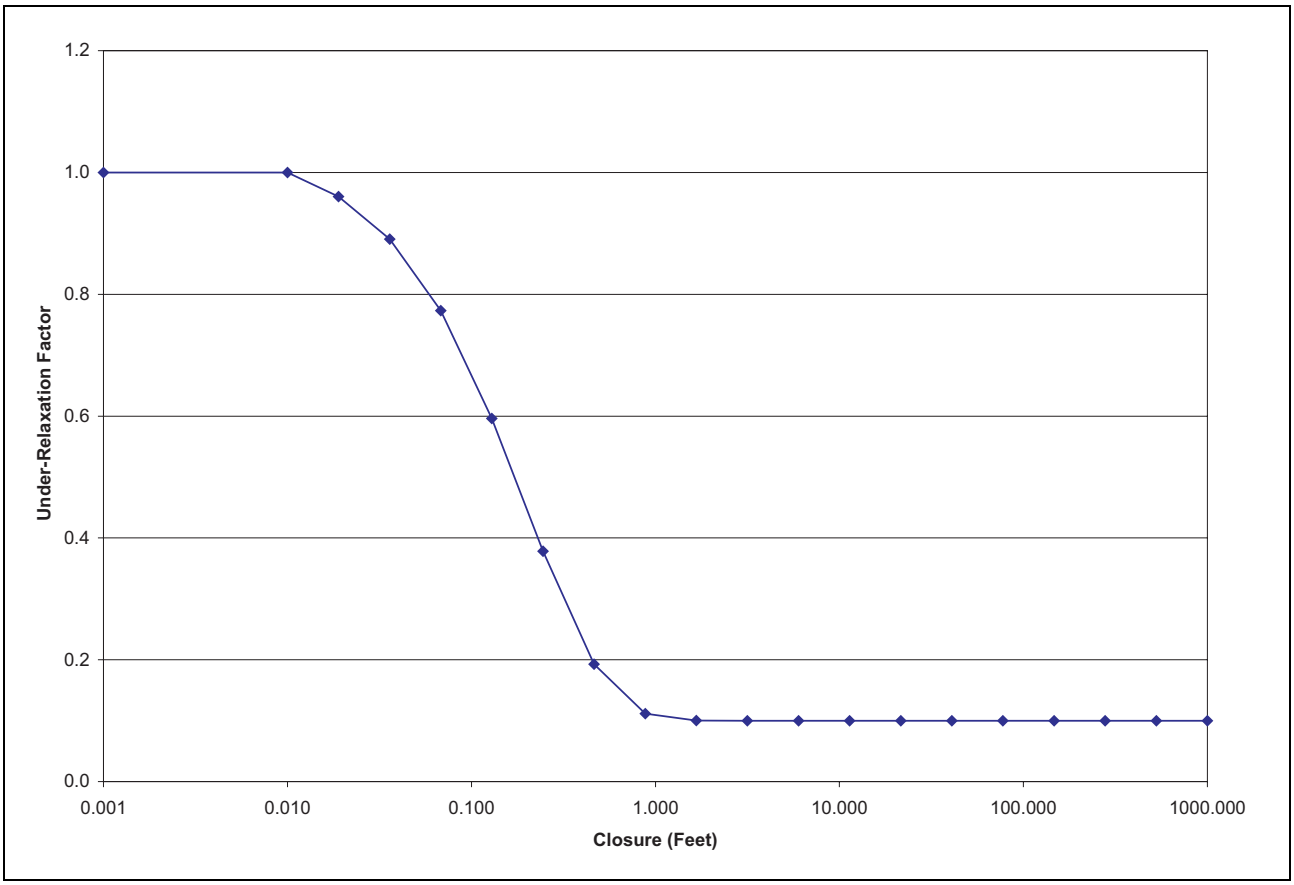

Figure 2-1
Relation Between Under-Relaxation Factor and Iterative Closure

2.4 Subroutine SRELAX

2.4.1 Background

Subroutine SRELAX is used to solve a system of linear equations using the point-over-relaxation method (Hager, 1988). Subroutine SRELAX includes entry points SRELAX1 and SRELAX2. Entry points SRELAX1 and SRELAX2 are called only if the user selects the point over-relaxation method of solving the linear equations. Entry point SRELAX1 reads in parameters that relate to solving a system of linear equations using the point over-relaxation method. Entry point SRELAX2 is called at each within-time-step iteration to iteratively solve the system of linear equations.

2.4.2 Mathematical Basis

2.4.2.1 The Governing Linear Equation

Subroutine SRELAX2 is called by subroutine WFLOW2 to iteratively solve a system of linear equations with the form (Pinder and Gray, 1977)

$$\left([A] + \frac{1}{\Delta t}[B]\right)\{X^{(t)}\} = \frac{1}{\Delta t}[B]\{X^{(t-\Delta t)}\} + \{F\} \quad (2\text{-}6)$$

where

$[A]$ = an $n \times n$ matrix of coefficients, with each of the n rows corresponding to a particular node in the finite-element mesh, and each of the n columns corresponding to the geometry of the groundwater system and its hydraulic parameters for the elements of the finite-element mesh that share the particular node,

$[B]$ = an $n \times n$ matrix of coefficients, with each of the n rows corresponding to a particular node in the finite-element mesh, and each of the n columns corresponding to the geometry of the groundwater system and its storage parameters, for the elements of the finite-element mesh that share the particular node,

$\{X\}$ = an $n \times 1$ vector of unknown heads. $\{X^{(t)}\}$ is the calculated vector of unknowns at the end of the current time-step, and $\{X^{(t-\Delta t)}\}$ is the calculated vector of unknowns at the end of the last time-step, and

$\{F\}$ = an $n \times 1$ vector of sources and sinks.

The derivation of this system of equations is described within the description of subroutine WFLOW.

2.4.2.2 The Point Over-Relaxation Method

The point over-relaxation method is one way in which the system of linear equations described by Equation 2-6 can be solved. Equation 2-6 can be expressed in terms of the left-hand and right-hand sides of the equation. The left-hand side can be expressed by the matrix $[L]$ as

$$[L] = \left([A] + \frac{1}{\Delta t}[B]\right) \quad (2\text{-}7)$$

The right-hand side can be expressed by the vector$\{R\}$ as

$$\{R\} = \frac{1}{\Delta t}[B]\{X^{(t-\Delta t)}\} + \{F\} \quad (2\text{-}8)$$

With these substitutions, Equation 2-6 can be re-expressed as

$$[L]\{X^{(t)}\} = \{R\} \quad (2\text{-}9)$$

Under the point over-relaxation method, the matrix $[L]$ can be expressed in the form

$$[L] = [D] - [l] - [u] \quad (2\text{-}10)$$

where

$[D]$ = a diagonal matrix consisting of the diagonal coefficients of the matrix $[L]$, (i.e., diag $\{L_{11}, L_{22},...,L_{nn}\}^T$),

$[l]$ = a matrix consisting of the negatives of the coefficients of matrix $[L]$ that lie below the main diagonal (i.e., the lower triangular matrix), and

$[u]$ = a matrix consisting of the negatives of the coefficients of matrix $[L]$ that lie above the main diagonal (i.e., the upper triangular matrix).

Substituting Equation 2-10 into Equation 2-9 yields

$$([D]-[l]-[u])\{X^{(t)}\} = \{R\} \quad (2\text{-}11)$$

Equation 2-11 can be rearranged to obtain

$$[D]\{X^{(t)}\} = [l]\{X^{(t)}\} + [u]\{X^{(t)}\} + \{R\} \quad (2\text{-}12)$$

Premultiplying each term by $[D]^{-1}$ yields

$$\{X^{(t)}\} = [D]^{-1}[l]\{X^{(t)}\} + [D]^{-1}[u]\{X^{(t)}\} + [D]^{-1}\{R\} \quad (2\text{-}13)$$

Equation 2-13 can be expressed as a summation based on three principles of the following matrix operations.

Inverse of a Diagonal Matrix

Equation 2-13 first involves calculating the inverse of matrix $[D]$ to obtain $[D]^{-1}$. $[D]$ is a diagonal matrix whose only non-zero entries are on the main diagonal. Under the principles of matrix operations, the inverse of a diagonal matrix is a diagonal matrix whose entries are the inverse of the entries of the original diagonal matrix. That is, if d_{II} are the diagonal coefficients of the diagonal matrix $[D]$, then the diagonal coefficients of the inverse diagonal matrix $[D]^{-1}$ will be $1/d_{II}$.

Product of Two Matrices

Equation 2-13 also involves taking the products of two matrices ($[D]^{-1}[l]$ and $[D]^{-1}[u]$). Under these principles, the product of two matrices $[A]$ and $[B]$ where $[A]$ has n columns and $[B]$ has n rows yields a matrix that has the same number of rows as $[A]$ and the same number of columns as $[B]$. If matrix $[C]$ is the product of matrices $[A]$ and $[B]$, the entries C_{IJ} in matrix $[C]$ can be derived from the expression

$$C_{IJ} = \sum_{k=1}^{n} (A_{Ik}B_{kJ}) \quad (2\text{-}14)$$

where

n = the number of columns in matrix [A] and the number of rows in matrix [B].

Product of a Matrix and a Vector

Equation 2-13 finally involves taking the product of a matrix and a vector (the result of the products of $[D]^{-1}[l]$ and $[D]^{-1}[u]$ are multiplied by vector $\{X^{(t)}\}$). The same principle expressed in Equation 2-15 applies when you take the product of matrix [A] and vector {B}, where matrix [A] has n columns and vector {B} has n entries. Regardless of the value of n, the result is a vector that has the same number of entries as the number of rows of matrix [A]. If matrix [C] is the product of matrix [A] and vector {B}, the entries C_I in vector {C} can be derived from the following expression

$$C_I = \sum_{k=1}^{n} (A_{Ik} B_I) \tag{2-15}$$

Using the concepts above, Equation 2-13 can be expressed in summation form as

$$X_I = \sum_{J=1}^{n} \frac{l_{IJ}}{D_{IJ}} X_J + \sum_{J=1}^{n} \frac{u_{IJ}}{D_{IJ}} X_J + \sum_{J=1}^{n} \frac{R_J}{D_{IJ}} \tag{2-16}$$

Note that the superscript t has been dropped from the unknown X for convenience, as the equation above is iteratively solved until convergence is achieved. Because [l] and [u] are the negatives of the upper and lower triangular matrix of [L] (per Equation 2-10), we can use the following equations to express [l], and [u] in terms of [L]:

$$\sum_{J=1}^{n} (l_{Ik} X_J) = -\sum_{J=1}^{I-1} (L_{Ik} X_J) \tag{2-17}$$

$$\sum_{J=1}^{n} (u_{Ik} X_J) = -\sum_{J=I+1}^{n} (L_{Ik} X_J) \tag{2-18}$$

If we substitute Equations 2-17 and 2-18 into the first two summation terms on the right-hand side of Equation 2-16, we get

$$X_I = -\sum_{J=1}^{I-1} \frac{L_{IJ}}{D_{IJ}} X_J - \sum_{J=I+1}^{n} \frac{L_{IJ}}{D_{IJ}} X_J + \sum_{J=1}^{n} \frac{R_J}{D_{IJ}} \tag{2-19}$$

Because $[D]^{-1}$ is a diagonal matrix where $D_{IJ} = 0$ for $i \neq j$, three summation terms on the right-hand side of Equation 2-19 only will have non-zero values for D_{II}. Thus, Equation 2-19 can be expressed

as

$$X_I = -\sum_{J=1}^{I-1}\frac{L_{IJ}}{L_{II}}X_J - \sum_{J=I+1}^{n}\frac{L_{IJ}}{L_{II}}X_J + \frac{R_I}{L_{II}} \tag{2-20}$$

If k is an iteration counter for each successive update of the vector $\{X\}$, then at any one calculation of Equation 2-20 for a given column J at a new iteration k+1, X_J will have a newly updated value $X_J^{(k+1)}$ for $J < I$ and a not yet updated value $X_J^{(k)}$ for $J > I$. This means that X_J will have a newly updated value $X_J^{(k+1)}$ for the first term in Equation 2-20 (where J will always be less than I) and X_J will not yet have an updated value $X_J^{(k)}$ for the second term in Equation 2-20 (where J will always be greater than I). Thus, Equation 2-20 can be expressed with an iteration counter as

$$X_I^{(k+1)} = -\sum_{J=1}^{I-1}\frac{L_{IJ}}{L_{II}}X_J^{(k+1)} - \sum_{J=I+1}^{n}\frac{L_{IJ}}{L_{II}}X_J^{(k)} + \frac{R_I}{L_{II}} \tag{2-21}$$

At each iteration, a new value for $X_J^{(k+1)}$ is calculated. At the next iteration, the previous value for $X_J^{(k+1)}$ substituted for $X_J^{(k)}$. Convergence is reached when the difference between $X_J^{(k+1)}$ and $X_J^{(k)}$ for all rows in vector $\{X\}$ is less than or equal to a convergence factor ε, which is specified by the user. As stated before in Section 2.3, convergence is achieved when, for all rows I:

$$\max_I\left(\left|X_I^{(k+l)} - X_I^{(k)}\right|\right) \le \varepsilon \tag{2-22}$$

Under the point over-relaxation method, convergence is accelerated by applying an over-relaxation factor ω, which is specified by the user. Using this over-relaxation factor, the value $X_I^{(k+1)}$ at a given iteration is accelerated by a weighted difference between what $\tilde{X}_I^{(k+1)}$ would have been without any acceleration and $X_J^{(k)}$. This is mathematically expressed as follows:

$$X_I^{(k+1)} = X_I^{(k)} + \omega(\tilde{X}_I^{(k+1)} - X_I^{(k)}) \tag{2-23}$$

where

$\tilde{X}_I^{(k+1)}$ = the unaccelerated value of $X_I^{(k+1)}$, and
ω = the over-relaxation factor, which has a value between 1 and 2.

Substituting Equation 2-21 into Equation 2-23, we get the ultimate equation that governs SRELAX2.

$$X_I^{(k+1)} = X_I^{(k)} + \omega\left(-\sum_{J=1}^{I-1}\frac{L_{IJ}}{L_{II}}X_J^{(k+1)} - \sum_{J=I+1}^{n}\frac{L_{IJ}}{L_{II}}X_J^{(k)} + \frac{R_I}{L_{II}} - X_I^{(k)}\right) \tag{2-24}$$

If no acceleration occurs (ω = 1), Equation 2-24 reduces to Equation 2-21.

2.5 Subroutine SITPACK

2.5.1 Background

Subroutine SITPACK includes entry points SITPACK1 and SITPACK2. Entry points SITPACK1 and SITPACK2 are called only if the user selects the conjugate-gradient method of solving the system of linear equations. Subroutine SITPACK1 reads in parameters that relate to solving a system of linear equations using the conjugate-gradient method. Subroutine SITPACK2 solves the system of linear equations.

2.5.2 Mathematical Basis

2.5.2.1 The Governing Linear Equation

Subroutine SITPACK2, which is called by subroutine WFLOW2, iteratively solves a system of linear equations with the form

$$\left([A] + \frac{1}{\Delta t}[B]\right)\{X^{(t)}\} = \frac{1}{\Delta t}[B]\{X^{(t-\Delta t)}\} + \{F\} \qquad (2\text{-}25)$$

where

$[A]$ = an $n \times n$ matrix of coefficients, with each of the n rows corresponding to a particular node in the finite-element mesh, and each of the n columns corresponding to the geometry of the groundwater system and its hydraulic parameters for the elements of the finite-element mesh that share the particular node,

$[B]$ = an $n \times n$ matrix of coefficients, with each of the n rows corresponding to a particular node in the finite-element mesh, and each of the n columns corresponding to the geometry of the groundwater system and its storage parameters, for the elements of the finite-element mesh that share the particular node,

$\{X\}$ = an $n \times 1$ vector of unknown heads. $\{X^{(t)}\}$ is the calculated vector of unknowns at the end of the current time-step, and $\{X^{(t-\Delta t)}\}$ is the calculated vector of unknowns at the end of the last time-step, and

$\{F\}$ = an $n \times 1$ vector of sources and sinks.

The derivation of this system of equations is described within the description of subroutine WFLOW.

2.5.2.2 The Jacobi Conjugate-Gradient Method

Subroutine SITPACK calls subroutine ITPACK, which was downloaded from a University of Texas website and used here unaltered. Subroutine ITPACK uses the Jacobi conjugate-gradient method to solve the system of equations represented by Equation 2-25. ITPACK is a collection of iterative

methods developed at the University of Texas (Hageman and Young, 1981; Kincaid and Young, 1980; Kincaid et al., 1982; Young, 1971; and Young and Kincaid, 1980). ITPACK is tailored to systems whose coefficient matrix is sparse, nearly symmetric, and positive definite. ITPACK contains basic iterative procedures such as the Jacobi method, successive overrelaxation, and symmetric successive overrelaxation with acceleration procedures such as Chebyshev and conjugate-gradient acceleration. The ITPACK automatically determines the appropriate acceleration parameters.

2.6 Subroutine SAMG

2.6.1 Background

Subroutine SAMG includes entry points SAMG1 and SAMG2. Entry points SAMG1 and SAMG2 are called only if the user selects the algebraic multigrid method of solving the system of linear equations. Subroutine SAMG1 reads in parameters that relate to solving a system of linear equations using the conjugate-gradient method. Subroutine SAMG2 solves the system of linear equations.

2.6.2 Mathematical Basis

2.6.2.1 The Governing Linear Equation

Subroutine SAMG2, which is called by subroutine WFLOW2, iteratively solve a system of linear equations with the form

$$\left([A] + \frac{1}{\Delta t}[B]\right)\{X^{(t)}\} = \frac{1}{\Delta t}[B]\{X^{(t-\Delta t)}\} + \{F\} \qquad (2\text{-}26)$$

where

$[A]$ = an $n \times n$ matrix of coefficients, with each of the n rows corresponding to a particular node in the finite-element mesh, and each of the n columns corresponding to the geometry of the groundwater system and its hydraulic parameters for the elements of the finite-element mesh that share the particular node,

$[B]$ = an $n \times n$ matrix of coefficients, with each of the n rows corresponding to a particular node in the finite-element mesh, and each of the n columns corresponding to the geometry of the groundwater system and its storage parameters for the elements of the finite-element mesh that share the particular node,

$\{X\}$ = the $n \times 1$ vector of unknown heads. $\{X^{(t)}\}$ is the calculated vector of unknowns at the end of the current time-step, and $\{X^{(t-\Delta t)}\}$ is the calculated vector of unknowns at the end of the last time-step, and

$\{F\}$ = an $n \times 1$ vector of sources and sinks.

The derivation of this system of equations is described within the description of subroutine WFLOW.

2.6.2.2 The Algebraic Multigrid

Subroutine SAMG calls subroutine AMG1R5, which was developed by the German National Resource Center for Information Technology. The version used here was downloaded from the U.S. Geological Survey (Mehl and Hill, 2001) and used here unaltered, except for a programming error corrected by Granville Swell, Texas A&M University (written communication, 2005). Subroutine SAMG uses the algebraic multigrid method to solve the system of equations represented by Equation 2-26 (Ruge and Stüben, 1987). The multigrid method is an iterative approach that improves the efficiency by which updates of the vector of unknowns are propagated through the overall system equations. With either conjugate-gradient or simpler point over-relaxation methods, the updating of a particular unknown affects typically, only a small region of the system of equations. With the multigrid method, the updating affects a larger region by taking advantage of connections within the system of equations as represented by the magnitude and position of the non-zero coefficients.

2.7 Subroutine NODES

2.7.1 Background

Subroutine NODES reads in the user-defined nodes for the individual compartments in the finite-element mesh, including the *x*, *y*, and *z* coordinates for these nodes and the scaling factors (if any) for these coordinates. Additionally, NODES reads in the parameters required for the contraction or expansion of the mesh to follow a moving water table. The coordinate system must be right handed with the *z*-axis vertically upward. Right handed means that the *y*-axis is 90 degrees counter-clockwise from the *x*-axis when looking backward along the *z*-axis. For example, if the positive *x*-direction is eastward, then the positive *y*-direction is northward.

2.7.2 Mathematical Basis

Subroutine NODES has three entry points. Entry point NODES1 reads the coordinates for each node, entry point NODES2 performs mesh adjustments, and entry point NODES3 outputs the mesh adjustments.

Within NODES2, mesh adjustments are made at each time step (and each time-step iteration) so that the elevations of the nodes comprising the water table equal the computed heads for the nodes as described by Durbin and Berenbrock (1985). If the water table rises within a time step, the nodal elevations are adjusted upward. If the water table falls, the node elevations are adjusted downward. However, if the downward adjustment position of node is too close to the next node below, the next node below is adjusted downward to maintain a specified minimum spacing between vertically adjacent nodes.

2.8 Subroutine ELEMS

Subroutine ELEMS first reads in the user-defined elements for the individual compartments in the finite-element mesh, including each element number and the node numbers of the nodes that form the vertices of each element. In most cases, an element will be wedge-shaped and contain six nodes. In cases where layers of the finite-element mesh pinchout, an element may contain only four or five nodes. A wedge-shaped element with a one zero-height edge ultimately reduces to a five-node pyramid, and a wedge-shaped element with two zero-height edges reduces to a four-node tetrahedron.

After reading in the element number and corresponding nodes, subroutine ELEMS translates these wedge-shaped elements into tetrahedral elements. However, the mesh is specified by the user as wedge elements, including wedges with zero-height edges, because the wedges are easier to work with than tetrahedrons. The wedge-shaped elements are oriented wherein the triangular faces are horizontal or sub-horizontal, the edges connecting the triangular faces are horizontal or sub-horizontal, and the quadrilateral faces are vertical or sub-vertical. Subroutine ELEMS automatically fits three, two, or one tetrahedron into each wedge-shaped element depending on whether the wedge has no, one, or two zero-height edges (Figures 2-2 and 2-3).

While FEMFLOW3D accommodates hydrogeologic units that pinch out within the model domain, the creation of a finite-element mesh with pinchouts can be difficult because GMS does not include that ability. However, meshes with pinchouts can be approximated in GMS by continuing the pinched out unit beyond the geographic extent of the unit as a thin layer.

Subroutine ELEMS creates an output file of the mesh geometry that can be opened in the Groundwater Modeling System (GMS). Within GMS the mesh can be viewed with various options.

2.9 Subroutine WFLOW

2.9.1 Background

Subroutine WFLOW is the central module of the groundwater-flow component within FEMFLOW3D. This subroutine controls data input for FEMFLOW3D and executes the principal calculations relating to the implementation of the finite-element method. Subroutine WFLOW includes entry points WFLOW1 and WFLOW2. Note that generally, the “1”-suffix entry points in FEMFLOW3D relate to reading in the relevant parameters, the “2”-suffix entry points relate to performing appropriate mathematical calculations on these parameters, and the “3”-suffix entry points relate to outputting the solution derived from these calculations.

Entry point WFLOW1 inputs hydraulic parameters, initial conditions, observation-well information, specified-heads, specified fluxes, groundwater evapotranspiration, stream-aquifer interactions, and faults. WFLOW1 calls subroutines WPARAMS1 (which reads in aquifer parameters such as hydraulic conductivity, specific storage, specific yield, and the orientation of the hydraulic-conductivity tensor with respect to coordinate axes), WSTART (which reads in global initial heads or initial heads for specific compartments), WOUTPUT1 (which reads in data for

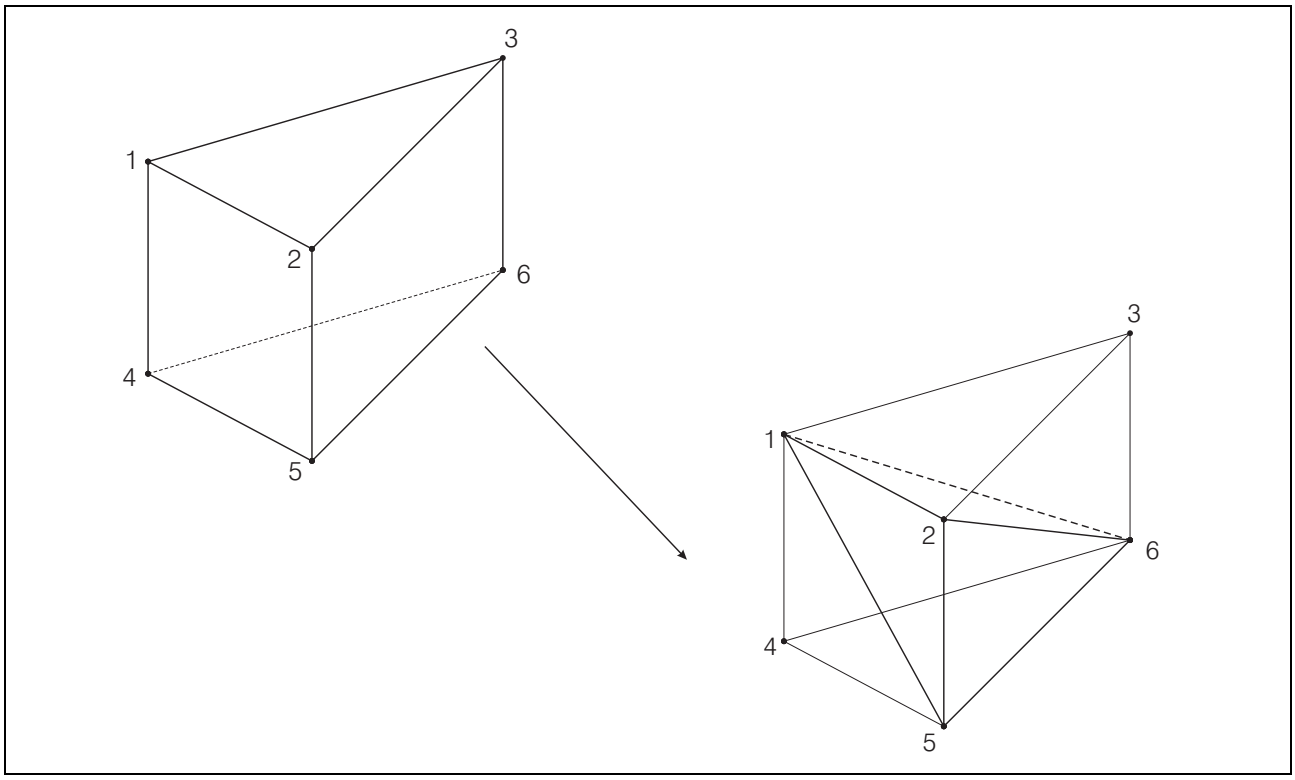

Figure 2-2
Disaggregation of Wedge-Shaped Element Into Three Tetrahedrons

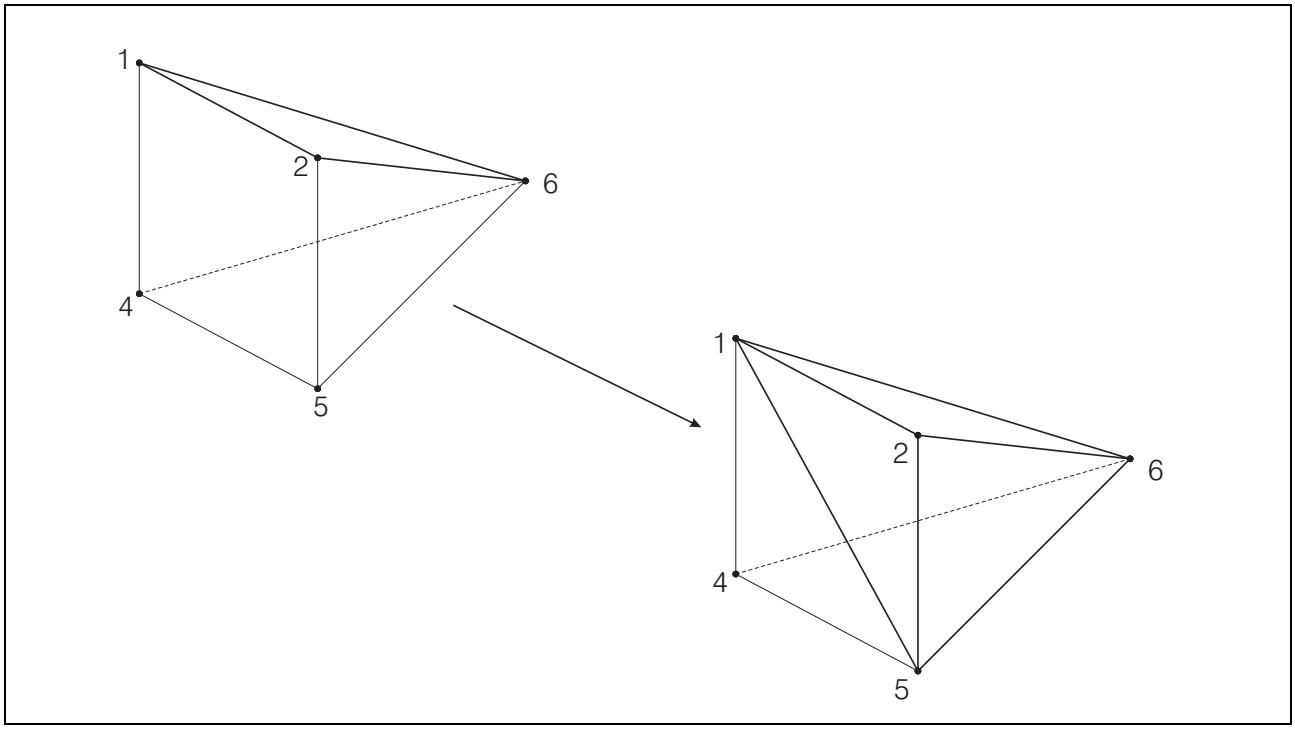

Figure 2-3
Disaggregation of Pyramid-Shaped Element Into Two Tetrahedrons

observation wells and hydrographs), WCHEAD1 (which reads in specified heads), WFLUX1 (which reads in specified fluxes), WEVAP1 (which reads in the specification of groundwater evapotranspiration), WRIVER1 (which reads in a description of a streamflow network), WFAULT1 (which reads in the specification of faults), and PACK1 (which creates the structure of the relevant matrices in Equation 2-6).

The matrices [*A*] and [*B*] are sparse, which means that most of their coefficients have a value of zero. Furthermore, the structures of non-zero coefficients are static within a particular simulation, even though the coefficient values within that structure are dynamic. The structure is dependent on only the geometric relations within the three-dimensional finite-element mesh used to represent the groundwater system, the two-dimensional mesh used to represent faults, and the links between the two. For a particular row *I* in [*A*] or [*B*], the non-zero columns firstly include all the nodes associated with all the elements that share node *I*. If node *I* is within the three-dimensional mesh, the elements will be all the tetrahedral elements that share the node. If node *I* is within the two-dimensional mesh, the elements will be all the triangular elements that share the node. The non-zero columns secondly include all the nodes associated with links between the three-dimensional mesh and the two-dimensional fault mesh. If node *I* in the three-dimensional mesh is linked to node *J* in the two-dimensional fault mesh, column *J* in row *I* will be non-zero. Likewise, column *I* in row *J* will be non-zero. The call to PACK1 identifies the structure of non-zero coefficients for each row in matrices [*A*] and [*B*].

Entry point WFLOW2 is called at each time-step iteration to construct Equation 1-3. WFLOW2 in turn calls subroutines WPARAMS2 (which performs integrations required by the finite-element method and populates the matrices [*A*] and [*B*] in Equation 1-3), WFLUX2 (which implements the specified fluxes by populating the vector {*F*} and, for the case of multilayer wells, the vector [*A*]). WEVAP2 (which implements groundwater evapotranspiration by populating the matrix [*A*] and vector{F}), WRIVER2 (which implements the stream-aquifer interactions by populating the matrix [*A*] and vector {*F*}), and WFAULT2 (which implements faults by populating the matrices [*A*] and [*B*]). Finally, Equation 1-3 is solved for the heads at the current time step by calling either SRELAX2 or SITPACK2.

After the new heads are obtained, the simulation results for the time step are output with calls to WOUPUT2, WCHEAD3, WFLUX3, WEVAP3, WRIVER3 and WFAULT3. Subroutine WOUTPUT2 outputs printed heads and the water budget for the groundwater system. It additionally outputs a file that can be read by the GMS to display the computed heads with various viewing options. The calls to WCHEAD3, WFLUX3, WEVAP3, WRIVER3, and WFAULT3 invoke outputs from those subroutines and compute the water-budget contribution from the respective processes represented by the subroutines.

2.9.2 Mathematical Basis

2.9.2.1 Governing Equation

The calculations in subroutine WFLOW2 are based on the three-dimensional equation of groundwater flow in the form

$$\frac{\partial}{\partial x_i}\left(K_{ij}\frac{\partial h}{\partial x_j}\right) + W = S\frac{\partial h}{\partial t} \quad \text{for } i = 1,2,3 \text{ and } j = 1,2,3 \tag{2-27}$$

where

h = the hydraulic head [L],
K_{ij} = a component of the hydraulic conductivity tensor [Lt^{-1}],
S = the specific storage [L^{-1}],
W = the source injection rate per unit volume [t^{-1}],
X = the coordinates in the x-direction of a right-hand Cartesian coordinate system [L],
t = time [t].

The form of the governing equation makes no assumption about the alignment of the coordinate system with respect to the alignment of the principal components of the hydraulic conductivity tensor.

2.9.2.2 Finite-Element Approximation

In subroutine WFLOW2, Equation 2-27 is solved using the Galerkin finite-element method described by Durbin and Berenbrock (1985). In this method, the exact continuous solution to Equation 2-27 is replaced by an approximate piecewise-continuous solution. This piecewise-continuous solution is defined by coefficient values specified at nodes in the model mesh. Solution values between the nodes are calculated using piecewise-continuous interpolation, or basis functions that depend on the coefficients and are defined over the elements in the mesh. FEMFLOW3D uses tetrahedral and triangular elements and linear interpolation functions.

Application of the Galerkin finite-element method to the spatial domain results in a system of ordinary differential equations in time. To solve this system of equations for each time step, the time derivative is approximated using a first-order, implicit, finite-difference scheme. Corresponding to the implicit approximation of the time derivative, the coefficients of the system of equations generated by the finite-element method are evaluated for each time step at the end of the new time step.

The coefficients of the system of equations are dependent, in part, on calculated hydraulic heads, causing the system of ordinary differential equations to be nonlinear. The nonlinearity of the system of equations results from both the adjustable mesh and nonlinear head-dependent fluxes. The nonlinear head-dependent fluxes in turn result from (1) the use of the drainage-node form of the specified-head boundary condition, (2) the representation of stream-aquifer interactions, and (3) the representation of evapotranspiration from groundwater. Because the nonlinearities typically are not

severe, a solution to the nonlinear system of ordinary differential equations can be obtained by simple iteration, which is sometimes referred to as Picard iteration. At each iteration, a system of linear equations is generated using the hydraulic heads from the last iteration to evaluate the coefficients of the system of equations. The coefficients are updated at each iteration until convergence is obtained. These iterations are referred to here as time-step iterations. The time-step iterations are not to be confused with solver iterations, which are used to solve the linearized system of equations within each time-step iteration.

Application of Galerkin Method

To apply the finite-element method, the linear operator $L[\ ]$ corresponding to Equation 2-27 is defined as

$$L[h'] = \frac{\partial}{\partial x_i}\left(K_{ij}\frac{\partial h'}{\partial x_j}\right) + W - S\frac{\partial h'}{\partial t} \quad \text{for } i = 1,2,3 \text{ and } j = 1,2,3 \tag{2-28}$$

where

$$h'(x_1, x_2, x_3, t) = \sum_{I=1}^{n} H_I(t)\phi_I(x_1, x_2, x_3) \quad \text{for } I = 1, 2, ..., n, \tag{2-29}$$

and where

L = the linear operator,
h' = a series approximation to h [L],
x_1 = the coordinate in the x-direction of a right-hand Cartesian coordinate system [L],
x_2 = the coordinate in the y-direction [L],
x_3 = the coordinate in the z-direction, which has the same datum as the hydraulic head [L],
K_{ij} = a component of the hydraulic conductivity tensor [Lt^{-1}],
W = the source injection rate per unit volume [t^{-1}],
H_I = the undetermined coefficients [L],
t = time [t],
S = the specific storage [L^{-1}], and
n = the number of nodes within the finite-element mesh.
ϕ_I = a linear interpolating (or basis) function [L^0]

The series approximation to Equation 2-28 will provide an exact representation as the number of nodes n approaches infinity. For a finite series however, the approximation will not satisfy exactly Equation 2-28, and a residual R will result. The residual is defined by

$$R(x_1, x_2, x_3, t) = L\left[\sum_{I=1}^{n} H_I(t)\phi_I(x_1, x_2, x_3)\right]. \tag{2-30}$$

If the solution h' was exact, the residual would vanish. However, for any non-exact solution, the residual locally will be non-zero. In the Galerkin method, the average residual within the domain is forced to zero through the selection of the undetermined coefficients H_I. In particular, the undetermined coefficients are calculated by setting the weighted integrals of the residual to zero. The interpolating functions are used as weighting functions (Pinder and Gray, 1977).

$$\int_{\Omega} L\left[\sum_{I=1}^{n} H_I(t)\phi_I(x_1, x_2, x_3)\right]\phi_J(x_1, x_2, x_3)d\omega = 0 \qquad (2\text{-}31)$$

for I = 1,2, ..., n and J = 1,2, ..., n, and where

Ω = the volume of three-dimensional flow domain [L^3],
t = time [t],
H_I = the undetermined coefficients [L],
ϕ_I = linearly independent interpolating functions defined over the volume of three-dimensional flow domain Ω [L^0], and
n = the number of nodes within the finite-element mesh.

The n equations can be solved for the n values of H_I.

System of Ordinary Differential Equations

To solve the system of equations, Equation 2-31 can be simplified. First, Equation 2-31 is expanded to obtain the system of n equations

$$\int_{\Omega}\left[\frac{\partial}{\partial x_i}\left(K_{ij}\frac{\partial}{\partial x_j}\sum_{I=1}^{n} H_I\phi_I\right) + W - S\frac{\partial h'}{\partial t}\right]\phi_J d\omega = 0 \qquad (2\text{-}32)$$

for I = 1,2, ..., n and J = 1,2, ..., n.

Second, the second-order terms in Equation 2-32 are eliminated by applying Green's theorem (Pinder and Gray, 1977). By assuming that hydraulic conductivity is constant for each element and by recalling that H_I is a function of time only, the application of Green's theorem yields

$$\int_{\Omega}\sum_{I=1}^{n}\left(K_{ij}\frac{\partial\phi_J}{\partial x_i}\frac{\partial\phi_I}{\partial x_j}\right)H_I d\omega + \int_{\Omega}\sum_{I}^{n}\left(S\phi_J\phi_I\frac{dH_I}{dt}\right)d\omega - \int_{\Omega} W\phi_J d\omega - \int_{\Gamma} q_B\phi_J d\lambda + \qquad (2\text{-}33)$$

$$\int_{\Gamma_F} S_y\phi_J\phi_I\frac{dH_I}{dt}d\lambda = 0$$

for I = 1,2, ..., n, and J = 1,2, ..., n, i = 1,2,3 and j = 1,2,3, and where

K_{ij} = a component of the hydraulic conductivity tensor [Lt^{-1}],
x_1 = the coordinate in the x-direction of a right-hand Cartesian coordinate system [L],
x_2 = the coordinate in the y-direction [L],
x_3 = the coordinate in the z-direction, which has the same datum as the hydraulic head [L],
H_I = the undetermined coefficients [L],
S = the specific storage [L^{-1}],
S_y = the specific yield [L^0],
W = the source injection rate per unit volume [t^{-1}],
t = time [t],
Ω = the volume of three-dimensional flow domain [L^3],
Γ = the boundary surface of the three-dimensional flow domain Ω [L^2],
Γ_F = the surface represented by the water table [L^2], and
q_B = the inward flux normal to the surface Γ [Lt^{-1}].

The n equations of Equation 2-33 can be written in matrix form as

$$[A]\{H\} + [B]\left\{\frac{dH}{dt}\right\} = \{F\} \tag{2-34}$$

where the typical elements of the matrices [A] and [B] and the vector {F} are

$$A_{IJ} = \int_{\Omega}\left(K_{ij}\frac{\partial\phi_J}{\partial x_i}\frac{\partial\phi_I}{\partial x_j}\right)d\omega, \tag{2-35}$$

$$B_{IJ} = \int_{\Omega} S\phi_J\phi_I d\omega + \int_{\Gamma_F} S_y\phi_J\phi_I d\lambda \tag{2-36}$$

and

$$F_I = \int_{\Omega} W\phi_J d\omega + \int_{\Gamma} q_B\phi_J d\lambda \tag{2-37}$$

which, respectfully, are referred to as the conductance matrix, the storage matrix, and the force vector.

2.9.2.3 Interpolating Functions

To generate the set of algebraic equations represented by Equation 2-34, integrations of the interpolating functions must be carried out in the form

$$\int \frac{\partial\phi_J}{\partial x_i}\frac{\partial\phi_I}{\partial x_j}d\omega,$$

$\int \phi_J \phi_I d\omega,$

$\int \phi_J d\omega,$

$\int \phi_J \phi_I d\lambda$

and

$\int \phi_J d\lambda.$

To facilitate these integrations, the interpolating functions are defined separately for each element, but when combined produce the global-interpolating functions within the flow domain. The elemental interpolating functions used in this work are linear and are defined for tetrahedral elements within the interior of the flow domain and for triangular elements on the boundary surfaces of the flow domain.

Volume Integrations

Linear tetrahedral elements are used for the volume integrations. Within a tetrahedral element, the approximate solution (Equation 2-29) can be expressed as

$$h' = \sum_{I=1}^{4} H_I \phi_I^e \qquad (2\text{-}38)$$

where

ϕ_I^e = an elemental interpolating function defined only within the element e (L^0).

The interpolating functions for the node I is given by the relation (Zienkiewicz, 1988)

$$\phi_I^e = \frac{1}{6V}(a_I + b_I x + c_I y + d_I z) \qquad (2\text{-}39)$$

where

V = the volume of the element [L^3],
x = the coordinate in the x-direction,
y = the coordinate in the y-direction,
z = the coordinate in the z-direction,
a_I = the intercept coefficient of the function [L^3],
b_I = the slope coefficient of the function in the direction x [L^2],
c_I = the slope coefficient of the function in the direction y [L^2], and
d_I = the slope coefficient of the function in the direction z [L^2].

The coefficients and volume within Equation 2-39 are given by the determinants

$$a_I = \begin{bmatrix} x_J & y_J & z_J \\ x_M & y_M & z_M \\ x_P & y_P & z_P \end{bmatrix}, \tag{2-40}$$

$$b_I = \begin{bmatrix} 1 & y_J & z_J \\ 1 & y_M & z_M \\ 1 & y_P & z_P \end{bmatrix}, \tag{2-41}$$

$$c_I = \begin{bmatrix} x_J & 1 & z_J \\ x_M & 1 & z_M \\ x_P & 1 & z_P \end{bmatrix}, \tag{2-42}$$

$$d_I = \begin{bmatrix} x_J & y_J & 1 \\ x_M & y_M & 1 \\ x_P & y_P & 1 \end{bmatrix}, \tag{2-43}$$

and

$$6V = \begin{bmatrix} 1 & x_I & y_I & z_I \\ 1 & x_J & y_J & z_J \\ 1 & x_M & y_M & z_M \\ 1 & x_P & y_P & z_P \end{bmatrix}, \tag{2-44}$$

and where

V = the volume of a tetrahedral element [L^3].

The indices *P*, *I*, *J*, and *M* are the nodal numbers for a tetrahedral element. The ordering of nodal numbers must follow the right-hand rule, that is, the first three nodes (*P*, *I*, and *J*) are numbered in a counter-clockwise manner when viewed from the last (*M*).

Integrations using derivatives of interpolating functions are given for Equation 2-35 by the relations (Zienkiewicz, 1988)

$$\int_e K_{xx} \frac{\partial \phi_I^e}{\partial x} \frac{\partial \phi_J^e}{\partial x} d\omega = \frac{K_{xx}}{36V} b_I b_J, \tag{2-45}$$

$$\int_e K_{xy} \frac{\partial \phi_I^e}{\partial x} \frac{\partial \phi_J^e}{\partial y} d\omega = \frac{K_{xy}}{36V} b_I c_J, \tag{2-46}$$

$$\int_e K_{xz} \frac{\partial \phi_I^e}{\partial x} \frac{\partial \phi_J^e}{\partial z} d\omega = \frac{K_{xz}}{36V} b_I d_J, \tag{2-47}$$

$$\int_e K_{yx} \frac{\partial \phi_I^e}{\partial y} \frac{\partial \phi_J^e}{\partial x} d\omega = \frac{K_{yx}}{36V} c_I b_J, \tag{2-48}$$

$$\int_e K_{yy} \frac{\partial \phi_I^e}{\partial y} \frac{\partial \phi_J^e}{\partial y} d\omega = \frac{K_{yy}}{36V} c_I c_J, \tag{2-49}$$

$$\int_e K_{yz} \frac{\partial \phi_I^e}{\partial y} \frac{\partial \phi_J^e}{\partial z} d\omega = \frac{K_{yz}}{36V} c_I d_J, \tag{2-50}$$

$$\int_e K_{zx} \frac{\partial \phi_I^e}{\partial z} \frac{\partial \phi_J^e}{\partial x} d\omega = \frac{K_{zx}}{36V} d_I b_J, \tag{2-51}$$

$$\int_e K_{zy} \frac{\partial \phi_I^e}{\partial z} \frac{\partial \phi_J^e}{\partial y} d\omega = \frac{K_{zy}}{36V} d_I c_J, \tag{2-52}$$

and

$$\int_e K_{zz} \frac{\partial \phi_I^e}{\partial z} \frac{\partial \phi_J^e}{\partial z} d\omega = \frac{K_{zz}}{36V} d_I d_J. \tag{2-53}$$

Finally,

$$A_{IJ}^e = \frac{1}{36V} (K_{xx} b_I b_J + K_{xy} b_I c_J + K_{xz} b_I d_J + K_{yx} c_I b_J + K_{yy} c_I c_J + K_{yz} c_I d_J + K_{zx} d_I b_J + K_{zy} d_I c_J + K_{zz} d_I d_J) \tag{2-54}$$

where the hydraulic-conductivity tensor is assumed to be constant for an element, and A_{IJ}^{e} is the contribution to elemental matrix $[A^e]$ for I = 1,2,3,4 and J = 1,2,3,4 locally.

The global matrix $[A]$ is obtained by summing the contribution from each node for each element matrix $[A^e]$. For example, if nodes I and J in the element nodal system correspond to nodes P and Q in the global nodal system, then A_{IJ}^{e} in the element stiffness matrix is added to A_{PQ} in the global stiffness matrix. This procedure is repeated for each node in an element and for all elements in the domain Ω.

Integrations with only the interpolating function, and not its derivatives, are given for Equation 2-36 by the relations (Zienkiewicz, 1988)

$$B_{IJ}^{e} = \int_{e} S\phi_I^e \phi_J^e \, d\omega = \frac{SV}{20} \text{ for } I \neq J \tag{2-55}$$

and

$$B_{IJ}^{e} = \int_{e} S\phi_I^e \phi_J^e \, d\omega = \frac{SV}{10} \text{ for } I = J \tag{2-56}$$

where the storage coefficient is assumed constant over an element and B_{IJ}^{e} is the elemental contribution to the matrix $[B^e]$ for I = 1,2,3,4 and J = 1,2,3,4 locally. The global matrix $[B]$ is obtained by summing the contributions from each elemental matrix $[B^e]$ as described above for matrices $[A]$ and $[A^e]$.

The integration for the first right-hand term in Equation 2-37 is given by the relation (Zienkiewicz, 1988)

$$F_I^e = \int_{e} W\phi_I d\omega = \frac{WV}{4} \tag{2-57}$$

where the internal flux rate is assumed constant over an element and F_I^e is the elemental contribution to the vector $\{F^e\}$ for I = 1,2,3,4 locally, but Equation 2-57 represents only the contribution associated with the first right-hand term of Equation 2-37. The global vector $\{F\}$ is obtained by summing the contributions from each elemental vector $\{F^e\}$ as described previously for matrices $[A]$ and $[A^e]$.

Surface Integrations

Surface integrations, rather than volume integrations, are performed for the implementation of the water-table condition and when fault planes have been identified in the finite-element mesh. Recall that the elements of a fault plane are two-dimensional triangular elements, rather than three-dimensional tetrahedral elements. Surface integrations over the flow domain involve the second right-hand term of Equation 2-37. The interpolating function for the node I is given by the relation (Zienkiewicz, 1988)

$$\phi_I^e = \frac{1}{2A}(a_I + b_I x' + c_I y') \tag{2-58}$$

where

ϕ_I^e = the elemental interpolating function defined only within the element e [L^0],
A = the area of the element [L^2],
x' = a local coordinate in the plane of the triangular element [L],
y' = a local coordinate in the plane of the triangular element [L],
a_I = the intercept coefficient of the function [L^2],
b_I = the slope coefficient of the function in the direction x' [L], and
c_I = the slope coefficient of the function in the direction y' [L].

The local coordinate axes lie within the plane of the triangular element, and the x' axis is the outward-pointing normal. The orientation and origin of the coordinate system within that plane can be assigned arbitrarily. Because the normal to boundary surface of the flow domain changes direction over the surface, the local coordinates system must be redefined for each triangular element on the surface.

The coefficient and area within Equation 2-58 are given by the relations (Zienkiewicz, 1988)

$$a_I = \begin{vmatrix} x'_J & y'_J \\ x'_M & y'_M \end{vmatrix} \tag{2-59}$$

$$b_I = -\begin{vmatrix} 1 & y'_J \\ 1 & y'_M \end{vmatrix} \tag{2-60}$$

$$c_I = \begin{vmatrix} x'_J & 1 \\ x'_M & 1 \end{vmatrix} \tag{2-61}$$

and

$$2A = \begin{vmatrix} 1 & x'_I & y'_I \\ 1 & x'_J & y'_J \\ 1 & x'_M & y'_M \end{vmatrix} \tag{2-62}$$

The indexes I, J, and M are the nodal numbers for a triangular element. The ordering of nodal numbers must follow the right-hand rule, that is, the nodes are numbered in a counter-clockwise direction when viewed from above the plane of the triangle.

For the second right-hand term of Equation 2-37, the integration of the interpolating function is given by the relation (Zienkiewicz, 1988)

$$F_I^e = \int_e q_B \phi_I d\lambda = \frac{q_B A}{3} \tag{2-63}$$

where the boundary flux rate is assumed constant over an element and F_I^e is the elemental contribution to the vector $\{F^e\}$ for I = 1, 2, 3 locally, but Equation 2-63 represents only the contribution associated with the second right-hand term of Equation 2-37. The global vector $\{F\}$ is obtained by summing the contributions from each elemental vector $\{F^e\}$ as described previously for matrices $[A]$ and $[A^e]$.

For the second right-hand term of Equation 2-36, the integration of the interpolating function is given by the relation (Zienkiewicz, 1988)

$$B_{IJ}^e = \int_e S_y \phi_J \phi_I d\lambda = S_y \frac{A}{12} \quad \text{for } I \neq J \tag{2-64}$$

and

$$B_{IJ}^e = \int_e S_y \phi_J \phi_I d\lambda = S_y \frac{A}{6} \quad \text{for } I = J \tag{2-65}$$

where the specific yield is assumed to be constant over an element and B_{IJ}^e is the elemental contribution to the matrix $[B^e]$ for I = 1, 2, 3 locally, but Equations 2-64 and 2-65 represent only the contribution associated with the second right-hand term of Equation 2-36. The global matrix [B] is obtained by summing the contribution from each elemental matrix $[B^e]$.

2.9.2.4 Integration in Time

Although the matrices $[A]$ and $[B]$ and the vector $\{F\}$ can now be evaluated, the system of ordinary differential equations must still be solved. To do this, the time derivative is approximated using the first-order, implicit, finite-difference scheme

$$[A]\{H^{(t)}\} + [B]\frac{\{H^{(t)} - H^{(t-\Delta t)}\}}{\Delta t} = \{F\} \tag{2-66}$$

which can be rearranged to obtain

$$\left([A] + \frac{1}{\Delta t}[B]\right)\{H^{(t)}\} = \frac{1}{\Delta t}[B]\{H^{(t-\Delta t)}\} + \{F\} \tag{2-67}$$

where Δt is the time step (t). By the implicit approximation of the time derivative, the matrices $[A]$ and $[B]$ and the vector $\{F\}$ are evaluated at the new time step $t + \Delta t$.

2.9.2.5 Iterative Solution of Non-Linear Equations

Because the coefficients of the matrices [A] and [B] and the vector {F} are dependent, in part, on the hydraulic head, Equation 2-67 represents a system of nonlinear algebraic equations. However, the nonlinearities introduced by deforming grid and head-dependent sources and sinks are not severe. Therefore, the solution of Equation 2-67 can be obtained by a simple iterative procedure, in which, at the k-th iteration, Equation 2-67 takes the form

$$\left([A]^{(k-1)} + \frac{1}{\Delta t}[B]^{(k-1)}\right)\{H^{(t)}\}^{(k)} = \frac{1}{\Delta t}[B]^{(k-1)}\{H^{(t-\Delta t)}\} + \{F\}^{(k-1)} \quad (2\text{-}68)$$

At each iteration, the matrices [A] and [B] and the vector {F} are updated, and a solution is obtained for the new values of $\{H^{(t)}\}$. The process is repeated until convergence is achieved. In most applications, convergence is obtained in two to ten iterations.

Within FEMFLOW3D, the convergence criterion is based on the absolute difference in the computed head between sequential iterations. Convergence is defined by the relation

$$\max_I \left(\left|H_I^{\,k} - H_I^{\,k-1}\right|\right) \le \varepsilon \quad \text{for } I = 1,2,3, \ldots, n \quad (2\text{-}69)$$

where

n = the number of nodes, and
ε = the convergence condition.

By this criterion, convergence occurs when the maximum difference in the computed head at any node is less than the specified value.

2.10 Subroutine WPARAMS

2.10.1 Background

As explained in Section 2.5, FEMFLOW3D iteratively solves the system of linear equations expressed by Equation 2-67 to arrive at groundwater parameters within each time step. Subroutine WPARAMS2 is one of the entry points that contribute to populating the matrices [A] and [B] in Equation 2-67 at each iteration. Subroutine WPARAMS includes entry points WPARAMS1, WPARAMS2, and WPARAMS3. WPARAMS1 is called by subroutine WFLOW1, and WPARAMS2 and WPARAMS3 are called by subroutine WFLOW2. WPARAMS1 reads in aquifer parameters such as hydraulic conductivity, specific storage, specific yield, specific head, and the orientation of the hydraulic-conductivity tensor with respect to the coordinate axes. WPARAMS2, which is called at each time-step iteration, calculates the volume and area integrals contained within Equations 2-35 and 2-36 and populates the matrices [A] and [B] in Equation 2-67. WPARAMS2 performs these calculations by making calls to subroutines WSHAPE1 (which performs the

integrations described by Equation 2-54 through 2-57) and PACK2 (which populates the relevant matrices in Equation 2-67 with coefficients). WPARAMS3, which is called at each flow time-step, computes the storage change associated with the computed head change.

2.10.2 Mathematical Basis

Hydraulic Conductivity Tensor

WPARAMS2 calculates the off-diagonal terms of the hydraulic conductivity tensor. The principal components of the tensor are inputs into WPARAMS1, along with the rotational angles of the principal components with respect to the axes of the coordinate system. The rotation is given by the matrix equation (Voss and Provost, 2003)

$$[K] = [H][K_p][H]^T \tag{2-70}$$

where

$[K]$ = the hydraulic conductivity tensor [Lt^{-1}],
$[K_p]$ = the principal component of the hydraulic conductivity tensor [Lt^{-1}], and
$[H]$ = the rotation matrix.

The tensor $[K_p]$ is given by the relation

$$[K_p] = \begin{bmatrix} K_{xx} & 0 & 0 \\ 0 & K_{yy} & 0 \\ 0 & 0 & K_{zz} \end{bmatrix} \tag{2-71}$$

and the rotation matrix is given by the coefficients (Voss and Provost, 2003)

$$h_{11} = \cos\alpha_1 \cos\alpha_2 \tag{2-72}$$

$$h_{12} = -\sin\alpha_1 \cos\alpha_3 - \cos\alpha_1 \sin\alpha_2 \cos\alpha_3 \tag{2-73}$$

$$h_{13} = \sin\alpha_1 \cos\alpha_3 - \cos\alpha_1 \sin\alpha_2 \cos\alpha_3 \tag{2-74}$$

$$h_{21} = \sin\alpha_1 \cos\alpha_2 \tag{2-75}$$

$$h_{22} = \cos\alpha_1 \cos\alpha_3 - \sin\alpha_1 \sin\alpha_2 \sin\alpha_3 \tag{2-76}$$

$$h_{23} = -\cos\alpha_1, \sin\alpha_3 - \sin\alpha_1, \sin\alpha_2 \cos\alpha_3 \tag{2-77}$$

$$h_{31} = \sin\alpha_2 \tag{2-78}$$

$$h_{32} = \cos\alpha_2 \sin\alpha_2 \quad (2\text{-}79)$$

$$h_{33} = \cos\alpha_2 \sin\alpha_3 \quad (2\text{-}80)$$

where

α_1 = the counter-clockwise angle in the *x*-*y* plane from the *x*-coordinate axis to the *x*-principal axis of the hydraulic-conductivity tensor,

α_2 = the counter-clockwise angle in the vertical plane (i.e., plane perpendicular to *x*-*y* plane) from the *x*-*y* plane to the *x*-principal axis of the hydraulic conductivity tensor, and

α_3 = the counter-clockwise angle in the plane perpendicular to the *x*-principal axis of the hydraulic-conductivity tensor from the intersection with the *x*-*y* plane to the *y*-principal axis of the hydraulic conductivity tensor. If $\alpha_2 = 0$, α_1 is the strike and α_3 is the negative of the dip.

2.10.2.1 Groundwater Storage

The change in groundwater storage for the groundwater system is calculated with a call to WPARAMS3. For each tetrahedral element, the storage change is given by

$$\Delta V_w = \sum_{\Omega} \sum_{I=1}^{4} \left(\frac{V^e}{4}\right)(H_I^{(t)} - H_I^{(t-\Delta t)})S + \sum_{\Gamma_F} \sum_{J=1}^{3} \left(\frac{A^e}{3}\right)(H_J^{(t)} - H_J^{(t-\Delta t)})S_y \quad (2\text{-}81)$$

where

ΔV_w = the change in groundwater storage within the groundwater system [L^3],

V^e = the volume of a tetrahedral element [L^3],

A^e = the area of the top surface of a wedge-shaped element as projected on a horizontal plane [L^2],

S = the specific storage [L^{-1}],

S_y = the specific yield [L^0],

H_I = the computed head at node I,

t = the current time [t],

Δt = the time-step length [t].

I = the local node numbers for the tetrahedral element,

J = the local node numbers representing the top surface of a wedge-shaped element,

Ω = the model domain, and

Γ_F = the water table surface of the model domain.

The volume is calculated using Equation 2-44, and the area is calculated using Equation 2-62. The specific-yield term in Equation 2-81 applies only to top face of the wedge-shaped elements representing the water table surface of the groundwater system.

2.11 Subroutine WSTART

Subroutine WSTART reads in the user-defined initial heads. Initial heads can be input using compartment-by-compartment datasets or globally as a single dataset for all compartments. If initial heads are input separately for each compartment, they can be specified as either a uniform value for all nodes in the compartment or individual values for each node. If initial heads are input globally, initial heads are specified as individual values for all nodes in all compartments. This option can be used to initialize a simulation with heads computed within a previous simulation.

2.12 Subroutine WOUTPUT

Subroutine WOUTPUT encompasses entry points WOUTPUT1 and WOUTPUT2. WOUTPUT1 opens the output files, including the print output file, plot output file, graph output file, and budget output file, and reads in data on groundwater observation wells. WOUTPUT2 writes the computed heads and groundwater budget to the output files.

Observation wells are specified in terms of nodes within the finite-element mesh. One or more nodes are specified, and FEMFLOW3D takes the average computed head at the nodes as the water level in the observation well. The water level in an observation well is specified according to the relation

$$h_{obs}^{(t)} = \sum_{I=1}^{m} H_I^{(t)} W_I \qquad (2\text{-}82)$$

where

$$\sum_{I=1}^{m} W_I = 1$$

and where

h_{obs} = the head at the observation well [L],
H_I = the computed head at a node [L],
W_I = the weight assigned to the node [L^o],
t = the current time [t], and
m = the number of nodes associated with the observation well.

Both horizontal and vertical weighting is embedded in the nodal weights in order to represent an observation well at a particular location and with a particular screened interval.

The assignment of weights to nodes in the finite-element grid depends on the location of the well and the depth interval of the well screen or perforations. For a well that is screened entirely within one element, as shown on Figure 2-4A, the weights are distributed proportionally to each of the six nodes that define that element. Two weighting distributions occur: one distribution is horizontal and one distribution is vertical.

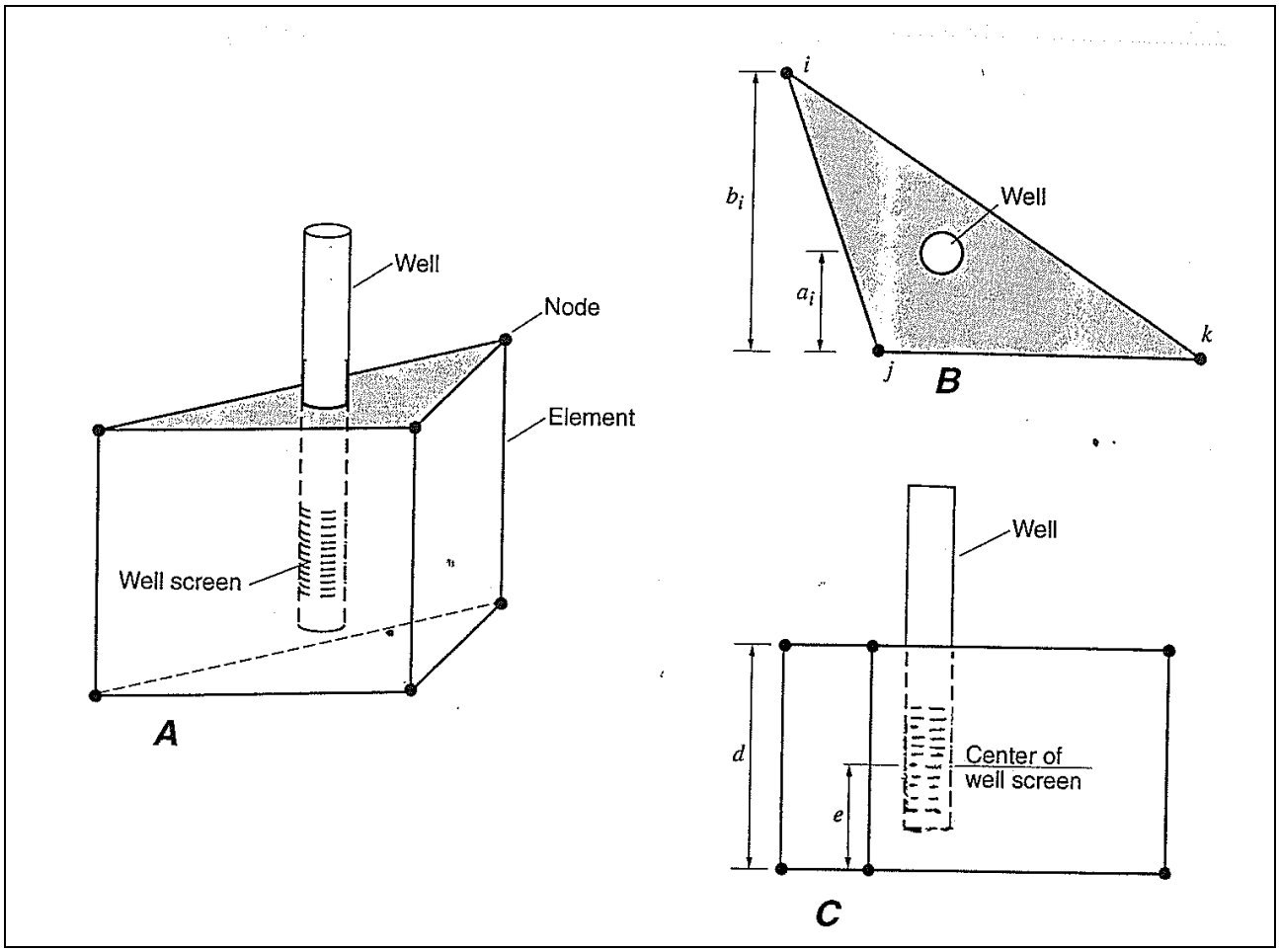

Figure 2-4
Assignment of Nodal Weight to Observation Wells

The geometry for he horizontal weighting is shown on Figure 2-4B. For the horizontal distribution, the weight assigned to node *i* is given by the relation

$$p_i = \frac{a_i}{b_i}, \tag{2-83}$$

where

p_i = the weight for node i [L^0]
a_i = the perpendicular distance from the side opposite node i to the well [L], and
b_i = the perpendicular distance from the side opposite node i to node i [L]

The weights for the nodes *j* and *k* are given by similar relations. The sum of the weights for the three nodes, *i*, *j*, and *k* will equal 1.0.

The geometry for the vertical distribution is shown on Figure 2-4C. For the vertical distribution, the proportion of pumpage assigned to the top of the element is given by the relation

$$p_T = \frac{e}{d}, \tag{2-84}$$

where

p_T = the weight for the top of the element [dimensionless],
e = the distance from the bottom of the element to the center of the well screen [L], and
d = the height of the element [L].

The weight assigned to the bottom of the element is given by the relation

$$p_B = l - p_T \tag{2-85}$$

where p_B is the weight for the bottom of the element [dimensionless]. The sum of these proportions will equal 1.0.

The horizontal and vertical distribution of pumpage must be combined. Using node i as an example, the combined proportion is given by the relation

$$P_i = p_i p_T \tag{2-86}$$

where P_i is the combined proportion [L^0]. The proportions for the other nodes that define the top and bottom of the element are similar.

WOUTPUT2 produces a variety of outputs. WOUTPUT2 creates an output file that contains listings of the computed heads for each observation well at each time step within the simulation. WOUTPUT2 creates also an output file of computed heads for input to the GMS. GMS then can be used to view the computed heads based on different display options, including the creation of animations. Additionally, WOUTPUT2 creates an output file representing the water budget for the groundwater system. For each time step, the file lists the respective fluxes for the groundwater-storage change, specified heads, specified fluxes, groundwater evapotranspiration, stream-aquifer interactions, and fault-aquifer exchanges. The file also includes the storage change within the faults.

2.13 Subroutine WCHEAD

2.13.1 Background

Subroutine WCHEAD is used to represent specified-head boundary conditions, which can take two different forms. In the first form, discharge can occur into or from the groundwater system through the specified-head nodes. An example of this type of boundary condition is with constantly flowing rivers that maintain a hydraulic connection to the water table. In the second form, discharge can occur from the groundwater system through specified-head nodes, but no recharge can occur into the groundwater system through the nodes. This boundary condition is used to represent drainage systems. Such a condition might exist where groundwater can discharge to a subsurface drain pipe.

However, if water otherwise does not flow in the pipe, water cannot discharge from the pipe to the groundwater system.

The heads specified in the subroutine WCHEAD either may be constant or may vary with time. A single head elevation for each specified-head node may be assigned for the entire simulation to represent temporally invariant conditions, such as the elevation of a subsurface drain pipe. Alternatively, the head elevation for each specified-head node may vary in time in accordance with a specified hydrograph, which is input to the model as a table of hydraulic heads at specified times. For each time-step heads are interpolated from the table. The resulting specified head is given by the relation

$$H_B^{(t)} = H_o + H_T(t) \tag{2-87}$$

where

H_B = the specified head at time t [L],
H_o = a baseline specified head [L],
H_T = the head interpolated from a table for time t [L], and
t = the current time.

Subroutine WCHEAD is structured into three basic blocks. A call to entry point WCHEAD1 reads in data on specified-head nodes in the finite-element grid. Entry point WCHEAD2 creates the coefficients to be added to the matrices [A] and [B] in Equation 2-67. Entry point WCHEAD3 calculates the actual groundwater discharge through each specified-head node and creates outputs.

2.13.2 Mathematical Basis

2.13.2.1 Specified-Head Flux Coefficients

System of Linear Equations

As mentioned before, FEMFLOW3D solves a system of linear equations having the form

$$\left([A] + \frac{1}{\Delta t}[B]\right)\{H^{(t)}\} = \frac{1}{\Delta t}[B]\{H^{t-\Delta t}\} + \{F\} \tag{2-88}$$

The vector $\{F\}$ in Equation 2-88 is associated with head-independent fluxes (such as a well pumping at a fixed rate) and head-dependent fluxes (such as specified-head boundaries). Populating vector $\{F\}$ is simple in the context of head-independent fluxes: the vector simply is populated with the user-defined flux values. However, populating vector $\{F\}$ is more complicated in the context of head-dependant fluxes. WCHEAD2 is one among several subroutines called by subroutine WFLOW2 that populate vector $\{F\}$.

The implementation of the specified-head nodes can be illustrated by first examining an individual row in Equation 2-88. Equation 2-88 can be expressed in terms of the left-hand side matrix [*L*] and right-hand vector as follows

$$[L]\{H^{(t)}\} = \{R\} \tag{2-89}$$

where

$$[L] = \left([A] + \frac{1}{\Delta t}[B]\right) \tag{2-90}$$

and

$$\{R\} = \frac{1}{\Delta t}[B]\{H^{(t-\Delta t)}\} + \{F\} \tag{2-91}$$

For a particular row, Equation 2-89 can be expressed as

$$\sum_{J=1}^{n} (L_{IJ}\, H_J^{(t)}) = \frac{1}{\Delta t} \sum_{J=1}^{n} (B_{IJ}\, H_J^{(t-\Delta t)}) + F_I \tag{2-92}$$

where

I = the particular row, which corresponds to the node I in the finite-element mesh, and
J = a column within the row.

Discharge Equation

The general equation for groundwater flow through a specified-head node can be expressed as

$$q_{BI} = C_{BI}(H_{BI} - H_I) \tag{2-93}$$

where

q_{BI} = the groundwater discharge due to the specified-head boundary condition at node I [Lt^{-1}],
C_{BI} = the coefficient representing the leakance of the specified-head boundary condition for node I, as assigned by the user [L^2t^{-1}],
H_{BI} = the specified head for node I, as assigned by the user [L], and
H_I = the unknown hydraulic head for node I [L].

The flux q_{BI} is the discharge necessary to produce the calculated hydraulic head H_I at node I that are approximately equal to the boundary heads H_{BI} at the node I. This relation between specified and calculated heads can be achieved if the coefficient C_{BI} in Equation 2-93 is sufficiently large. The practical application of the specified-head boundary condition does not require the careful determination of values for the coefficient C_{BI}. It is sufficient to choose a value that is large enough

that H_I will be close to H_{BI}. Nevertheless, the value should not be so large that the difference between H_I and H_{BI} is lost in the precision of the calculations.

Substitution Into Force Vector

In the system of linear equations solved by FEMFLOW3D (Equation 2-93), F_I is a quantity representing the internal and boundary fluxes for the model domain. F_I can be expressed as follows:

$$F_I = \int_{\Omega} W\phi_I d\omega + \int_{\Gamma} q\phi_I d\lambda \qquad (2\text{-}94)$$

where

Ω = the three-dimensional flow domain [L^3],
ϕ_I = the linearly independent interpolating functions defined over the flow domain Ω [L^0],
Γ = the part of the boundary surface across which fluxes occur [L^2],
W = the source injection rate per unit volume [t^{-1}], and
q = the inward discharge normal to the surface Γ [Lt^{-1}],

Equation 2-93 is an expression for the boundary fluxes representing specified-head boundaries. Equations 2-94 and 2-93 can be combined into the form

$$F_I = F'_{BI} + C_{BI}(H_{BI} - H_I) \qquad (2\text{-}95)$$

where F'_{BI} represents the internal and boundary fluxes associated with node I except for the boundary fluxes associated with the specified-head boundary conditions. The right-hand side of Equation 2-95 includes the dependent variable H_I, which, in the system of equations set forth in Equation 2-92, represents the head $H_I^{(t)}$ at node I at the end of the current time step. Substituting Equation 2-95 for F_I in Equation 2-92 yields

$$\sum_{J=1}^{n} (L_{IJ}\, H_J^{(t)}) = \frac{1}{\Delta t} \sum_{J=1}^{n} (B_{IJ}\, H_J^{(t-\Delta t)}) + F'_{BI} + C_{BI}(H_{BI} - H_I^{(t)}) \qquad (2\text{-}96)$$

Multiplying through the right-most term in Equation 2-96, and rearranging the equation to bring all of the unknown terms to the left-hand side, yields

$$\sum_{J=1}^{n} (L_{IJ}\, H_J^{(t)}) + C_{BI} H_I^{(t)} = \frac{1}{\Delta t} \sum_{J=1}^{n} (B_{IJ}\, H_J^{(t-\Delta t)}) + F'_{BI} + C_{BI} H_{BI} \qquad (2\text{-}97)$$

This essentially means that, when $J=I$, the quantity C_{BI} is added to the entry L_{II} on the left-hand side of the equation. In matrix form, this is equivalent to adding the quantities C_{BI} to the diagonal of the left-hand matrix [L] in Equation 2-89 and to adding the quantities $C_{BI}H_{BI}$ to right-hand vector {R} of Equation 2-89. Thus, Equation 2-97 can be re-expressed in matrix form as follows

$$([L] + diag\{C_B\})\{H^{(t)}\} = \{R\} + diag\{C_B\}\{H_B\} \quad (2\text{-}98)$$

Where $\{R\}$ in this case contains all the internal and boundary sources and sinks except those associated with the specified-head boundaries. Accordingly, in FEMFLOW3D the quantities C_{BI} are referred to as the "left-hand coefficients" and the quantities $C_{BI}H_{BI}$ are referred to as the "right-hand coefficients."

2.13.2.2 Water Budget

In subroutine WCHEAD3, the discharge of groundwater through individual nodes in the finite-element grid is calculated from the expression

$$\{ q_B^{(t)} \} = diag\{C_B\}\{H_B\} - diag\{C_B\}\{H^{(t)}\} \quad (2\text{-}99)$$

where an element of $\{q_B\}$ is given by

$$q_{BI} = C_{BI}H_{BI} - C_{BI}H_I \quad (2\text{-}100)$$

The cumulative discharge through all specified-head nodes is given by

$$Q_B = \sum_{I=1}^{n} q_{BI} \quad (2\text{-}101)$$

where

Q_B = the cumulative discharge [L^3t^{-1}], and
n = the number of nodes.

2.14 Subroutine WFLUX

2.14.1 Background

Subroutine WFLUX is used to represent specified-flux boundary conditions and internal sources and sinks. Whereas WCHEAD calculates fluxes resulting from specified-head boundaries, WFLUX represents fluxes resulting from specified-flux boundaries or internal sources and sinks. The flux at a particular node also can vary with time as specified by the user in a table. At each time step, flux values are interpolated from the table. The specified flux for a node or well for a time step is given by the relation

$$Q_I = a_I(t) Q_{BI} \tag{2-102}$$

where

Q_I = the specified flux for a node or well [L^3t^{-1}],
Q_{BI} = a baseline flux [L^3t^{-1}],
a_I = a temporal factor for adjusting the baseline flux [L^0], and
t = the current time [t].

FEMFLOW3D includes also a feature for representing pumping from or injection to a well that is screened over multiple layers in the finite-element mesh. The discharge from a particular layer is proportional to the differential head between the well and the mesh layer and the leakance between the mesh and the well. The leakance represents the translation of the mesh-scale hydraulic heads into a within-well hydraulic head. The leakance is specified to capture the effects of converging flow from near the well and well-skin resistance at the well that are not represented in the mesh-scale simulation.

Subroutine WFLUX is structured into three basic blocks. A call to entry point WFLUX1 reads in data on specified-flux nodes in the finite-element grid. Subroutine WFLUX2 creates the coefficients to be added to the vector $\{F\}$ and, for multi-layer wells, the matrix $[A]$. Entry point WFLUX3 calculates the actual fluxes through each node in the finite-element mesh and compiles an element of the water budget for the time step.

2.14.2 Mathematical Basis

2.14.2.1 Specified-Flux Flux Coefficients

System of Linear Equations

As with subroutine WCHEAD, we begin with the system of linear equations that is solved by FEMFLOW3D in the form

$$\left([A] + \frac{1}{\Delta t}[B]\right)\{H^{(t)}\} = \frac{1}{\Delta t}[B]\{H^{(t-\Delta t)}\} + \{F\} \tag{2-103}$$

Equation 2-103 can be expressed in terms of the left-hand side matrix $[L]$ and right-hand vector as follows

$$[L]\{H^{(t)}\} = \{R\} \tag{2-104}$$

where

$$[L] = \left([A] + \frac{1}{\Delta t}[B]\right) \tag{2-105}$$

and

$$\{R\} = \frac{1}{\Delta t}[B]\{H^{(t-\Delta t)}\} + \{F\} \; . \tag{2-106}$$

At a particular row, Equation 2-104 can be expressed as

$$\sum_{J=1}^{n} (L_{IJ} \, H_J^{(t)}) = \frac{1}{\Delta t} \sum_{J=1}^{n} (B_{IJ} \, H_J^{(t-\Delta t)}) + F_I \tag{2-107}$$

where

I = the particular row, which corresponds to the node I in the finite element mesh, and
J = a column within the row.

Discharge Equation

For the specified fluxes that are not associated with a multilayer well, the fluxes are implemented by simply loading the flux value for node I into F_I in Equation 2-107. However, for multilayer wells, the implementation is more complex. As for the specified-heads in subroutine WCHEAD, the approach starts with a discharge equation in the form

$$q_W = C_{WI}(H_W - H_I) \tag{2-108}$$

where

$$\sum q_W = Q_W \tag{2-109}$$

and where

q_W = the groundwater discharge due to a well link to node I [Lt^{-1}],
Q_W = the pumping or injection for a well [L^3t^{-1}],
C_{WI} = the coefficient representing the leakance at node I [L^2t^{-1}],
H_W = the unknown head in the well [L], and
H_I = the unknown hydraulic head for node I [L].

The discharge q_W represents the well-link fluxes. The well-node leakance represents, the drawdown effects at spatial scales less than those represented by finite-element mesh, including well-skin effects.

Substitution Into Force Vector

In the system of linear equations solved by FEMFLOW3D (Equation 2-103), F_I is a quantity representing the internal and boundary fluxes for the model domain. F_I can be expressed as follows

$$F_I = \int_{\Omega} W\phi_I \, d\omega + \int_{\Gamma} q\phi_I \, d\lambda \tag{2-110}$$

where

Ω = the three-dimensional flow domain [L^3],
ϕ_I = the linearly independent interpolating functions defined over the flow domain Ω [L^0],
Γ = the part of the boundary surface across which fluxes occur [L^2],
W = the source injection rate per unit volume [t^{-1}], and
q = the inward discharge normal to the surface Γ [Lt^{-1}].

Equation 2-110 is an expression for the boundary fluxes representing specified-head boundaries. Equations 2-110 and 2-108 can be combined into the form

$$F_I = F'_W + C_{WI}(H_W - H_I) \tag{2-111}$$

where F'_W represents the internal and boundary fluxes associated with a node except for the well-link fluxes. The right-hand side of Equation 2-111 includes the two unknowns H_I and H_W. Substituting Equation 2-111 for F_I in Equation 2-107 yields

$$\sum_{J=1}^{n} (L_{IJ} H_J^{(t)}) = \frac{1}{\Delta t} \sum_{J=1}^{n} (B_{IJ} H_J^{(t-\Delta t)}) + F'_W + C_{WI}(H_W^{(t)} - H_I^{(t)}) \tag{2-112}$$

Multiplying through the right-most term in Equation 2-112 and rearranging the equation to bring all of the unknown terms to the left-hand side yields

$$\sum_{J=1}^{n} (L_{IJ} H_J^{(t)}) + C_{WI} H_I^{(t)} - C_{WI} H_W^{(t)} = \frac{1}{\Delta t} \sum_{J=1}^{n} (B_{IJ} H_J^{(t-\Delta t)}) + F'_W \tag{2-113}$$

Mass Balance Equation

Because a new unknown $H_W^{(t)}$ has been introduced by specifying a pumping or injection well, an additional equation is needed in order to solve for both $H_I^{(t)}$ as well as $H_W^{(t)}$. The following basic mass balance equation for a particular well node will provide this additional equation.

$$\sum_{I} [C_{WI}(H_W^{(t)} - H_I^{(t)})] = Q_W \tag{2-114}$$

where

Q_W = the pumping or injection rate of the well [L^3t^{-1}], and
I = the set of nodes linked to the well.

Separating the two unknowns into separate terms yields

$$\sum_I C_{WI}\, H_W^{(t)} - \sum_I C_{WI}\, H_I^{(t)} = Q_W \tag{2-115}$$

Solving for Additional Unknowns

Equations 2-113 and 2-114 together allow FEMFLOW3D to solve for the unknowns $H_I^{(t)}$ as well as $H_W^{(t)}$. To solve for these terms, FEMFLOW3D adds another row and column to the left-hand matrix [L], another entry to the vector of unknowns {H}, and another entry to the right-hand vector {R}. The coefficients of the new mass balance Equation 2-115 are added to the new row, and the coefficients of unknown $H_W^{(t)}$ can be added to the new column. The addition of a well transforms Equation 2-103 into the form

$$\left(\begin{bmatrix} [A] + diag\{C_W\} & \{C_W\} \\ \{C_W\}^T & -\sum C_W \end{bmatrix} + \frac{1}{\Delta t} \begin{bmatrix} [B] & \{0\} \\ \{0\}^T & 0 \end{bmatrix} \right) \begin{Bmatrix} \{H^{(t)}\} \\ H_W^{(t)} \end{Bmatrix} \tag{2-116}$$

$$= \frac{1}{\Delta t} \left[\begin{Bmatrix} [B] & \{0\} \\ \{0\}^T & 0 \end{Bmatrix} \right] \begin{Bmatrix} \{H^{(t-\Delta t)}\} \\ 0 \end{Bmatrix} + \begin{Bmatrix} \{F'\} \\ \{0\} \end{Bmatrix}$$

where

$\{C_W\}$ = an $n\times1$ vector that has non-zero values for the nodes linked to the well, and
$\{C_W\}^T$ = a $1\times n$ transpose of vector $\{C_W\}$.

For each additional well specified by the user, another row and column is added to [L] and another entry is added to vectors {H} and {R} to enable FEMFLOW3D to solve for the new head variable associated with the new well.

In WFLUX3, the discharges through individual well-links for a particular well is calculated from the expression

$$\{\, q_W^{(t)} \,\} = diag\{C_W\}\{H_W\} - diag\{C_W\}\{H^{(t)}\} \tag{2-117}$$

where an element of $\{q_W\}$ is given by

$$q_{WI} = C_{WI} H_W - C_{WI} H_I \tag{2-118}$$

The cumulative discharge through a node associated with a well is given by

$$Q_W = \sum_I q_{WI} \tag{2-119}$$

where

Q_W = the pumping or injection rate for the well [L^3t^{-1}], and
I = the set of all nodes associated with the well.

2.15 Subroutine WEVAP

2.15.1 Background

Subroutine WEVAP is used to simulate the discharge of groundwater from a shallow water table owing to evapotranspiration from vegetated areas or evaporation from bare-soil areas. The simulation is done by assuming that the discharge is linearly related to the depth below the land surface to the water table. The linear relation holds until a maximum depth (extinction depth) is reached. If the water table drops below the extinction depth, evapotranspiration (or evaporation) ceases. In subroutine WEVAP, the evapotranspiration rate depends on the local depth to the water table, the extinction depth, the potential evapotranspiration rate, and the size of the discharge area.

Subroutine WEVAP is structured into three basic blocks. A call to entry point WEVAP1 reads in data on the discharge of water due to evapotranspiration, including data on the discharge area, extinction depth, and potential evapotranspiration rate. Entry point WEVAP2 creates the coefficients to be added to the matrices [A] and [B] in Equation 2-68. Entry point WEVAP3 calculates the actual groundwater discharge due to evapotranspiration.

2.15.2 Mathematical Basis

2.15.2.1 Groundwater Evapotranspiration Flux Coefficients

System of Linear Equations

As usual, we begin with the following system of linear equations that is iteratively solved by FEMFLOW3D:

$$\left([A] + \frac{1}{\Delta t}[B]\right)\{H^{(t)}\} = \frac{1}{\Delta t}[B]\{H^{(t-\Delta t)}\} + \{F\} \quad (2\text{-}120)$$

Equation 2-120 can be expressed in terms of the left-hand side matrix [L] and right-hand vector as follows

$$[L]\{H^{(t)}\} = \{R\} \quad (2\text{-}121)$$

$$[L] = \left([A] + \frac{1}{\Delta t}[B]\right) \quad (2\text{-}122)$$

and

$$\{R\} = \frac{1}{\Delta t}[B]\{H^{(t-1)}\} + \{F\} \quad (2\text{-}123)$$

At a particular node I in the finite-element mesh, Equation 2-121 can be expressed as follows

$$\sum_{J=1}^{n} (L_{IJ}\, H_J^{(t)}) = \frac{1}{\Delta t} \sum_{J=1}^{n} (B_{IJ}\, H_J^{(t-\Delta t)}) + F_I \qquad (2\text{-}124)$$

Discharge Equation

The discharge of groundwater from a shallow water table has the general form

$$q_{EI} = C_{EI}(H_{EI} - H_I) \qquad (2\text{-}125)$$

where

q_{EI} = the groundwater discharge due to the specified-head boundary condition at node I [L^3t^{-1}],
C_{EI} = the coefficient representing the leakance at node I [L^2t^{-1}],
H_{EI} = the elevation of the extinction depth for node I [L], and
H_I = the unknown hydraulic head for node I [L].

The discharge q_{EI} has a non-zero value at nodes where source-sink fluxes occur and a zero value elsewhere.

The coefficient C_{EI} in Equation 2-125 depends on several factors, as indicated in the expression

$$C_{EI} = \frac{A_I E_{\max}}{H_{LI} - H_{EI}} \qquad (2\text{-}126)$$

where

A_I = the discharge area associated with node I [L^2],
$E_{\max}$ = the maximum evapotranspiration rate per unit area [Lt^{-1}],
H_{LI} = the land-surface elevation at the node I [L], and
H_{EI} = the extinction-depth elevation at the node I [L].

The extinction-depth elevation is given by the relation

$$H_{EI} = H_{LI} - d_o \qquad (2\text{-}127)$$

where

d_o = the extinction depth [L].

Substitution Into Force Vector

In the system of linear equations solved by FEMFLOW3D (Equation 2-124), F_I is a quantity representing the internal and boundary fluxes for the model domain. F_I can be expressed as follows

$$F_I = \int_{\Omega} W\phi_I \, d\Omega + \int_{\Gamma_R} q\phi_I \, d\Gamma \qquad (2\text{-}128)$$

where

Ω = the three-dimensional flow domain [L^3],
ϕ_I = the linearly independent interpolating functions defined over the flow domain Ω [dimensionless],
Γ = the overall boundary surface of the flow domain Ω [L^2],
Γ_R = the part of the boundary surface that is not a free surface [L^2],
W = the source injection rate per unit volume [t^{-1}], and
q = the inward discharge normal to the surface Γ [Lt^{-1}].

Equation 2-128 is an expression for the internal and boundary fluxes for the model domain. Correspondingly, Equation 2-125 is an expression for the boundary fluxes representing evapotranspiration nodes. Equations 2-125 and 2-128 can be combined into the form

$$F_I = F'_{EI} + C_{EI}(H_{EI} - H_I) \qquad (2\text{-}129)$$

where F'_{EI} represents the internal and boundary fluxes associated with node I except for the boundary fluxes associated with the evapotranspiration nodes. The right-hand side of Equation 2-129 includes the dependent variable H_I, which, in the system of equations set forth in Equation 2-124, represents the head $H_I^{(t)}$ at node I at the end of the current time step. Substituting Equation 2-129 for F_I in Equation 2-124 yields

$$\sum_{J=1}^{n} (L_{IJ} H_J^{(t)}) = \frac{1}{\Delta t} \sum_{J=1}^{n} (B_{IJ} H_J^{(t-\Delta t)}) + F'_{EI} + C_{EI}(H_{EI} - H_I^{(t)}) \qquad (2\text{-}130)$$

Multiplying through the right-most term in Equation 2-130 and rearranging the equation to bring all of the unknown terms to the left-hand side yields

$$\sum_{J=1}^{n} (L_{IJ} H_J^{(t)}) + C_{EI} H_I^{(t)} = \frac{1}{\Delta t} \sum_{J=1}^{n} (B_{IJ} H_J^{(t-\Delta t)}) + F'_{EI} + C_{EI} H_{EI} \qquad (2\text{-}131)$$

This essentially means that, when $J=I$, the quantity C_{EI} is added to the entry L_{II} on the left-hand side of the equation. In matrix form, this is equivalent to adding the quantities to the diagonal of the left-hand matrix [L] in Equation 2-121 and to adding the quantities $C_{EI}H_{EI}$ to right-hand vector {R} of Equation 2-121. Thus, Equation 2-131 can be re-expressed in matrix form as follows

$$(\{L\} + diag\{C_E\})\{H^{(t)}\} = \{R\} + diag\{C_E\}\{H_E\} \quad (2\text{-}132)$$

Accordingly, in FEMFLOW3D, the quantities C_{EI} are referred to as the "left-hand coefficients" and the quantities $C_{EI}H_{EI}$ are referred to as the "right-hand coefficients."

The value of C_{EI} is based on the relationship between the calculated hydraulic head $H_I^{(t)}$, the extinction depth, and the land surface. First, if the calculated hydraulic head $H_I^{(t)}$ is above the extinction depth and below the land surface, then C_{EI} is given by Equation 2-126. Second, if the calculated hydraulic head $H_I^{(t)}$ is below the extinction depth, then C_{EI} equals zero, and no discharge occurs from the shallow water table.

2.15.2.2 Water Budget

At entry point WEVAP3, the discharge of groundwater due to evapotranspiration through individual nodes in the finite-element grid is calculated from the expression

$$\{ q_E^{(t)} \} = diag\{C_E\}\{H_E\} - diag\{C_E\}\{H^{(t)}\} \quad (2\text{-}133)$$

where an element of $\{q_E\}$ is given by

$$q_{EI} = C_{EI}(H_{EI} - H_I) \quad (2\text{-}134)$$

and where $\{q_E\}$ is a vector of inward discharges [L^3t^{-1}]. The cumulative discharge through all nodes is given by

$$Q_{EI} = \sum_{I=1}^{n} q_{EI} \quad (2\text{-}135)$$

where Q_E is the cumulative discharge [Lt^{-1}], and n is the number of nodes.

2.16 Subroutine WRIVER

2.16.1 Background

Subroutine WRIVER is used to simulate river-aquifer interactions. The simulation is performed by routing inflows through a river network (or networks) that consist of a main river channel and tributary channels, while accounting for riverflow depletions and accretions owing to the exchange of water between the river and the groundwater system. Each river channel consists of a series of channel links associated with nodes in the model. In subroutine WRIVER, the exchange of water is dependent on the river stage, river width, river-bed thickness, river-bed hydraulic conductivity, and groundwater levels at each node within the river network.

Subroutine WRIVER is structured into three basic blocks. A call to entry point WRIVER1 reads in data on the river network, including the physical properties of the channel links and river inflows.

Entry point WRIVER2 creates the coefficients to be added to the matrix [*A*] and vector {*F*} in Equation 2-67. Entry point WRIVER3 calculates the components of the water budget for the river network, including the exchanges of water between the river network and the groundwater system.

2.16.2 Mathematical Basis

2.16.2.1 River Flux Coefficients

System of Linear Equations

As usual, we begin with the following system of linear equations that is iteratively solved by FEMFLOW3D:

$$\left([A] + \frac{1}{\Delta t}[B]\right)\{H^{(t)}\} = \frac{1}{\Delta t}[B]\{H^{(t-\Delta t)}\} + \{F\} \tag{2-136}$$

Equation 2-136 can be expressed in terms of the left-hand side matrix [*L*] and right-hand vector as follows

$$[L]\{H^{(t)}\} = \{R\} \tag{2-137}$$

where

$$[L] = \left([A] + \frac{1}{\Delta t}[B]\right) \tag{2-138}$$

and

$$\{R\} = \frac{1}{\Delta t}[B]\{H^{(t-\Delta t)}\} + \{F\} \tag{2-139}$$

At a particular row, Equation 2-137 can be expressed as

$$\sum_{J=1}^{n} (L_{IJ}\, H_J^{(t)}) = \frac{1}{\Delta t}\sum_{J=1}^{n} (B_{IJ}\, H_J^{(t-\Delta t)}) + F_I \tag{2-140}$$

Discharge Equation

The exchange of water between the river and the groundwater system has the general form

$$q_{RI} = C_{RI}(H_{RI} - H_I) \tag{2-141}$$

where

q_{RI} = the rate of groundwater exchange at node *I* [Lt^{-1}],
C_{RI} = the coefficient representing the river-bed leakance at node *I*, as assigned by the user [Lt^{-1}],

H_{RI} = the stage elevation in the river reach for node I [L], and
H_I = the unknown hydraulic head for node I [L].

The coefficient C_{RI} in Equation 2-141 depends on several factors, as indicated in the expression

$$C_{RI} = L_I W_I \frac{K_I'}{B_I'} \tag{2-142}$$

where

L_I = the reach length associated with the node I [L],
W_I = the river width at node I [L],
K_I' = the vertical hydraulic conductivity of the river bed at node I [Lt^{-1}], and
B_I' = the thickness of the river bed at node I [L].

Accordingly, the coefficient C_{RI} is the product of the wetted area of the river reach ($L_I W_I$) and the river-bed leakance (K_I'/B_I'). The river width is specified as a table of widths and the corresponding flows; and the width for a particular flow can be obtained from the table by interpolation between the tabulated values. The river depth is specified as a table of depths and the corresponding flows; and the depth for a particular discharge can be obtained from the table by interpolation between the tabulated values.

Substitution Into Force Vector

In the system of linear equations solved by FEMFLOW3D (Equation 2-141), F_I is a quantity representing the internal and boundary fluxes for the model domain. F_I can be expressed as follows

$$F_I = \int_{\Omega} W\phi_I \, d\Omega + \int_{\Gamma_R} q\phi_I \, d\Gamma \tag{2-143}$$

where

Ω = the three-dimensional flow domain [L^3],
ϕ_I = the linearly independent interpolating functions defined over the flow domain Ω [dimensionless],
Γ = the overall boundary surface of the flow domain Ω [L^2],
Γ_R = the part of the boundary surface that is not a free surface [L^2],
W = the source injection rate per unit volume [t^{-1}], and
q = the inward discharge normal to the surface Γ [Lt^{-1}].

Equation 2-143 is an expression for the internal and boundary fluxes for the model domain. Correspondingly, Equation 2-141 is an expression for the boundary fluxes representing river nodes. Equations 2-141 and 2-143 can be combined into the form

$$F_I = F'_{RI} + C_{RI}(H_{RI} - H_I) \tag{2-144}$$

where F'_{RI} represents the internal and boundary fluxes associated with nodes except for the fluxes associated with the river nodes. The right-hand side of Equation 2-144 includes the dependent variable H_I, which, in the system of equations set forth in Equation 2-140, represents the head $H_I^{(t)}$ at node I at the end of the current time step. Substituting Equation 2-144 for L_I in Equation 2-140 yields

$$\sum_{J=1}^{n} (L_{IJ}\, H_J^{(t)}) = \frac{1}{\Delta t} \sum_{J=1}^{n} (B_{IJ}\, H_J^{(t-\Delta t)}) + F'_{RI} + C_{RI}(H_{RI} - H_I^{(t)}) \qquad (2\text{-}145)$$

Multiplying through the right-most term in Equation 2-145 and rearranging the equation to bring all of the unknown terms to the left-hand side yields

$$\sum_{J=1}^{n} (L_{IJ}\, H_J^{(t)}) + C_{RI}\, H_I^{(t)} = \frac{1}{\Delta t} \sum_{J=1}^{n} (B_{IJ}\, H_J^{(t-\Delta t)}) + F'_{RI} + C_{RI} H_{RI} \qquad (2\text{-}146)$$

This essentially means that, when $J=I$, the quantity C_{RI} is added to the entry L_{II} on the left-hand side of the equation. In matrix form, this is equivalent to adding the quantities C_{RI} to the diagonal of the left-hand matrix [L] in Equation 2-137 and to adding the quantities $C_{RI}\, H_{RI}$ to right-hand vector {R} of Equation 2-137. Thus, Equation 2-146 can be re-expressed in matrix form as follows

$$(\{L\} + diag\{C_R\})\{H^{(t)}\} = \{R\} + diag\{C_R\}\{H_R\} \qquad (2\text{-}147)$$

Accordingly, in FEMFLOW3D, the quantities C_{RI} are referred to as the “left-hand coefficients” and the quantities $C_{RI}\, H_{RI}$ are referred to as the “right-hand coefficients.”

Several different conditions determine the values of C_{RI}. First, if water flows to the lower end of the reach associated with the node I in the finite-element grid, then C_{RI} is given by Equation 2-142 where L_I is the entire length of the reach. Second, if water does not flow to the lower end of the reach, then C_{RI} again is given by Equation 2-142, except that L_I is the wetted length of the reach. Third, if no flow occurs within the reach, then C_{RI} equals zero. Finally, if the groundwater at the node I is below the bottom of the river-bed thickness B'_I, then C_{RI} equals zero, but the coefficient F_I in Equation 2-143 is replaced by

$$F'_{RI} + C_{RI}[H_{RI} - (H_{BI} - B'_I)] \qquad (2\text{-}148)$$

where

H_{BI} = the elevation of the river channel at node I [L].

The quantity $(H_{BI} - B'_I)$ is equal to the elevation of the base of the river bed material [L]. In this condition, the left-hand side of Equation 2-137 is unchanged. The length L_I is always the wetted length of the reach. Furthermore, in this condition, the hydraulic connection between the river and

the groundwater system is broken. The recharge rate to the groundwater system from the river is independent of the hydraulic heads in the groundwater system. For the condition of hydraulic disconnection, the seepage through the river-bed material depends on the head differential across the river-bed material. The head at the upper surface of the river-bed material is the river-surface elevation H_{RI}. The head at the bottom surface of the river-bed material is defined based on the assumption of unit hydraulic gradient from the bottom surface to the groundwater table. With that assumption, the head equals the water-table elevation plus the distance from the water table to the bottom surface. However, the sum of these quantities equals the elevation of the bottom surface of the bed materials $(H_{BI} - B'_I)$.

2.16.2.2 Water Budget

In subroutine WRIVER3, the exchange of water between the river and the groundwater system through individual nodes in the finite-element grid is calculated from the expression

$$\{q_R\} = diag\{C_R\}\{H_R\} - diag\{C_R\}\{H(t)\} \quad (2\text{-}149)$$

where an element of $\{q_R\}$ is given by

$$q_{RI} = C_{RI}H_R - C_{RI}H_I \quad (2\text{-}150)$$

and where $\{q_R\}$ is a vector of inward discharges [L^3t^{-1}]. The cumulative discharge through all nodes is given by

$$Q_R = \sum_{I=1}^{n} q_{RI} \quad (2\text{-}151)$$

where Q_R is the cumulative discharge [L^3t^{-1}], and n is the number of nodes.

2.17 Subroutine WFAULT

2.17.1 Background

Subroutine WFAULT simulates groundwater flow in a two-dimensional fault plane within the three-dimensional finite-element mesh, including the exchange of water between the fault plane and the adjacent three-dimensional groundwater system. FEMFLOW3D can simulate faults in one of two modes. In the first, a fault acts as a barrier to transverse groundwater flow and may facilitate longitudinal flows. This mode is implemented by making the three-dimensional mesh for the groundwater system discontinuous across the fault. Correspondingly, the resistance to groundwater flow into or across the fault plane is represented by fault links that connect the fault plane to the adjacent groundwater system. In the second mode, a fault readily allows transverse groundwater flow and is a conduit for longitudinal flow. For this mode, the three-dimensional mesh for the groundwater system does not need to be discontinuous, but it can be if that is desired. However, the fault plane

simply can be superimposed within a continuous three-dimensional mesh. In either mode, FEMFLOW3D simulates two-dimensional flow within the fault plane.

Subroutine WFAULT is structured into three basic blocks. A call to entry point WFAULT1 reads in data on the physical characteristics of the fault plane and the links between the fault plane and the adjacent three-dimensional groundwater system. Entry point WFAULT2 creates the coefficients to be added to the matrices [*A*] and [*B*] in Equation 2-67. Entry point WFAULT3 calculates the actual groundwater discharge through the links between node pairs and the water budget for the faults.

2.17.2 Mathematical Basis

2.17.2.1 Finite-Element Formulation

Groundwater Flow Within Fault Plane

If the *x*-*y* plane of a Cartesian coordinate system is coincident with the fault plane, groundwater flow in the fault plane is described by the equation

$$\frac{\partial}{\partial x'}\left(T\frac{\partial h}{\partial x'}\right) + \frac{\partial}{\partial y'}\left(T\frac{\partial h}{\partial y'}\right) = S\frac{\partial h}{\partial t} \qquad (2\text{-}152)$$

where

x' = the x-coordinate coincident with the fault plane [L],
y' = the y-coordinate coincident with the fault plane [L],
T = the transmissivity of the fault plane [L^2t^{-1}],
S = the storage coefficient for the fault plane [L^0], and
h = the hydraulic head within the fault plane [L].

System of Linear Equations for Groundwater Flow Within Fault Plane

Recall that the following system of equations is solved by FEMFLOW3D for groundwater flow in a three-dimensional system

$$\left([A] + \frac{1}{\Delta t}[B]\right)\{H^{(t)}\} = \frac{1}{\Delta t}[B]\{H^{(t-\Delta t)}\} + \{F\} \qquad (2\text{-}153)$$

However, in this case the groundwater flow is through two-dimensional fault planes, rather than the three-dimensional groundwater system. The system of equations is slightly modified as follows

$$\left([A]' + \frac{1}{\Delta t}[B]'\right)\{H^{(t)}\}' = \frac{1}{\Delta t}[B]'\{H^{(t-\Delta t)}\} + \{F\}' \qquad (2\text{-}154)$$

where

$[A]'$ = the coefficients related to the geometry and transmissivity of the fault plane, as compared to matrix [A],
$[B]'$ = the coefficients related to the geometry and storage coefficient of the fault plane,
$\{H^{(t)}\}'$ = the vector of unknown heads calculated at the current time-step t for the fault plane [L],
$\{H^{(t-\Delta t)}\}'$ = the vector of unknown heads calculated at the last time-step t-1 for the fault plane [L],
$\{F\}'$ = the head-dependent water exchanges between the fault plane and the groundwater system, but note that FEMFLOW3D does not provide for assigning recharge or discharge directly to or from the fault plane,
t = the current time [t], and
Δt = the change in time between time steps [t].

Thus, when fault planes are specified, FEMFLOW3D not only has to populate matrices $[A]$ and $[B]$ in Equation 2-153, but also has to populate matrices $[A]'$ and $[B]'$ in Equation 2-154. Furthermore, FEMFLOW3D not only has to solve for unknown $\{H^{(t)}\}$, but it also has to solve for the additional unknown $\{H^{(t)}\}'$.

To solve for the new vector of unknowns introduced by fault, Equation 2-153 and Equation 2-154 can be combined to yield the system of equations

$$\left(\begin{bmatrix}[A] & [0]\\ [0] & [A]'\end{bmatrix} + \frac{1}{\Delta t}\begin{bmatrix}[B] & [0]\\ [0] & [B]'\end{bmatrix}\right)\begin{Bmatrix}\{H^{(t)}\}\\ \{H^{(t)}\}'\end{Bmatrix} = \frac{1}{\Delta t}\begin{bmatrix}[B] & [0]\\ [0] & [B]'\end{bmatrix} + \begin{Bmatrix}\{F\}\\ \{F\}'\end{Bmatrix} \qquad (2\text{-}155)$$

Discharge Equations for Groundwater Flow Between Fault Plane and Three-Dimensional Groundwater System

Although Equation 2-155 governs flow of groundwater within the fault plane, it does not represent the exchange of groundwater between the fault plane and the adjacent three-dimensional groundwater system. This connectivity is described by creating a link between a node within the fault plane and a node in the groundwater system. In this simulation, the outflow from the first node is equal to the inflow to the second node. The exchange of water between the node I in the fault plane and node J in the three-dimensional groundwater system can be described by the relation

$$q_I = C_F(H_J - H_I), \qquad (2\text{-}156)$$

$$q_J = -C_F(H_J - H_I), \qquad (2\text{-}157)$$

where

q_I = the groundwater outflow at node I, which lies in the fault plane [Lt^{-1}],
q_J = the groundwater inflow at node J, which lies in the three-dimensional groundwater system [Lt^{-1}],

C_F = the coefficient representing the leakance of the link between nodes I and J, as assigned by the user [L^2t^{-1}],
H_I = the hydraulic head at node I in the fault plane [L], and
H_J = the hydraulic head at node J in the adjacent groundwater system [L].

Because the discharge q_J represents the exchange of groundwater out of node I in the fault plane, we can substitute Equation 2-156 for $\{F\}'$ in Equation 2-155. Likewise, because the discharge q_J represents the exchange of groundwater into node J in the three-dimensional groundwater system, we can substitute Equation 2-157 for $\{F\}$ in Equation 2-155. The resulting equation for the I-J node-pair at time-step t is:

$$\left(\begin{bmatrix}[A] & [0]\\ [0] & [A]'\end{bmatrix} + \frac{1}{\Delta t}\begin{bmatrix}[B] & [0]\\ [0] & [B]'\end{bmatrix}\right)\begin{Bmatrix}\{H^{(t)}\}\\ \{H^{(t)}\}'\end{Bmatrix} = \frac{1}{\Delta t}\begin{bmatrix}[B] & [0]\\ [0] & [B]'\end{bmatrix} + \begin{Bmatrix}\{H^{(t-\Delta t)}\}\\ \{H^{(t-\Delta t)}\}'\end{Bmatrix} + \tag{2-158}$$

$$\begin{Bmatrix}\{-C_F(H^{(t)} - H'^{(t)})\}\\ \{C_F(H^{(t)} - H'^{(t)})\}\end{Bmatrix}$$

Multiplying through the right-hand term in Equation 2-158 and rearranging the equation to bring the coefficients of both unknowns $H^{(t)}$ and $H'^{(t)}$ to the left-hand side yields the following equation.

$$\left(\begin{bmatrix}[A] + diag\{C_F\} & diag\{-C_F\}\\ diag\{-C_F\} & [A]' + diag\{C_F\}\end{bmatrix} + \frac{1}{\Delta t}\begin{bmatrix}[B] & [0]\\ [0] & [B]'\end{bmatrix}\right)\begin{Bmatrix}\{H^{(t)}\}\\ \{H^{(t)}\}'\end{Bmatrix} = \tag{2-159}$$

$$\frac{1}{\Delta t}\begin{bmatrix}[B] & [0]\\ [0] & [B]'\end{bmatrix} + \begin{Bmatrix}\{H^{(t-\Delta t)}\}\\ \{H^{(t-\Delta t)}\}'\end{Bmatrix} + \begin{Bmatrix}\{F\}\\ \{F\}'\end{Bmatrix}$$

Orientation of Fault Plane

A triangular element representing part of a fault plane can have any orientation in three-dimensional space. The application of the finite-element method to Equation 2-152 requires integrations over the fault plane to generate the coefficients of $[A]'$ and $[B]'$ based on the relations

$$A'_{IJ} = \int_A T\frac{\partial\phi_J}{\partial x}\frac{\partial\phi_I}{\partial y}\,d\omega \tag{2-160}$$

and

$$B'_{IJ} = \int_A S\phi_J\phi_I\,d\omega \tag{2-161}$$

where

ϕ = one linearly independent interpolating function defined over the area of the fault plane [L^0],
T = the transmissivity of the fault plane [L^2t^{-1}], and
S = the storage coefficient for the fault plane [L^0].

and where x and y are coordinates and the x-y plane is coincident with the fault plane.

Surface Integrations

Surface integrations, rather than volume integrations, are performed when fault planes have been identified in the finite-element mesh. Recall that the elements of a fault plane are two-dimensional triangular elements, rather than three-dimensional tetrahedral elements. Surface integrations over the flow domain involve the second right-hand term of Equation 2-37. The interpolating function for the node I is given by the relation (Zienkiewicz, 1988)

$$\phi_I^e = \frac{1}{2A}(a_I + b_I x' + c_I y') \qquad (2\text{-}162)$$

where

ϕ_I^e = the elemental interpolating function defined only within the element e [L^0],
A = the area of the element [L^2],
x' = a local coordinate in the plane of the triangular element [L],
y' = a local coordinate in the plane of the triangular element [L],
a_I = the intercept coefficient of the function [L^2],
b_I = the slope coefficient of the function in the direction x' [L^1], and
c_I = the slope coefficient of the function in the direction y' [L^1].

The local coordinate axes lie within the plane of the triangular element, and the z' axis is the outward-pointing normal. The orientation and origin of the coordinate system within that plane can be assigned arbitrarily. Because the normal to boundary surface of the flow domain changes direction over the surface, the local coordinates system must be redefined for each triangular element on the surface.

The coefficient and area within Equation 2-162 are given by the relations (Zienkiewicz, 1988)

$$a_I = \begin{vmatrix} x'_J & y'_J \\ x'_M & y'_J \end{vmatrix}, \qquad (2\text{-}163)$$

$$b_I = -\begin{vmatrix} 1 & y'_J \\ 1 & y'_M \end{vmatrix}, \qquad (2\text{-}164)$$

$$c_I = \begin{vmatrix} x'_J & 1 \\ x'_M & 1 \end{vmatrix}, \tag{2-165}$$

and

$$2A = \begin{vmatrix} 1 & x'_I & y'_I \\ 1 & x'_J & y'_J \\ 1 & x'_M & y'_M \end{vmatrix}, \tag{2-166}$$

and

The indexes *I*, *J*, and *M* are the nodal numbers for a triangular element. The ordering of nodal numbers must follow the right-hand rule, that is, the nodes are numbered in a counter-clockwise direction when viewed from above the plane of the triangle.

Now the integrations represented by Equations 2-160 and 2-161 are given by

$$\int_e T \frac{\partial \phi_I^e}{\partial x} \frac{\partial \phi_J^e}{\partial x} d\omega = T \frac{b_I b_J}{4A} \tag{2-167}$$

$$\int_e T \frac{\partial \phi_I^e}{\partial y} \frac{\partial \phi^e}{\partial y} d\omega = T \frac{c_I c_J}{4A} \tag{2-168}$$

$$\int_e S \phi_I^e \, \phi_J^e \, d\omega = \frac{SA}{12} \quad \text{for } I \neq J \tag{2-169}$$

$$\int_e S \phi_I^e \, \phi_J^e \, d\omega = \frac{SA}{6} \quad \text{for } I = J \tag{2-170}$$

The integrations represented in Equations 2-160 and 2-161 must be calculated in the plane of the triangular element. This is accomplished by first describing the triangular element in the local *x-y-z* coordinate plane and performing the required integrations, and then performing a rotation using vector algebra.

A triangular element is defined by the coordinates of the nodes at the three respective vertices. Consider the points, P_1 (x_1, y_1, z_1), P_2 (x_2, y_2, z_2), and P_3 (x_3, y_3, z_3), which are the vertices in the counter-clockwise direction when the triangular element is viewed in three-dimensional space from

the appropriate side. When viewed from one side of the element, P_1, P_2, and P_3, will occur in a counter-clockwise order. However, when viewed from the other side, they will occur in a clockwise order. The counter-clockwise view is obtained when looking backward along a vector normal to the plane that is defined by the cross product

$$\vec{C} = \vec{A} \times \vec{B} \tag{2-171}$$

where

$$\vec{A} = \overrightarrow{P_1 P_2} \tag{2-172}$$

which is a vector from P_1 to P_2, and where

$$\vec{B} = \overrightarrow{P_1 P_3} \tag{2-173}$$

which is a vector from P_1 to P_3.

The vectors $\vec{A}$ and $\vec{B}$ can be used to determine the coordinates of P_1, P_2, and P_3 within an $x' - y'$ coordinate system that is in the plane of the triangular element. In this system, the origin is at P_1 and the x' axis is coincident with the vector $\vec{A}$. Correspondingly, the coordinates of P_1 are $P_1(0,0)$, and the coordinates of P_2 are P_2 (|A|,0) where

$$|A| = \sqrt{(x_2 - x_1)^2 + (y_2 - y_1)^2 + (z_2 - z_1)^2} \ . \tag{2-174}$$

The coordinates of P_3 are derived from the dot product of vectors $\vec{A}$ and $\vec{B}$, or

$$\vec{A} \bullet \vec{B} = \left|\vec{A}\right|\left|\vec{B}\right| \cos\theta \tag{2-175}$$

where θ is the angle between $\vec{A}$ and $\vec{B}$ in the plane defined by $\vec{A} \times \vec{B}$. The angle θ is given in turn by the expression

$$\cos\theta = \frac{(x_2 - x_1)(x_3 - x_1) + (y_2 - y_1)(y_3 - y_1) + (z_2 - z_1)(z_3 - z_1)}{|A||B|} \tag{2-176}$$

and

$$\theta = \cos^{-1}(\cos\theta) \tag{2-177}$$

where

$$|B| = \sqrt{(x_3 - x_1)^2 + (y_3 - y_1)^2 + (z_3 - z_1)^2} \ . \tag{2-178}$$

Correspondingly, the coordinates of P_3 are P_3 (|B|cosθ, |B|sinθ).

2.17.2.2 Water Budget

At entry point WFAULT3, the discharge of groundwater through fault-node pairs is calculated from the expression

$$\{q_F\} = diag\{C_F\}\{H\}' - diag\{C_F\}\{H\} \quad (2\text{-}179)$$

with respect to the groundwater system where

q_F = the discharge from the fault to the adjacent groundwater system [L^3t^{-1}],
C_F = the leakance of the link between the fault and the adjacent groundwater system [L^2t^{-1}],
H' = the calculated head in the fault [L], and
H = the calculated head in the adjacent groundwater system [L].

An element of $\{q_F\}$ is given by

$$q_{FI} = C_{FI}H_{FI} - C_{FI}H_{GI} \ . \quad (2\text{-}180)$$

The cumulative discharge through all nodes is given by

$$Q_F = \sum_{I=1}^{n} q_{FI} \ , \quad (2\text{-}181)$$

where

Q_F is the cumulative discharge [L^3t^{-1}], and n is the number of nodes.

2.18 Subroutine PACK

2.18.1 Background

Subroutine PACK is called by each subroutine that creates coefficients for the matrices in the linear system of equations described by Equation 2-68. Subroutine PACK is executed in two basic blocks. A call to entry point PACK1 creates the structures for the matrices. Entry point PACK2, which is called by WPARAMS2, WCHEAD2, WFLUX2, WFAULT2, WEVAP2, and WRIVER2, actually populates the matrices with coefficients that are calculated by the calling routines.

2.18.2 Mathematical Basis

FEMFLOW3D employs a compressed storage scheme for matrices [*A*] and [*B*]. The non-zero coefficients of the matrices are stored row-by-row in a vector format. This storage scheme is implemented using three FORTRAN one-dimensional arrays. For the matrix [*A*], the real one-dimensional array *A*( ) contains the non-zero coefficient values. The integer one-dimensional

array *JA*( ) identifies the column number for each element in the real array *A*( ), and the integer one-dimensional array *IA*( ) identifies the element in the array *JA*( ) representing the first non-zero column in a row. The storage scheme can be demonstrated by considering the simple matrix

$$[A] = \begin{bmatrix} a_{11} & a_{12} & 0 & 0 \\ a_{21} & a_{22} & a_{23} & 0 \\ 0 & a_{32} & a_{33} & a_{34} \\ 0 & 0 & a_{43} & a_{44} \end{bmatrix}, \tag{2-182}$$

which contains $n = 4$ rows and $m = 10$ non-zero coefficients. For this matrix, the vector *A*( ) has *m* elements as given by

$$A( ) = \{a_{11}, a_{12}, a_{21}, a_{22}, a_{23}, a_{32}, a_{33}, a_{34}, a_{43}, a_{44}\}^T, \tag{2-183}$$

the vector *JA*( ) also has *m* elements as given by

$$JA( ) = \{1, 2, 1, 2, 3, 2, 3, 4, 3, 4\}^T, \tag{2-184}$$

and the vector *IA*( ) has $n + 1$ elements as given by

$$IA( ) = \{1, 3, 6, 9, 11\}^T . \tag{2-185}$$

Correspondingly, the starting position of the *I*-th row in *JA*( ) and *A*( ) is *IA*(*I*), and the ending position of the row is *IA*(*I*+1) - 1. For the last row, the ending position is *IA*(*n* +1) – 1. Subroutine PACK is used within FEMFLOW3D to assemble the arrays *A*( ), *JA*( ), and *IA*( ).

2.18.2.1 Constructing Structures of Matrices [A] and [B]

Entry point PACK1 is called by subroutine WFLOW1. PACK1 creates the structure of the matrices [*A*] and [*B*] in the system of linear equations described by Equation 2-68. The structure of matrices [*A*] and [*B*] is determined strictly from the topology of the finite-element mesh, and not on any groundwater flow parameters. Specifically, PACK1 assembles the arrays *JA*( ) and *IA*( ) based on the element incidences specified by user inputs with calls to ELEMS, WFLUX1 and WFAULT1. The element incidences specify the nodes associated with either a three-dimensional tetrahedral aquifer element, a one-dimensional well-link element, a two-dimensional triangular fault element, or a one-dimensional fault-link element. These element incidences all are stored in the array *IN2*( ), which contains four, three, or two node specifications for an element depending on whether the element is three-, two, or one-dimensional. The array *IN2*( ) represents a collection of incident sets, where each member of the collection in turn represents the element nodes for a particular element. Subroutine PACK1 constructs *JA*( ) for row *I* such that the set of columns for the row is the union of all the incident sets containing node *I*.

2.18.2.2 Populating Matrices [A] and [B]

PACK2 is called by subroutines WPARAMS2, WCHEAD2, WFLUX2, WFAULT2, WEVAP2, and WRIVER2, all of which calculate the values for the coefficients of matrices [*A*] and [*B*] in the system of linear equations described by Equation 2-68. Once the relevant coefficient values are calculated, PACK2 is used to populate matrices [*A*] and [*B*] with these coefficients. Specifically, PACK2 inserts the coefficient values into the array *A*( ).

2.19 Subroutine WSHAPE

2.19.1 Background

Subroutine WSHAPE includes subroutines WSHAPE1, WSHAPE2, and WSHAPE3. WSHAPE1, WSHAPE2, and WSHAPE3 are called by various subroutines to perform necessary integrations that determine the values of the coefficients in matrices [*A*] and [*B*] and vector {*F*} in Equation 2-68. WSHAPE1 is called by WPARAMS2, WSHAPE2 is called by WFAULT2, and WSHAPE3 is called by WFLUX2.

2.19.2 Mathematical Basis

As explained in detail in Section 2.9, FEMFLOW3D solves the following system of linear equations

$$[A]\{H\} + [B]\left\{\frac{dH}{dt}\right\} = \{F\} \tag{2-186}$$

where the typical elements of the matrices [*A*] and [*B*] and the vector {*F*}are

$$A_{IJ} = \int_{\Omega}\left(K_{ij}\frac{\partial\phi_J}{\partial x_i}\frac{\partial\phi_I}{\partial x_j}\right)d\omega\ , \tag{2-187}$$

$$B_{IJ} = \int_{\Omega} S\phi_J\phi_I d\omega\ , \tag{2-188}$$

$$F_I = \int_{\Omega} W\phi_J\, d\omega + \int_{\Gamma} q_B\phi_J\, d\varphi\ , \tag{2-189}$$

$$A'_{IJ} = \int_{\Gamma} T\frac{\partial\phi_J}{\partial x'}\frac{\partial\phi_I}{\partial y'}\, d\lambda\ , \tag{2-190}$$

and

$$B'_{IJ} = \int_{\Gamma'} S\phi_J \phi_I d\lambda \qquad (2\text{-}191)$$

for I = 1,2, ..., n, J = 1,2, ..., n, i = 1,2,3, and j = 1,2,3, and where

K_{ij} = a component of the hydraulic conductivity tensor [Lt^{-1}],
S = the storage coefficient [L^{-1}],
W = the source injection rate per unit volume [t^{-1}],
Ω = the volume of three-dimensional flow domain [L^3],
Γ = the boundary surface of the three dimensional flow domain Ω [L^2],
Γ' = the surface of faults [L^2],
q_B = the inward flux normal to the surface Γ [Lt^{-1}], and
ϕ = linearly independent interpolating functions defined over the volume of three-dimensional flow domain Ω [L^0].

WSHAPE1, which is called from subroutine WPARAMS1, calculates these integrals for tetrahedral elements in the finite-element mesh. WSHAPE2, which is called from subroutine WFAULT2, calculates these integrals for triangular elements in the finite-element mesh. Triangular elements result from the definition of fault-planes in the mesh. WSHAPE3, which is called from subroutines WFAULT2 and WFLUX2, calculates these integrals for one-dimensional elements in the finite-element mesh. In WFLUX2, one-dimensional elements represent links connecting a node in a well to multiple nodes in the groundwater system. In WFAULT2, the one-dimensional elements represent links that connect fault nodes to multiple nodes in the groundwater system.

3.0 INPUT FILE FORMATS

For each of the subroutines below, variables identified with parentheses (e.g., "NPT( )") represent arrays, and variables identified without parentheses (e.g., "FTYPE") represent scalar values. Additionally, Tables 3-1 through 3-13 indicates the file format for the respective subroutine and file.

3.1 Subroutine SETFILES

File Type Identifier: SUP or FLS
Record Formats:

Table 3-1
File Structure for Subroutine SETFILES
File Type SUP

Record	Condition	Variables Read
1		RNAME
2		FTYPE,FNAME Repeat record for each required and optional file.

Record	Columns	Type	Variable	Definition
1	1-12	A12	RNAME1	Name of simulation.
2	1-3	A3	FTYPE	File type identifier for input file.
	10-69	A60	FNAME()	Input file name.

Notes:

1. The character string RNAME1 is used to construct automatically the names of output files. The constructed file names are created by adding an extension to RNAME1. Correspondingly, RNAME1 can include only those characters that can be used in a file name.

2. Record 2 is repeated for each input file to create a list of input files. File list is terminated with an additional occurrence of Record 1 with FTYPE = END and FNAME = blank.

3. For both the flow and transport models, file types BAS, XYZ, ELE, PAR, INT, and HED must appear in file list. The associated files respectively represent inputs of basic simulation parameters, node coordinates, element incidences, aquifer properties, initial heads, and head output control. The files may occur in any order and file types should be in Upper Case.

4. For both the flow and transport models, other file types occur in the list only if the associated subroutine is to be used in simulation. The additional file types are CHD, FLX, GET, RIV, FLT, and FNT. The associated files respectively represent specified heads, specified fluxes, groundwater evapotranspiration, stream-aquifer interactions, faults, and initial fault heads. The files may occur in any order.

3.2 Subroutine BASIC

File Type Identifier: BAS
Record Formats:

Table 3-2
File Structure for Subroutine BASIC
File Type BAS

Record	Condition	Variables Read
1		TITLE1
2		TITLE2
3		NCELL
4		CNAME Repeat NCELL times.
5		NITER, CONV, DMIN,SHAPE,RFACT
6		ISOLVE1, ISOLVE2, ISS, IMATRIX,ICHECK
7	ISOLVE1=1	NITER, OMEGA, CONV, NOUT
8	ISOLVE1=2	ITMAX, EPS, LEVEL
9	ISOLVE1=3	IDEFAULT
10	ISOLVE1=3 and IDEFAULT=0	IOUT, LEVELX, NCYC1, NCYC2, NCYC3, NCYC4, EPS
11		ISTEP1, ISTEP2, STIME0
12		NSTRESS
13		TIME, FDELT, NSTEP, NTRAN Repeat NSTRESS times.
14		NPRINT
15		IPRINT Repeat NPRINT times five values per record.
16		NPLOT
17		IPLOT Repeat NPLOT times five values per record.

Record	Columns	Type	Variable	Definition
1	1-80	A80	TITLE1	Primary title of simulation.
2	1-80	A80	TITLE2	Secondary title of simulation.
3	1-10	I10	NCELL	Number of compartments.
4	1-20	A20	CNAME()	Compartment name.
5	1-10	I10	NITER	Number of time-step iterations.
	11-20	F10.0	CONV	Convergence criteria for time-step iterations (L).
	21-30	F10.0	DMIN	Under-relaxation factor for solver minimum value (L^0).
	31-40	F10.0	SHAPE	Under-relaxation shape factor (L^0).
	41-50	F10.0	RFACT	Factor for reducing DMIN (L^0).
6	1-10	I10	ISOLVE1	Switch for selection of solver type for flow component of model.
	11-20	I10	ISOLVE2	Switch for selection of solver type for transport component of model.
	21-30	I10	ISS	Switch for steady state at first time step.
	31-40	I10	ITRAN	Switch for transport simulation.
	41-50	I10	IMATRIX	Switch for input or output of matrix structure.
	51-60	I10	ICHECK	Switch for input checking only.
7	1-10	I10	NITER	Number of solver iterations.
	11-20	F10.0	OMEGA	Over-relaxation factor for solver (L^0).
	21-30	F10.0	CONV	Convergence criteria for solver iterations (L).
	41-50	I10	NOUT	Interval between outputs from solver iterations.
8	1-10	I10	ITMAX	Maximum number of solver iterations.
	11-20	F10	EPS	Convergence criteria for solver iterations (L).
	21-30	I10	LEVEL	Switch for level of output detail on solver progress.
9	1-10	I10	IDEFAULT	Switch to set AMG solver input variables.
10	11-20	I10	IOUT	Switch for output control.
	21-30	I10	LEVELX	Maximum number of multigrid levels.
	31-40	I10	NCYC1	Switch for cycle type.
	41-50	I10	NCYC2	Switch for using conjugate gradient.
	51-60	I10	NCYC3	Switch for closure criterion type.
	61-70	I10	NCYC4	Maximum number of cycles.
	71-80	F10.0	EPS	Closure criterion.
11	1-10	I10	ISTEP1	Starting time step for simulation.
	11-20	I10	ISTEP2	Ending time step for simulation.
	21-30	F10.0	STIME0	Starting elapsed time for simulation (t).
12	1-10	I10	NSTRESS	Number of stress periods.
13	1-10	F10.0	TIME	Duration of stress period (t).

Record	Columns	Type	Variable	Definition
	11-20	F10.0	FDELT	Acceleration factor for time steps within stress period (L^0).
	21-30	I10	NSTEP	Number of time steps within stress period.
	31-40	I10	NTRAN	Number of transport steps within flow step.
14	1-10	I10	NPRINT	Number of steps with print output.
15	1-50	5I10	IPRINT	Flags steps with print output.
16	1-10	I10	NPLOT	Number of steps with plot output.
17	1-50	5I10	IPLOT	Flags steps with plot output.

Notes:

1. Record 4 is repeated for NCELL compartment names.

2. Record 11 is repeated for NSTRESS stress periods.

3. NITER = 1 if no time-step iterations are required. That is the case for a simulation with no deforming mesh, only specified-flux nodes, bi-directional specified-head nodes, or faults. With this limitation, the simulation is linear.

4. The value of ISOLVE1 can be 1, 2, or 3 depending on the solver method. ISOLVE1 = 1 for the point over-relaxation method. ISOLVE1 = 2 for the conjugate-gradient method. ISOLVE1 = 3 for the multi-grid method. If ISOLVE1 = 1, Records 8, 9 and 10 are omitted. If ISOLVE1 = 2, Records 7, 9 and 10 are omitted. If ISOLVE1 = 3, Records 7 and 8 are omitted.

5. ISOLVE1 = 3 and IDEFAULT = 0 will pass arguments in Record 10 to the solver. If ISOLVE1 = 3 and IDEFAULT = 1, default multi-grid arguments will be used, and Record 10 is omitted. The default parameters work well for many large-scale simulations. If the default parameters are not adequate, Mehl and Hill (2001) give guidance on the selection of alternative parameter values.

6. ISS = 1 for the calculation of steady-state heads at the first time step, which is when the time-step number equals ISTEP1 in Record 11. Otherwise, ISS = 0. This switch is used to create a transient-state simulation that starts with a computed steady state.

7. The under-relaxation acceleration factor must be within the range $0 < DMIN \leq 1$. The value for DMIN within this range depends greatly on the linearity of the problem, with DMIN approaching 1 for more linear problems. A value of 0.5 is a good starting point.

8. The reduction factor RFACT reduces DMIN if divergence occurs between two iterations. RFACT must be within the range $0 < RFACT < 1$. A value of 0.7 is a good starting point.

9. The under-relaxation shape factor SHAPE instructs the program to relax the under-relaxation by a certain factor in order to allow the results to converge more quickly on the convergence criteria CONV. SHAPE typically results in reasonably quick convergence within the range 2 ≤ SHAPE ≤ 10. A value of 2 is a good starting point.

10. The over-relaxation acceleration factor must be within the range 0 < OMEGA < 2. For the flow component of the model, the optimal factor usually is within the range 1.6 < OMEGA <1.85.

11. A simulation can start a time step either equal to or greater than 1, and it can end at a time step equal to or less than the maximum number of steps. The initial time step ISTEP1 can be in the range 1 ≤ ISTEP1 ≤ ISTEP2. The final time step ISTEP2 can be in the range ISTEP1 ≤ ISTEP2 ≤ Σ MSTEP().

12. The quantity STIME0 sets the initial elapsed time for the simulation. The elapsed time at any point in the simulation is given by the relation t^k = STIME0 + $\sum_{i=1}^{k} \Delta t_i$, where t is the elapsed time at the k-th time step and Δt is a time step. The value of STIME0 should be specified so as to preserve the match between the elapsed time at each time step and the elapsed time use in specified-head, specified-flux, groundwater evapotranspiration, and streamflow tables in subroutines WCHEAD, WFLUX, WEVAP, and WRIVER. To maintain that match, the value of the initial elapsed time will depend on the initial time step as specified by ISTEP1.

13. The IMATRIX switch is used either to write the vectors JA() and IA() to a file or read them from a file. If the vectors are input, the execution time for FEMFLOW3D can be reduced, especially for large-scale simulations. However, the vectors cannot be input unless they have been saved from a previous simulations. These vectors identify respectively the column numbers for the non-zero coefficients in the rows of a matrix and the number of non-zero coefficients in each row (see Section 2.8). For large scale simulations, considerable computational effort can be required to generate the vectors JA() and IA(). However, these vectors depend only on the assignment of nodes to elements (see Section 2.8), and the vectors only need to be created once, if they are saved to a file for future use. If IMATRIX = 1, a file is saved with a name RNAME1 (see Section 3.1) and an extension .PAK. If IMATRIX = 2, the file is read to retrieve the previously saved vectors JA() and IA(). However, the file must be listed in the SUP or FLS file with the file type identifier PAK (see Section 3.1).

14. The ICHECK switch is used to check all of the model input files. If ICHECK equals “1”, then model input files will be checked and no model run will be completed. If ICHECK equals “0”, no checking will be completed and the model will be run.

15. The switch LEVEL in Record 8 can have the values 1, 2, or 3. LEVEL = 1 produces the least detail, and LEVEL = 3 produces the most detail.

3.3 Subroutine NODES

File Type Identifier: XYZ
Record Formats:

Table 3-3
File Structure for Subroutine NODES
File Type XYZ

Record	Condition	Variables Read
1		XCNAME Repeat Records 1-3 as group for each compartment.
2		NNC, FACX, FACY, FACZ, IECHO1
3		Blank, X, Y, Z Repeat NNC times.
4		XCNAME Repeat Records as a group for each compartment.
5		NC, NMAX, IECHO2
6		ZMIN, ZMAX, COL, COL **…** Continue values of COL until all entered for node column, but not more than 20 values are allowed. Repeat record NC times.

Record	Columns	Type	Variable	Definition
1	1-20	A20	CNAME	Compartment name.
2	1-10	I10	NNC()	Number of nodes in compartment.
	11-20	F10.0	FACX	Factor for scaling *x*-coordinate (L^0).
	21-30	F10.0	FACY	Factor for scaling *y*-coordinate (L^0).
	31-40	F10.0	FACZ	Factor for scaling *z*-coordinate (L^0).
	41-50	I10	IECHO1	Switch for echo on coordinate inputs.
3	1-10	10X	Blank	Can be used to enter node number, but is not read because the node numbers are assumed to be sequential.
	11-20	F10.0	X()	*X*-coordinate of right-hand Cartesian coordinate system (L).
	21-30	F10.0	Y()	*Y*-coordinate (L).
	31-40	F10.0	Z()	*Z*-coordinate measured positive upward (L).
4	1-20	A20	CNAME	Compartment name.
5	1-10	I10	NC	Number of node columns.
	11-20	I10	NMAX	Maximum number of nodes in columns.
	21-30	I10	IECHO2	Switch for echo of collapsing mesh.
6	1-10	F10.0	ZMIN()	Minimum distance between collapsed nodes.
	11-20	F10.0	ZMAX()	Maximum elevation of top node.
	21-220	20I10	COL()	Column node number.

Notes:

1. Records 1 through 3 are repeated for each compartment. The compartments must be in the same order as identified in the inputs to subroutine BASIC.

2. Record 3 is repeated for the NNC() nodes in the compartment.

3. Columns 1-10 within Record 3 can be used to indicate the node number. However, that field is not read because the coordinates are assumed to be sequential by node. In other words, the first occurrence of Record 3 represents node number 1, the second occurrence represents node number 2, and so on. The node numbering restarts with 1 for each compartment. This is the "local" node numbering. The "global" numbering is sequential across all the compartments.

4. The scaling factors FACX, FACY, and FACZ can be used to transform the measurement units expressed in Record 3. The scaling factors are multipliers that are applied to the coordinates within a compartment.

5. The three-dimensional coordinate system must be orthogonal and right handed, with the *z*-coordinate positive upward. For example, if the *x*-coordinate is positive eastward, the *y*-coordinate must be positive northward. More generally, looking down on the *x*-*y* plane, the positive *y*-axis must be 90 degrees counter-clockwise from the positive *x*-axis.

6. Records 4 through 6 are repeated for each compartment. The compartments must be in the same order as identified in the inputs into subroutine BASIC. Figure 3-1 shows the layout of node columns used to deform the finite-element mesh, which shows the example of a collapsed mesh. ZMIN is the minimum spacing maintained between adjacent nodes when the mesh is collapsed. If the mesh were to be expanded, ZMAX is the maximum elevation of the top node. The variable COL is assigned the node numbers in the column in downward order, where COL = {10, 20, 14, 6} in the figure.

7. Record 6 is repeated for the NC columns in the compartment. If NC = 0, then Record 8 is omitted.

8. ZMIN should be small enough to remove the hydrologic unit from the simulation by collapsing the grid. However, ZMIN should be big enough to allow numerical problems to continue. ZMAX is equal to the top node in the column of nodes. COL is the series of nodes and must start at the top node of the grid and proceed down.

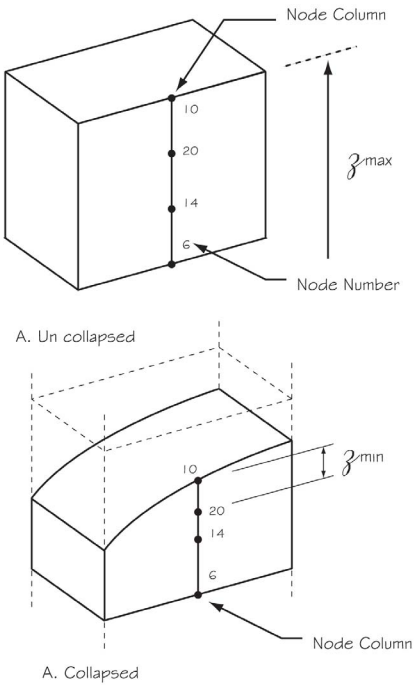

Figure 3-1
Collapsing Mesh Diagram

3.4 Subroutine ELEMS

File Type Identifier: ELE
Record Formats:

Table 3-4
File Structure for Subroutine ELEMS
File Type ELE

Record	Condition	Variables Read
1		IMESH
2		XCNAME Repeat Records 2-3 as a group for each compartment.
3		NEC, IECHO1, IECHO2
4		Blank, IN(,1), IN(,2), IN(,3), IN(,4), IN(,5), IN(,6), MAT Repeat record NEC times.

Record	Columns	Type	Variable	Definition
1	1-10	I10	IMESH	Switch for output of GMS 3dm file.
2	1-20	A20	CNAME	Compartment name.
3	1-10	I10	NEC()	Number of elements in compartment.
	11-20	I10	IECHO1	Switch for output of wedge elements.
	21-30	I10	IECHO2	Switch for output of tetrahedral elements.
4	1-10	10X	Blank	Can be used to enter element numbers, but is not read because the element numbers are assumed to be sequential.
	11-20	I10	IN(,1)	First top node of element.
	21-30	I10	IN(,2)	Second top node of element.
	31-40	I10	IN(,3)	Third top node of element.
	41-50	I10	IN(,4)	First bottom node of element.
	51-60	I10	IN(,5)	Second bottom node of element.
	61-70	I10	IN(,6)	Third bottom node of element.
	71-80	I10	MAT()	Material identifier for element material.

Notes:

1. Records 2 through 4 are repeated for each compartment. The compartments must be in the same order as identified in the inputs to subroutine BASIC.

2. Record 4 is repeated for NEC() elements within the compartment.

3. Columns 1-10 within Record 4 can be used to indicate the element number. However, that field is not read because the element incidences are assumed to be sequential by element. In other words, the first occurrence of Record 4 represents element number 1; the second occurrence represents element number 2, and so on. The element numbering restarts with 1 for each compartment. This is the “local” element numbering. The “global” numbering is sequential across all the compartments.

4. IN(,1) through IN(,6) for a particular element are referred to as the element incidences for the element. They identify the nodes, and hence the coordinates, that define the vertices of a wedge-shaped element. The elements are assumed to be oriented spatially such that triangular faces are generally subparallel with a horizontal plane. With this orientation, the element incidences are input first for the top nodes and then for the bottom nodes. Counter-clockwise around the top triangular face looking down, IN(,1) through IN(,3) represent the top nodes, and IN(,4) through IN(6,) represent the bottom nodes. The list of top nodes can start with any node

on the top face. However, the list of bottom nodes must start with the bottom node directly below the first listed top node.

5. Elements can be defined that have zero-height edges. Such elements are used to create the pinchout of a hydrogeologic unit. A wedge-shaped element that has one zero-height edge becomes a five-node pyramid, and a wedge-shaped element that has two zero-height edges becomes a four-node tetrahedron. If an element is to have one zero-height edge, IN(,6) = 0. Correspondingly, the listing of top nodes must start such that IN(,3) represents the top node on the zero-height edge. If an element is to have two zero-height edges, both IN(,5) = 0 and IN(,6) = 0. The listing of top nodes must start such that both IN(,2) and IN(,3) represent the top nodes on the zero-height edges.

6. IMESH is a switch for outputting 3dm files for input to GMS. If IMESH = 1, a global 3dm file is created that includes all the compartments. Additionally, a 2dm file is created for the fault planes. The nodes and elements within the files are represented by their global numberings. If IMESH = 0, neither a 3dm nor 2dm file is created. The material identifier MAT() in Record 4 is used in GMS to display individual hydrogeologic units.

7. MAT() is used only by GMS to give different colors to separate hydrogeologic units. MAT() is assigned an integer to each element comprising a hydrogeologic unit.

3.5 Subroutine WPARAMS

File Type Identifier: PAR
Record Formats:

Table 3-5
File Structure for Subroutine WPARAMS
File Type PAR

Record	Condition	Variables Read
1		XCNAME Repeat Records 1-5 as a group for each compartment.
2		NGROUP, FACKX, FACKY, FACKZ, FACSS, FACSY, IECHO1
3		LL1, LL2, XKX, XKY, XKZ, XSS, XSY, XTOP Repeat NGROUP times.
4		NGROUP, FAC1, FAC2, FAC3, IECHO2
5		LL1, LL2, XALPHA1, XALPHA2, XALPHA3 Repeat NFROUP times.

Record	Columns	Type	Variable	Definition
1	1-20	A20	CNAME	Compartment name.
2	1-10	I10	NGROUP	Number of parameter groups for compartment.
	11-20	F10.0	FACKX	Scaling factor for hydraulic conductivity along *x*-direction principal axis (L^0).
	21-30	F10.0	FACKY	Scaling factor for hydraulic conductivity along *y*-direction principal axis (L^0).
	31-40	F10.0	FACKZ	Scaling factor for hydraulic conductivity along *z*-direction principal axis (L^0).
	41-50	F10.0	FACSS	Scaling factor for specific storage (L^0).
	51-60	F10.0	FACSY	Scaling factor for specific yield (L^0).
	61-70	I10	IECHO1	Switch for echo of hydraulic parameters.
3	1-10	I10	LL1	First element number (local) within range for element group.
	11-20	F10.0	LL2	Last element number (local) within range for element group.
	21-30	F10.0	KX()	Hydraulic conductivity for element group along *x*-direction principal axis (Lt^{-1}).
	31-40	F10.0	KY()	Hydraulic conductivity for element group along *y*-direction principal axis (Lt^{-1}).
	41-50	F10.0	KZ()	Hydraulic conductivity for element group along *z*-direction principal axis (Lt^{-1}).
	51-60	F10.0	SS()	Specific storage for group (Lt^{-1}).
	61-70	F10.0	SY()	Specific yield for group (dimensionless).
	71-80	I10	ITOP	Flag to identify top element.
4	1-10	I10	NGROUP	Number of rotation groups for compartment.
	11-20	F10.0	FAC1	Scaling factor for strike (L^0).
	21-30	F10.0	FAC2	Scaling factor for rotation in dip plane (L^0).
	31-40	F10.0	FAC3	Scaling factor for dip (L^0).
	41-50	I10	IECHO2	Switch for echo of rotation inputs.
5	1-10	I10	LL1	First element number (local) within range for element group.
	11-20	I10	LL2	Last element number (local) within range for element group.
	21-30	F10.0	ALPHA1()	Counter-clockwise angle in *x*-*y* plane from *x*-coordinate axis to *x*-principal axis of hydraulic-conductivity tensor (degrees).

Record	Columns	Type	Variable	Definition
	31-40	F10.0	ALPHA2()	Counter-clockwise angle in vertical plane (i.e., plane perpendicular to *x*-*y* plane) from *x*-*y* plane to *x*-principal axis of hydraulic-conductivity tensor (degrees).
	41-50	F10.0	ALPHA3()	Counter-clockwise angle in plane perpendicular to *x*-principal axis of hydraulic-conductivity tensor from intersection with *x*-*y* plane to *y*-principal axis of hydraulic-conductivity tensor (degrees).

Notes:

1. Records 1 through 5 are repeated for each compartment. The compartments must be in the same order as identified in the inputs to subroutine BASIC.

2. Record 3 is repeated for NGROUP element groups for a compartment.

3. Record 5 is repeated for MGROUP orientation groups for a compartment.

4. The scaling factors FACKX, FACKY, FACKZ, FACSS, and FACSY can be used to transform measurement units. The scaling factors are multipliers that are applied to the respective parameters within a compartment. The scaling factors also can be used in model calibration to make compartment-wide adjustments to parameter values.

5. Hydraulic conductivities KX(), KY(), and KZ() represent the principal components of the hydraulic-conductivity tensor. The directions of the principal components need not be aligned with the coordinate system used to specify nodal coordinates. The rotation of the principal-component directions is specified in Record 5.

6. The principal *x, y,* and *z*-components of the hydraulic-conductivity tensor can be oriented in a different direction than the *x, y,* and *z*-coordinate axes. The orientation of the hydraulic-conductivity tensor with respect to the *x*-*y*-*z* coordinate system is specified by assigning values to ALPHA1(), ALPHA2(), and ALPHA3(). ALPHA1() is the counter-clockwise angle in the x-y plane from the x-coordinate axis to the x-principal axis of the hydraulic-conductivity tensor. ALPHA2() is the counter-clockwise angle in the vertical plane (i.e., plane perpendicular to x-y plane) from the x-y plane to the x-principal axis of hydraulic-conductivity tensor. ALPHA3() is the counter-clockwise angle in the plane perpendicular to the x-principal axis of the hydraulic-conductivity tensor from the intersection with the x-y plane to the y-principal axis of the hydraulic-conductivity tensor. If ALPHA2()= 0, ALPHA1() is the strike and ALPHA3() is the negative of the dip.

3.6 Subroutine WSTART

File Type Identifier: INT
Record Formats:

Table 3-6
File Structure for Subroutine WSTART
Record Type INT

Record	Condition	Variables Read
1		IGLOBAL, ISAVE, IWHEN, IECHO1
2	IGLOBAL=1	Blank, H Repeat H five times per record. Repeat record until values have been entered for the total number of nodes in all the compartments.
3	IGLOBAL=0	XCNAME Repeat Records 3-5 as a group for each compartment.
4	IGLOBAL=0	XNNC, ISTART, XH0, IECHO2
5	IGLOBAL=0 and ISTART=0	H Repeat H five times per record. Repeat record until values have been entered for XNNC values.

Record	Columns	Type	Variable	Definition
1	1-10	I10	IGLOBAL	Switch to input global initial heads from prior simulation.
	11-20	I10	ISAVE	Switch for overwriting global initial heads.
	21-30	I10	IWHEN	Step for overwriting global initial heads.
	31-40	I10	IECHO1	Switch for echo of global initial heads.
2	1-20	20X		
3	1-20	A20	CNAME	Compartment name.
4	1-10	I10	NNC	Number of nodes represented by initial heads for compartment.
	11-20	I10	ISTART	Switch for input of uniform initial heads for compartment.
	21-30	F10.0	XH0	Uniform initial head assigned to compartment (L).
	31-40	I10	IECHO1	Switch for echo of initial heads for compartment.
5	1-50	5F10.0	H()	Initial-head values for each node (L).
6	35-95	5F15.0	H()	Initial-head values for each node (L).

Notes:

1. Records 3 through 5 are repeated for each compartment. The compartments must be in the same order as identified in the inputs to subroutine BASIC.

2. Record 5 is skipped if ISTART = 1. Otherwise, Record 5 is repeated until NNC() nodal initial heads have been entered, entering five values per record. NNC() must equal the number of nodes in the compartment as specified for NNC() in subroutine NODES.

3. If ISTART = 0, the quantity XH0 is ignored.

4. IGLOBAL is a switch for entering the global initial heads. If IGLOBAL = 1, Records 3 through 5 are skipped, and the initial heads for all compartments are read as a continuous block based on Record 6. The total number of nodal heads read is Σ NNC(). If IGLOBAL = 0, the initial heads are entered separately for each compartment, and Record 6 is not used.

5. ISAVE is used to create a dataset of global initial heads representing time step IWHEN within the simulation. If ISAVE = 1, then the dataset is created. The data set overwrites the contents of the initial heads for the simulation. The dataset is written using the formats of Records 1 and 6.

3.7 Subroutine WOUTPUT

File Type Identifier: HED
Record Formats:

Table 3-7
File Structure for Subroutine WOUTPUT
File Type HED

Record	Condition	Variables Read
1		XCNAME Repeat Records 1-4 as a group for each compartment
2		NGPHC
3		NNODE, WNAME Repeat records 3-4 as a group NGPHC times.
4		WNODE, WEIGHT Repeat record NNODE times.

Record	Columns	Type	Variable	Definition
1	1-10	A20	CNAME	Compartment name.
2	1-10	I10	NGPHC	Number of hydrograph sites within compartment.
3	1-10	I10	NNODE()	Number of nodes associated with hydrograph site.
	12-21	A20	WNAME()	Name associated with hydrograph site.
4	1-10	I10	WNODEC()	Node number.
	11-20	F10.0	WEIGHT()	Nodal weight (L^0).

Notes:

1. Records 1 through 4 are repeated for each compartment. The compartments must be in the same order as identified in the inputs to subroutine BASIC.

2. Records 3 and 4 are repeated for NGPHC hydrograph sites within the compartment. If NGPHC = 0, Records 3 and 4 are omitted.

3. Record 4 is repeated for NNODE nodes for each hydrograph site. The weighting scheme is discussed in Section 2.12. The head for the hydrograph at a particular site is the weighted average head for the nodes associated with the site. The quantity WNODE() is a node number, and WEIGHT() is the weight given to the computed head at that node. Correspondingly, the hydrograph head at the site is given by the relation $H_t = \Sigma$ WEIGHT()h_t, where H_t is the weighted head at time t, h_t is the computed head at a node at time t, and the summation is over all the nodes associated with the hydrograph site. The weights for a site must sum to unity, or Σ WEIGHT() = 1.

4. See Figure 2-4 in Section 2.12.

3.8 Subroutine WCHEAD

File Type Identifier: CHD
Record Formats:

Table 3-8
File Structure for Subroutine WCHEAD
File Type CHD

Record	Condition	Variables Read
1		IECHO2
2		XCNAME Repeat Records 2-6 as a group for each compartment.
3		NCHNC, NTABC, IECHO1
4		CHNODE, CHBASE, LEAK,CHTAB, ITYPE, CHNAME Repeat record NCHNC times
5	NTABC>0	NPT, IGET Repeat Records 5-6 NTABC times.
6	NTABC>0	TTB, HTB Repeat record NPT times.

Record	Columns	Type	Variable	Definition
1	1-10	I10	IECHO2	Switch for time-step fluxes through specified-head nodes.
2	1-20	A20	CNAME	Compartment name.
3	1-10	I10	NCHNC	Number of specified-head nodes in compartment.
	11-20	I10	NTABC	Number of tables associated with compartment.
	21-30	I10	IECHO1	Switch for output of specified-head nodes.
4	1-10	I10	CHNODE()	Node number for specified-head node.
	11-20	F10.0	CHBASE()	Steady-state component of specified head (L).
	21-30	F10.0	LEAK()	Leakance for specified-head node (L^2t^{-1}).
	31-40	I10	CHTAB()	Table associated with node.
	41-50	I10	ITYPE()	Switch for flux conditions allowed.
	51-71	1X,A20	CHNAME()	Name associated with specified-head node.
5	1-10	I10	NPT()	Number of points in specified-head table.
	11-20	I10	IGET()	Switch for interpolation method.
6	1-10	F10.0	TTB()	Elapsed time associated with point in table (t).
	11-20	F10.0	HTB()	Transient-state head associated with point in table (L).

Notes:

1. Records 2 through 6 are repeated for each compartment. The compartments must be in the same order as identified in the inputs to subroutine BASIC.

2. Record 4 is repeated for NCHNC specified-head nodes within the compartment.

3. Records 5 and 6 are repeated for NTABC specified-head tables for the compartment. If NTABC = 0, then Records 5 and 6 are skipped.

4. The quantity CHNODE() represents local node numbers within the compartment, where each compartment includes node number 1 through NCHNC.

5. Record 6 is repeated for NTABC points within a table. A specification of CHTAB() = *i* assigns the *i*-th table among the NTABC tables to the node. If CHTAB() = 0, no table is assigned to the node, and the specified-head equals CHBASE() for all times. The table numbers are local to the compartment, which means that for the first table in any compartment i = 1. Correspondingly, a table in another compartment cannot be assigned to CHTAB().

6. The value of IGET can be 1 or 2. If IGET = 1, the point value at the end of the time step is used from the specified head table. If IGET = 2, the specified head over the time step is averaged from the specified head table.

7. The quantity LEAK() represents the resistance to water exchanges through a node between the groundwater system and a hydraulically connected water source, such as a pond, lake, channel, or subsurface drain. Two approaches can be used to assigning a value to LEAK(). Firstly, the value can represent the physical attributes of the hydraulic connection. Using a pond as an example, the leakance would represent the vertical hydraulic conductivity of the pond bed, the thickness of the pond bed, and the pond area associated with the node. Using a subsurface drain as an example, the leakance would represent not only the resistance to groundwater flow from the surrounding soil into the drain but also the resistance to groundwater flow within the soil that is not represented in the model. This latter resistance is related to converging groundwater-flow paths that cannot be represented in the model because of the spatial discretization used in constructing the finite-element mesh. Correspondingly, the leakance value assigned to a subsurface drain depends on that spatial discretization. Secondly, a leakance value can be assigned to approach a mathematical specified-head condition. This is accomplished by assigning a high value to the leakance such that the computed and specified heads are essentially identical. However, care must be taken to not assign an excessively high value such that the difference between the computed and specified heads exceeds digits of a double-precision number.

8. The quantity ITYPE() identifies the specified-head type. If ITYPE() = 1, bidirectional flow can occur at the specified-head node: water can flow either into or from the groundwater system. If ITYPE() = 2, only unidirectional flow can occur: water can flow only from the groundwater system.

9. The quantity CHTAB() in Record 4 is the specified-head table assigned to the node.

10. The quantity CHBASE() in Record 4 is the steady component of the specified head at a node. The specified-head at a particular time is the sum of CHBASE() and the transient-state head change interpolated from the specified-head table for the node. The head change is the transient-state change from the steady-state component CHBASE(). However, if CHTAB() = 0 for the node, the specified-head value does not have a transient component.

11. The specified-head tables have elapsed time TTB() as the independent variable and head HTB() as the dependent variable. The elapsed time TTB() assigned to a point in a table must be greater than the elapsed time for the previous point in the table. The transient component of the specified head is interpolated from the table based on the elapsed time in the simulation. The elapsed time at any time step in the simulation is given by the relation t^k = STIME0 + $\sum_{i=1}^{k} \Delta t_i$, where t is the elapsed time at the k-th time step and Δt is a time step. STIME0 and the time-step scheme are specified in subroutine BASIC.

3.9 Subroutine WFLUX

File Type Identifier: FLX
Record Formats:

Table 3-9
File Structure for Subroutine WFLUX
File Type FLX

Record	Condition	Variables Read
1		IECHO2
2		XCNAME Repeat Records 2-8 as group for each compartment.
3		NFXNC, NTABC, NWELC, IECHO1
4		FXNODE, FXRATE, FXTAB, FXNAME Repeat record NFXNC times
5	NTABX>0	NPT, IGET Repeat Records 5-6 NTABC times.
6	NTABC>0	TTB, QTB Repeat record NPT times.
7	NWELC>0	NWLN, WLRATE, WLTAB, WNAME Repeat Records 7-8 NWELC times.
8	NWELC>0	IN2, LEAK Repeat record NWLN timers.

Record	Columns	Type	Variable	Definition
1	1-10	I20	IECHO2	Switch for output of time-step fluxes.
2	1-20	A20	CNAME	Compartment name.
3	1-10	I10	NFXNC	Number of specified-flux nodes in compartment.
	11-20	I10	NTABC	Number of specified-flux tables assigned to compartment.
	21-30	I10	NWELC	Number of wells.
	31-40	I10	IECHO1	Switch for echo of specified-flux inputs.
4	1-10	I10	FXNODE()	Node number (local) for specified flux.
	11-20	F10.0	FXRATE()	Steady-state flux rate at node (L^3t^{-1}). A positive flux represents a groundwater recharge, and a negative flux represents a discharge.
	21-30	I10	FXTAB()	Specified-flux table assigned to node.
	31-51	1X,A20	FXNAME()	Specified-flux name assigned to node.
5	1-10	I10	NPT()	Number of points in specified-flux table.
	11-20	I10	IGET()	Switch for interpolation method.
6	1-10	F10.0	TTB()	Elapsed time associated with point in table (t).
	11-20	F10.0	QTB()	Transient-state scaling factor associated with point in table (L^0). The scaling factor is positive unless the user wants to reverse the sign in Record 4.
7	1-10	I10	NWLN()	Number of well nodes.
	11-20	IE10.2	WLRATE()	Well flux rate. ($L^3t\text{-}^1$)
	21-30	IE10.2	WLTAB()	Flux rate table.
	31-40	A20	WNAME()	Well name.
8	1-10	I10	IN2()	Well node
	11-20	F10.10	LEAK()	Leakance of well link (L^2t^{-1}).

Notes:

1. Records 2 through 6 are repeated for each compartment. The compartments must be in the same order as identified in the inputs to subroutine BASIC.

2. Record 4 is repeated for each of the NFXNC nodes in the flux data set. If NFXNC = 0, then Record 4 is skipped.

3. Records 5 and 6 are repeated for each of the NTABC tables for the compartment. If NTABC = 0, then Records 5 and 6 are skipped.

4. Record 6 is repeated for each of the NPT() entries in a table. A specification FXTAB() = *i* assigns the *i*-th table among the NTASBC tables to the node. If FXTAB() = 0, no table is assigned to the node, and the specified flux equals FXRATE () for all times. The table numbers are local to the

compartment, which means that for the first table in any compartment i = 1. Correspondingly, reference cannot be made to a table in another compartment.

5. Records 7 and 8 are repeated for each of the NWELC wells for the compartment. If NWELC = 0, then Records 7 and 8 are skipped.

6. Record 8 is repeated NWLN() times for each finite-element mesh node that is linked to a particular well node.

7. The quantity FXNODE() represents a local node number within the compartment, where the compartment includes nodes 1 through NNC().

8. The flux rate at any time is the flux rate FXRATE() in Record 4 scaled by an interpolated value from the evapotranspiration scaling-factor table.

9. Each elapsed time TTB() entered in a table must be greater than the previous entry in the table.

10. The scaling-factor tables have elapsed time TTB() as the independent variable and the flux-rate scaling factor QTB() as the dependent variable. The elapsed time TTB() assigned to a point in a table must be greater than the elapsed time for the previous point in the table. The flux-rate factor is interpolated from the table based on the elapsed time in the simulation. The elapsed time at any time step in the simulation is given by the relation t^k = STIME0 + $\sum_{i=1}^{k} \Delta t_i$, where t is the elapsed time at the k-th time step and Δt is a time step. STIME0 and the time-step scheme are specified in subroutine BASIC.

11. The value of IGET can be 1 or 2. If IGET = 1, the point value at the end of the time step is used from the specified flux table. If IGET = 2, the specified flux over the time step is averaged from the specified flux table.

12. The scaling used in the flux specification is the average inflow during a particular time step. To extract that average from the table, the tabulated function is integrated from time t^k - Δt to time t^k and then divided by Δt. Accordingly, the scaling-factor table should be constructed with this in mind.

13. The leakance of the well link LEAK() is related to skin effects (such as perforations in the well casing, gravel pack effects, plugging of the formation due to drilling, resistance to flow through the well screen, etc.) as well as near-field effects (for coarser grades of sediment, the heads are underrepresented). Thus, an appropriate value for LEAK() must be selected by the user based on these factors.

14. A physical well can be represented within a simulation by one of two approaches. Firstly, a well can be represented by identifying the appropriate node or nodes in the input FXNODE() in Record 4. Correspondingly, the pumping rate is assigned in the input FXRATE() in Record 4 or in FXRATE() along with a table assignment. If a well has its pumping assigned to more than one

node, the computed heads at the node in the general case will be different. Secondly, a well can be represented as a feature connected to the finite-element mesh with links that have a specified leakance. A water-level elevation in the well is calculated such that the inflow to the well from the groundwater system equals the pumping rate. Additionally, the inflows along the links to the well are proportional to the leakance of the link and the difference in the heads calculated for the well and the node within the finite-element mesh. The well casing is assumed to have an infinite leakance. Using this approach the dual effects of pumping and inter-aquifer exchanges are simulated for the well. The leakance assigned to a node represents the resistance to groundwater because of the local radial flow to the well, a scale not simulated by the model.

3.10 Subroutine WEVAP

File Type Identifier: GET
Record Formats:

Table 3-10
File Structure for Subroutine WEVAP
File Type GET

Record	Condition	Variables Read
1		IECHO2
2		XCNAME Repeat Records 2-6 as group for each compartment.
3		NETNC, NTABC, IECHO1
4		ETNODE, ETAREA, LAND, DELH0, ETMAX, ETTAB, ETNAME Repeat record NETNC times.
5	NTABC>0	NPT, IGET Repeat Records 5-6 NTABC times.
6	NTABC>0	TTB, FTB Repeat record NPT times.

Record	Columns	Type	Variable	Definition
1	1-10	I10	IECHO2	Switch for output of time step groundwater-evapotranspiration fluxes.
2	1-20	A20	CNAME	Compartment name.
3	1-10	I10	NETNC	Number of groundwater- evapotranspiration nodes in compartment.
	11-21	I10	NTABC	Number of groundwater- evapotranspiration tables associated with compartment.
	21-30	I10	IECHO1	Switch for echo of groundwater- evapotranspiration inputs.

4	1-10	I10	ETNODE()	Node number (local) for groundwater evapotranspiration.
	11-20	F10.0	ETAREA()	Area associated with groundwater-evapotranspiration node (L^2).
	21-30	F10.0	LAND()	Land-surface elevation at node (L).
	31-40	F10.0	DELH0()	Extinction depth for vegetation (L).
	41-50	F10.0	ETMAX()	Maximum evapotranspiration rate for vegetation (Lt^{-1}).
	51-60	I10	ETTAB()	Groundwater-evapotranspiration table associated with node.
	61-81	1X,A20	ETNAME()	Groundwater-evapotranspiration name associated with node.
5	1-10	I10	NPT()	Number of points in groundwater-evapotranspiration table.
	11-20	I10	IGET()	Switch for interpolation method.
6	1-10	F10.0	TTB()	Elapsed time associated with point in table (t).
	11-20	F10.0	FTB()	Transient-state scaling factor associated with point in table (L^0).

Notes:

1. Records 2 through 6 are repeated for each compartment. The compartments must be in the same order as identified in the inputs to subroutine BASIC.

2. Record 4 is repeated for each of the NETNC nodes in the flux data set.

3. Records 5 and 6 are repeated for each NTABC table for the compartment. If NTABC = 0, then Records 5 and 6 are skipped. A specification of ETTAB() = i assigns the *i*-th table among the NTABC tables to the node. If ETTAB() = 0, no table is assigned to the node, and the maximum evapotranspiration rate equals ETMAX () for all times. The table numbers are local to the compartment, which means that for the first table in any compartment *i* = 1. Correspondingly, reference cannot be made to a table in another compartment.

4. Record 6 is repeated for each NPT() in a table.

5. The value of IGET can be 1 or 2. If IGET = 1, the point value at the end of the time step is used from the specified head table. If IGET = 2, the specified head over the time step is averaged from the specified head table.

6. The quantity ETNODE() in Record 4 represents a local node number within the compartment, where the compartment includes nodes 1 through NNC().

7. The quantity ETMAX() in Record 4 represents the nominal maximum evapotranspiration rate ETMAX(), which occurs when the groundwater table is exactly at the land surface. However, that nominal rate can be scaled for any time step by an interpolated value from the

evapotranspiration scaling-factor table. The scaling-factor table is specified for each evapotranspiration node by the quantity TABQ(). If TABQ() = 0, then the maximum evapotranspiration rate is always ETMAX() without scaling.

8. The scaling-factor tables have elapsed time TTB() as the independent variable and the evapotranspiration-rate scaling factor QTB() as the dependent variable. The elapsed time TTB() assigned to a point in a table must be greater than the elapsed time for the previous point in the table. The flux-rate factor is interpolated from the table based on the elapsed time in the simulation. The elapsed time at any time step in the simulation is given by the relation t^k = STIME0 + $\sum_{i=1}^{k} \Delta t_i$, where t is the elapsed time at the k-th time step and Δt is a time step. STIME0 and the time-step scheme are specified in subroutine BASIC.

9. The scaling used in the evapotranspiration simulation is the average value during a particular time step. To extract that average from the table, the tabulated function is integrated from time $t^k - \Delta t$ to time t^k and then divided by Δt. Accordingly, the scaling-factor table should be constructed with this in mind.

3.11 Subroutine WRIVER

File Type Identifier: RIV
Record Formats:

Table 3-11
File Structure for Subroutine WRIVER
File Type RIV

Record	Condition	Variables Read
1		IECHO2
2		XCNAME Repeat Records 2-10 as group for each compartment.
3		NRC, NTABXC, NTABQC, NGPHC, IECHO1
4		NRN, LAST, FACK, SNAME Repeat Records 4-5 NRC times.
5		RNODE, LENGTH, ZBED, KBED, BBED, TABXC, TABQC, JOIN, CJOIN Repeat record NRN times.
6		NPTX Repeat Records 6-7 NTABXC times.
7		QXTB, WXTB, DXTB Repeat record NPTX times.
8	NTABQC>0	NPTQ, QFACT, IGET, QNAME Repeat Records 8-9 NTABQC times.
9	NTABQC>0	TTB, QTB Repeat record NPTQ times.
10	NGPHC>0	GREACHC, GLINK, GNAME Repeat record NGPHC times.

Record	Columns	Type	Variable	Definition
1	1-10	I10	IECHO2	Switch for output of river discharges and stream-aquifer exchanges.
2	1-20	A20	CNAME	Compartment name.
3	1-10	I10	NRC()	Number of river reaches in compartment.
	11-20	I10	NTBXC	Number of cross-section tables associated with compartment.
	21-30	I10	NTBQC	Number of inflow tables associated with compartment.
	31-40	I10	NGPHC	Number of hydrograph sites associated with compartment.
	41-50	I10	IECHO1	Switch for echo of river inputs.
4	1-10	I10	NRN()	Number of links in river reach.
	11-20	I10	LAST()	Flag to indicate a downstream reach in network.
	21-30	I10	FACK	Scaling factor for hydraulic conductivity of channel bed for links within reach.
	41-61	1X,A20	SNAME()	Name associated with river reach.
5	1-10	I10	RNODEC()	Node number (local) for river-reach link.
	11-20	F10.0	LENGTH()	Channel length for link (L).
	21-30	F10.0	ZBED()	Elevation of channel bed at node (L).
	31-40	F10.0	KBED()	Vertical hydraulic conductivity of channel bed for link (Lt^{-1}).
	41-50	F10.0	BBED()	Thickness of channel bed for link (L).
	51-60	I10	TABXC	Cross-section table assigned to link.
	61-70	I10	TABQC	Inflow table assigned to link.
	71-80	I10	JOIN()	River reach number joining at link.
	81-90	A20	CJOIN()	Compartment name for river reach joining at link.
6	1-10	I10	NPTX()	Number of points in cross-section table.
7	1-10	F10.0	QXTB()	Discharge associated with point in cross-section table (L^3t^{-1}). Assigned recharge is always positive.
	11-20	F10.0	WXTB()	Streamflow width (corresponding to discharge) associated with point in table (L).
	21-30	F10.0	DXTB()	Streamflow average depth (corresponding to discharge) associated with point in table (L).
8	1-10	I10	NPTQ()	Number of points in inflow table.
	11-20	F10.0	QFACT	Scaling factor for discharges in inflow table (L^0).
	21-30	I10	IGET()	Switch for interpolation method.
	31-51	1X,A20	QNAME()	Name associated with inflow.
9	1-10	F10.0	TTB()	Elapsed time associated with point in inflow table (t).

Record	Columns	Type	Variable	Definition
	11-20	F10.0	QTB()	Inflow associated with point in table (L^3t^{-1}). Inflow to channel is positive, and diversion from channel is negative.
10	1-10	I10	GREACHC	River reach associated with hydrograph site.
	11-20	I10	GLINK()	Link with reach associated with hydrograph site.
	21-41	1X,A20	GNAME()	Name associated with hydrograph site.

Notes:

1. Figure 3-2 shows the layout for a stream-channel network that covers two compartments. Compartment A has one reach (NRC=1) with six links (NRN=6). This reach is the last downstream in the network (LAST=1), and the first reach in Compartment B is tributary to this reach (JOIN=1 and CJOIN=Compartment B). Compartment B has two reaches (NRC=2) with five and four links respectively (NRN=5 and NRN=4). The first reach has a specified inflow at the upstream link, and the inflow values are contained in a second inflow table (TABQC=2). The second reach is tributary to the first (JOIN=2 and CJOIN=Compartment B for the first reach). The first reach has a specified inflow at the upstream link, and the inflow values are contained in a second inflow table (TABQC=1).

2. Records 2 through 10 are repeated for each compartment. The compartments must be in the same order as identified in the inputs to subroutine BASIC.

3. Records 4 and 5 are repeated for each of the NRC() reaches within a compartment.

4. For each reach, Record 5 is repeated for each of the NRN() links.

5. Records 6 and 7 are repeated for each of the NTBXC cross-section tables for a compartment.

6. For each cross-section table, Record 7 is repeated for NPTX() points within the table.

7. Records 8 and 9 are repeated for each of the NTBQC inflow tables for a compartment.

8. The value of IGET can be 1 or 2. If IGET = 1, the point value at the end of the time step is used from the specified head table. If IGET = 2, the specified head over the time step is averaged from the specified head table.

9. For each inflow table, Record 9 is repeated for each of the NPTQ() points within the table.

10. Record 10 is repeated for each of the NGPHC hydrograph points for the compartment.

11. The inflow tables have elapsed time TTB() as the independent variable and the inflow QTB() as the dependent variable. The elapsed time TTB() assigned to a point in a table must be greater than the elapsed time for the previous point in the table. The inflow is interpolated from the table

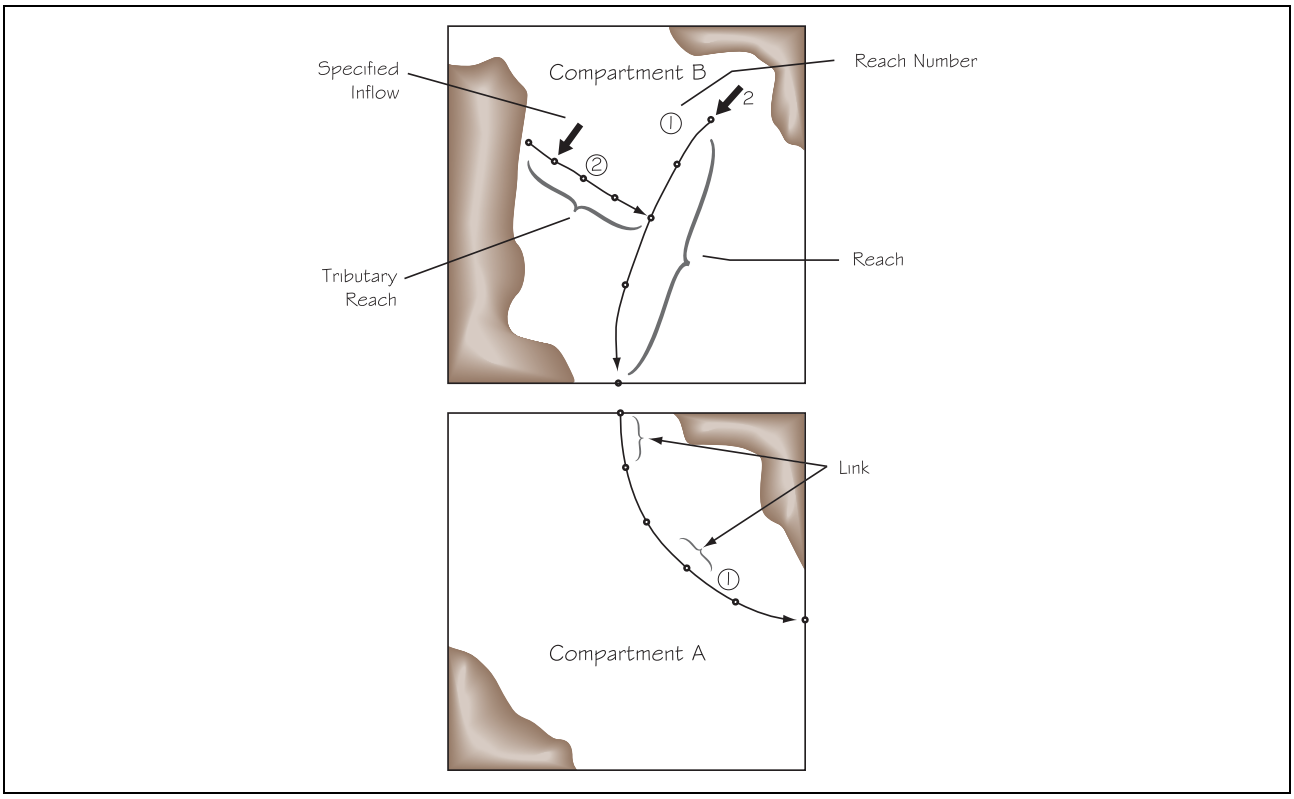

Figure 3-2
Layout for a Stream-Channel Network

based on the elapsed time in the simulation. The elapsed time at any time step in the simulation is given by the relation $t^k = \text{STIME0} + \sum_{i=1}^{k} \Delta t_i$, where t is the elapsed time at the k-th time step and Δt is a time step. STIME0 and the time-step scheme are specified in subroutine BASIC.

11. The inflow used in the river simulation is the average inflow during a particular time step. To extract that average from the table, the tabulated function is integrated from time $t^k - \Delta t$ to time t^k and then divided by Δt. Accordingly, the inflow table should be constructed with this in mind.

3.12 Subroutine WFAULT

File Type Identifier: FLT
Record Formats:

Table 3-12
File Structure for Subroutine WFAULT
File Type FLT

Record	Condition	Variables Read
1		IMESH
2		NFN, NFE, NFL, IECHO1, IECHO2, IECHO3, IECHO4
3		FACX, FACY, FACZ
4		Blank, X, Y, Z Repeat record NFN times.
5		NFC, NMAX
6		ZMIN, ZMAX, COL, COL, **…** Continue values of COL until all entered for node column, but not more than 20 values are allowed. Repeat record NFC times.
7		Blank, IN2(,1), IN2(,2), IN2(,3), MAT Repeat record NFE times.
8		Blank, IN2(,1), IN2(,2), XCNAME Repeat NFL times.
9		NGROUP, FACT, FACS
10		LL1, LL2, XTRAN, XSTOR Repeat record NGROUP times.
11		NGROUP, FACL
12		LL1, LL2, XLEAK Repeat record NGROUP times.

Record	Columns	Type	Variable	Definition
1	1-10	I10	IMESH	Switch for output of mesh file (2DM).
2	1-10	I10	NFN	Number of fault nodes.
	11-20	I10	NFE	Number of fault elements.
	21-30	I10	NFL	Number of fault links.
	31-40	I10	IECHO1	Switch for echo of fault inputs.
	41-50	I10	IECHO2	Switch for echo of fault initial heads.
	51-60	I10	IECHO3	Switch for echo of time-step fault heads.
	61-70	I10	IECHO4	Switch for echo of time-step fault-link fluxes.
3	1-10	F10.0	FACX	Scaling factor for *x*-coordinates of fault nodes (L^0).
	11-20	F10.0	FACY	Scaling factor for *y*-coordinates (L^0).
	21-30	F10.0	FACZ	Scaling factor for *z*-coordinates (L^0).

Record	Columns	Type	Variable	Definition
4	11-20	F10.0	X()	*X*-coordinate of fault node (L).
	21-30	F10.0	Y()	*Y*-coordinate of fault node (L).
	31-40	F10.0	Z()	*Z*-coordinate of fault node (L).
5	1-10	I10	NFC	Number of node columns.
	11-20	I10	NMAX	Maximum number of nodes in a column.
6	1-10	F10.0	ZMIN()	Minimum distance between collapsed nodes.
	11-20	F10.0	ZMAX()	Maximum elevation of top node.
	21-30	I10	COL()	Column node number.
7	11-20	I10	IN2()	First node of fault element.
	21-30	I10	IN2()	Second node of fault element.
	31-40	I10	IN2()	Third node of fault element.
	41-50	I10	MAT()	Identifier for fault material.
8	11-20	I10	IN2(,1)	Node in fault plane.
	21-30	I10	IN2(,2)	Node in adjacent groundwater system.
	32-51	A20	CNAME	Compartment name associated with node in groundwater system.
9	1-10	I10	NGROUP	Number of fault-parameter groups.
	11-20	F10.0	FACT	Scaling factor for fault transmissivity (L^0).
	21-30	F10.0	FACS	Scaling factor for fault storage coefficient (L^0).
10	1-10	I10	LL1	First element number within range for element group.
	11-20	I10	LL2	Last element number within range for element group.
	21-30	F10.0	TRAN()	Transmissivity of fault element normal to fault plane (L^2t^{-1}).
	31-40	F10.0	STOR()	Storativity of fault element (L^0).
11	1-10	I10	NGROUP	Number of parameter groups for fault links.
	11-20	I10	FACL	Scaling factor for leakance assigned to fault links.
12	1-10	I10	LL1	First element number within range for element group.
	11-20	I10	LL2	Last element number within range for element group.
	21-30	F10.0	XLEAK	Leakance assigned to elements within group (L^2t^{-1}).

Notes:

1. Figure 3-3 shows the layout of fault links. The first link connects fault node 20 to mesh node 9 in Compartment A (IN2(,1)=20, IN2 (,2)=9, and CNAME=Compartment A in Record 8). The second fault link connects fault node 20 to mesh node 3 in Compartment B (IN2(,1)=20,

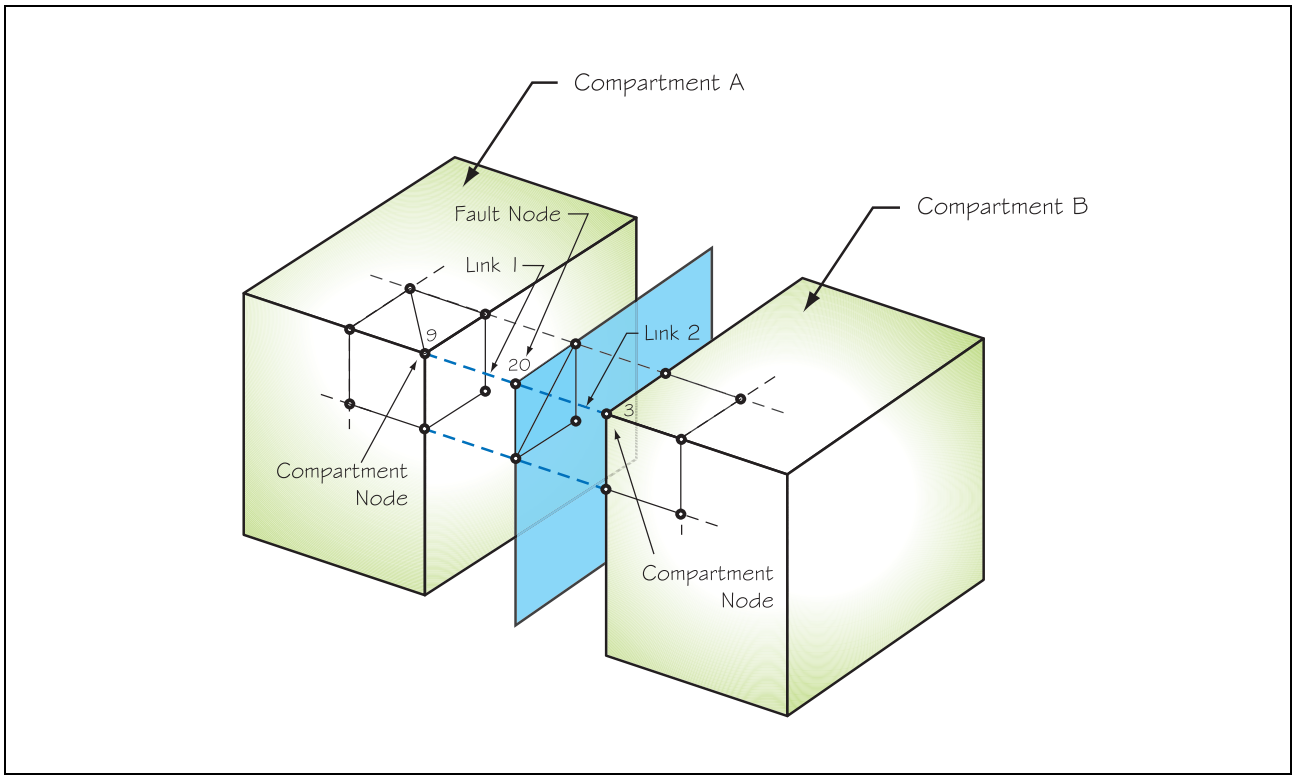

Figure 3-3
Layout for Fault Links

IN2(,2)=3, and CNAME=Compartment B). Link assignments such as these are repeated until all the fault-to-mesh connections are specified.

2. If IMESH = 1 in Record 1, then a file is created for input into GMS to display the fault mesh as a three-dimensional object. If IMESH = 0, then no file is created.

3. Faults are not compartmentalized.

4. Record 4 is repeated for NFN fault nodes.

5. Record 5 is repeated for NFE fault elements.

6. Record 6 is repeated for NFL fault links.

7. Record 8 is repeated for NGROUP groups of fault elements.

8. If ISTART = 0, Record 12 is repeated until NFN initial heads have been entered as five head values per record. Otherwise, Record 12 is omitted.

9. Record 10 is repeated for MGROUP groups of fault elements.

10. ZMIN should be small enough to remove the hydrologic unit from the simulation by collapsing

the grid. However ZMIN should be big enough to allow numerical problems to continue. ZMAX is equal to the top node in the column of nodes. COL is the series of nodes and must start the top node of the grid and proceed down.

3.13 File Type Identifier: FNT

Record Formats:

Table 3-13
File Structure for Subroutine WFAULT
File Type FNT

Record	Condition	Variables Read
1		XNFN, ISTART, XH0, ISAVE, IWHEN
2	ISTART=0	Blank, H Repeat H five times per record. Repeat record until values have been entered for XNFN values.

Record	Columns	Type	Variable	Definition
1	1-10	I10	NFN	Number of fault nodes.
	11-20	I10	ISTART	Switch for uniform initial heads.
	21-30	F10.0	XH0	Uniform initial head value (L).
	31-40	I10	ISAVE	Switch for overwriting initial heads.
	41-50	I10	IWHEN	Step for overwriting initial heads.
2	1-20	Blank		
	21-70	5F10.0	H()	Initial-head values for each node.

Notes:

1. Record 2 is skipped if ISTART = 1. Otherwise, Record 2 is repeated until XNFN nodal initial heads have been entered, entering five values per record.

2. If ISTART = 0, the quantity XH0 is ignored.

3. ISAVE is used to create a dataset of initial heads representing time step IWHEN within the simulation. If ISAVE = 1, then the dataset is created. The dataset overwrites the contents of the initial heads for the simulation. The dataset is written using the formats of Records 1 and 2.

4.0 MODEL VALIDATION

4.1 General Description

In order to validate the FEMFLOW3D model, four test cases with known analytical solutions were simulated. The simulation results were then compared with the known analytical solutions to verify that FEMFLOW3D accurately simulated these groundwater scenarios. These test cases can be summarized as follows.

The Theis Problem (Theis, 1935)

The Theis Problem examines transient, confined flow to a well in a horizontal, infinite, confined aquifer of constant thickness and with homogeneous and isotropic hydraulic properties. The problem is for constant pumping from a fully-penetrating well.

The Papadopulos Problem (Papadopulos, 1965)

The Papadopulos Problem examines transient, confined flow to a well in a horizontal, infinite, confined, constant-thickness, homogeneous, and isotropic aquifer. In this problem, the principal components of the transmissivity tensor have different values.

The Neuman Problem (Neuman, 1974)

The Neuman Problem examines transient, unconfined flow to a well in an infinite, constant-thickness, and homogeneous aquifer. The well and observation wells are partially penetrating. The groundwater system is isotropic in the radial and vertical directions.

The parameters for these test cases, the results of the simulation, and the comparison of analytical solutions versus simulation results are provided in further detail below.

4.2 The Theis Problem

4.2.1 Problem Description

In its simplest form, the Theis Problem (Theis, 1935) examines transient flow of groundwater to a well under the assumptions that the:

- Aquifer is horizontal,
- Aquifer is infinite in lateral extent,

- Aquifer is confined,
- Aquifer is of constant thickness,
- Aquifer has homogenous and isotropic hydrologic properties,
- Hydraulic head initially is uniform throughout the aquifer,
- Well fully penetrates the aquifer,
- Well has negligible diameter, and
- Well is pumping at a constant rate.

The analytical solution for these assumptions has the form

$$s = \frac{Q}{4\pi KB} W(u), \qquad (4\text{-}1)$$

where

s = the drawdown in the aquifer at the specified time and distance from the well [L],
Q = the pumping rate [L^3t^{-1}],
K = the radial hydraulic conductivity of the aquifer [Lt^{-1}],
B = the aquifer thickness [L],
$W()$ = the well function [L^0], and
u = is a parameter [L^0].

The parameter u is given by the relation

$$u = \frac{r^2 S}{4Kt}, \qquad (4\text{-}2)$$

where

r = the radial distance from the well [L],
t = the time since the start of pumping [t], and
S = the storage coefficient for the aquifer [L^0].

4.2.2 Model Simulation

The Theis model was simulated with FEMFLOW3D in a transient-state over 10 days and 40 time steps. The simulation was divided into a single stress period, with all 40 time steps occurring within the single stress period. Within each stress period, time-steps were accelerated by a factor of 1.2. The initial time step for the simulation was 0.00136 days.

The finite-element mesh used for the simulation is shown on Figure 4-1. The mesh is radially symmetric and represents an 18-degree wedge-shaped groundwater system with a single pumping well at the narrowest edge of the wedge. The radial length of the mesh is approximately 42,337 ft, which is sufficient to avoid adverse boundary effects. The grid-spacing in the radial direction begins at 1.0 ft from the well to the next node column, and increases in the radial direction by a factor of 1.1

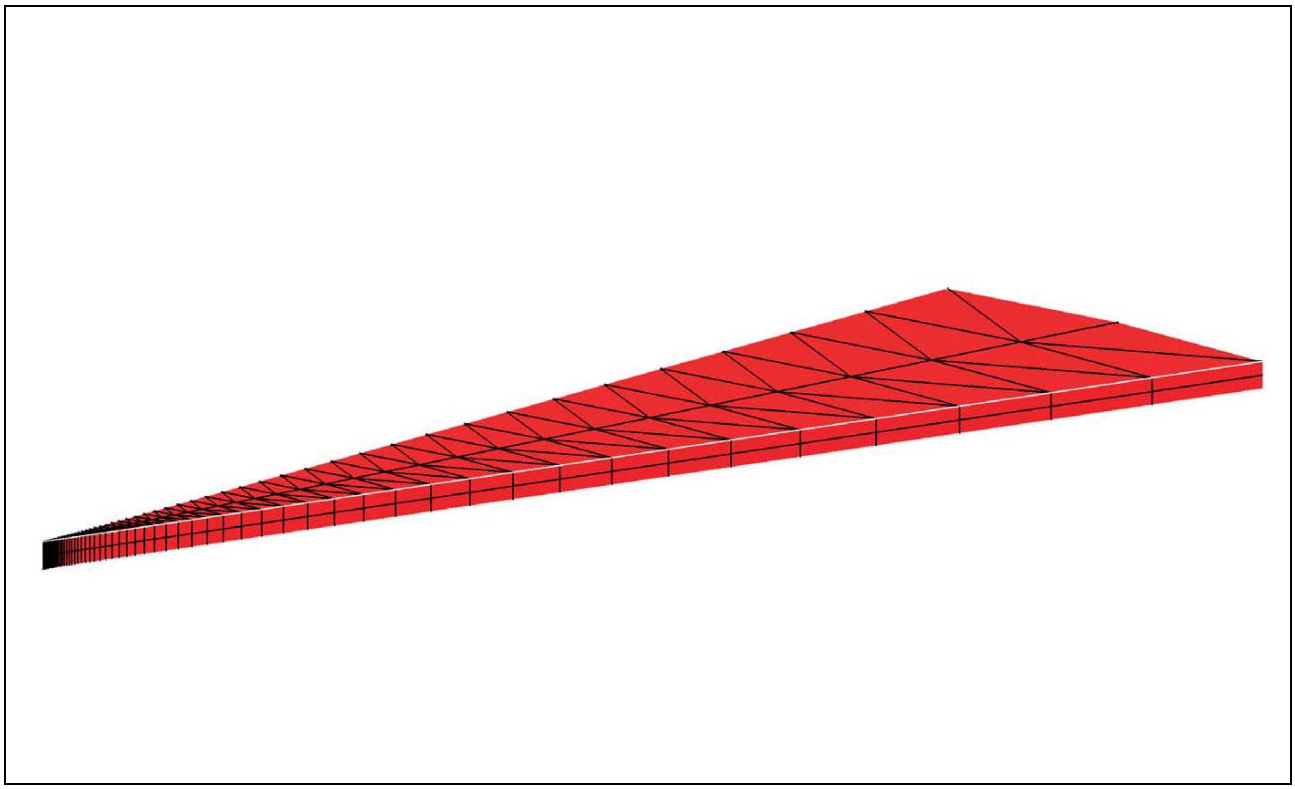

Figure 4-1
Finite-Element Mesh Used for Theis Model Simulation

with increasing distance from the well. The vertical thickness of the mesh is 100 ft. The wedge-shaped face of the mesh is parallel with the *x*-*y* coordinate plane, with the line between the centre of the narrowest edge of the wedge and the center of the widest edge of the wedge lying at a 45-degree angle between the *x* and *y*-coordinate axes. The quadrilateral face of the finite-element mesh lies parallel to the *z*-coordinate axis. The radius of the single pumping well is 1.0 ft, and the screened interval is assumed to fully penetrate the aquifer. The finite-element mesh contains a total of 912 wedge-shaped elements and 1,035 nodes. The hydraulic parameters assigned to the mesh are listed in Table 4-1, along with descriptions of the initial and boundary conditions.

Table 4-1
Parameters for the Theis Problem

Parameter	Value
Hydraulic Conductivity (K_x, K_y, K_z)	50 ft/d, 50 ft/d, 50 ft/d
Storage Coefficient (S)	0.01 ft^0
Pumping Rate of Well (Q)	400 ft^3/d

4.2.3 Results

Three fully-penetrating observation wells were placed in the finite-element mesh at 200, 400, and 800 feet from the pumping well. The FEMFLOW3D output files provided hydrographs for these wells over the simulation period. These hydrographs were translated into drawdowns in each observation well. The simulated drawdowns were then plotted on a graph along with the analytical solution for the drawdown calculated using the same parameters as those used in the FEMFLOW3D simulation. As shown in Figures 4-2, 4-3, and 4-4, the drawdowns simulated with FEMFLOW3D replicate the analytical solution for a range of distances and times.

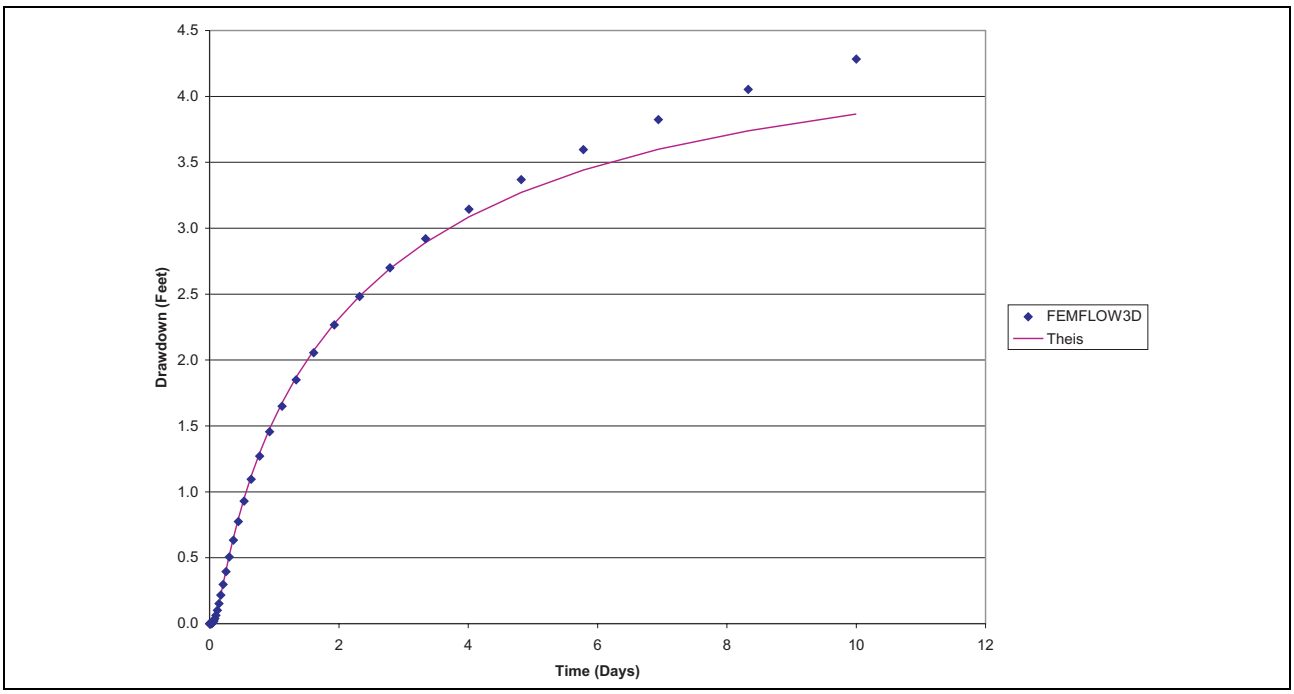

Figure 4-2
Comparison of FEMFLOW3D Simulated Drawdowns
With Theis Solution at a Distance of 200 Feet From Pumping Well

4.3 The Papadopulos Problem

4.3.1 Problem Description

The Papadopulos Problem (Papadopulos, 1965) is based on the assumption that the aquifer is homogenous and isotropic, where the principal components of the hydraulic-conductivity tensor have different values. Papadopulos (1965) developed an analytical solution for the drawdown distribution around a well pumping at a constant rate. The Papadopulos problem extends the Theis solution to an anisotropic medium and with the assumptions that the:

- Aquifer is horizontal,
- Aquifer is infinite in lateral extent,

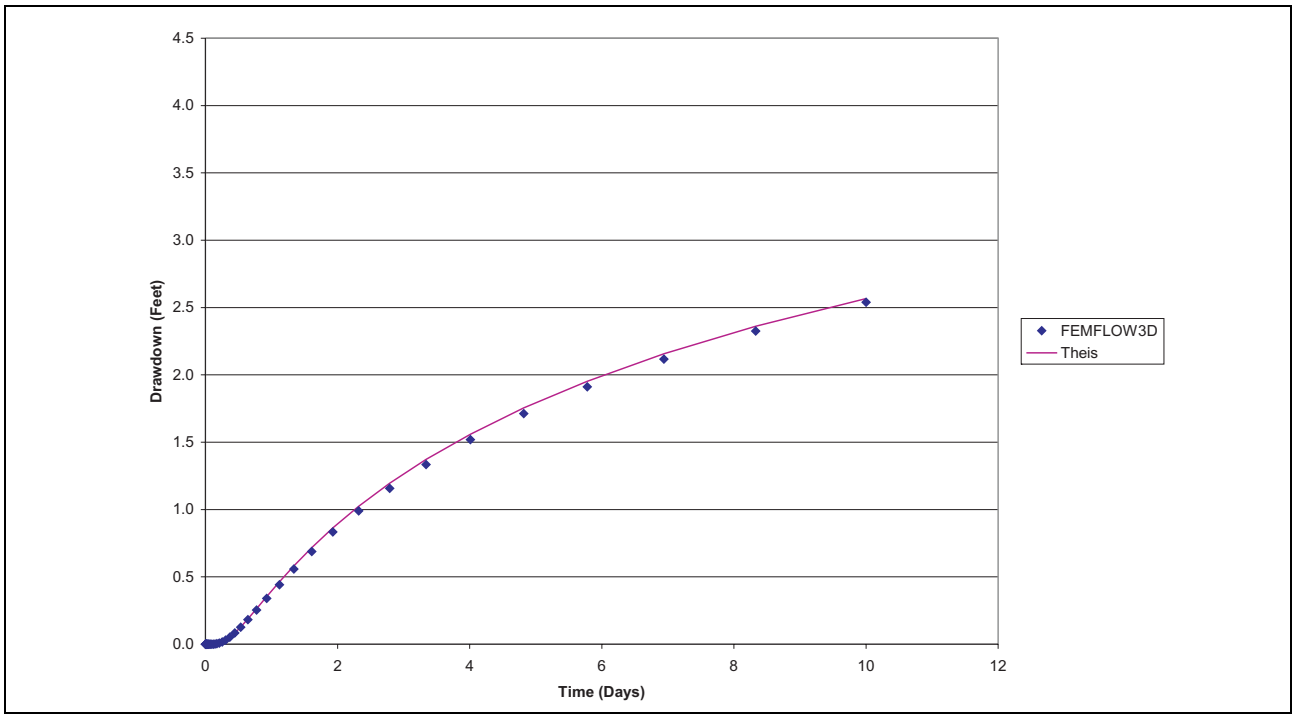

Figure 4-3
Comparison of FEMFLOW3D Simulated Drawdowns
With Theis Solution at a Distance of 400 Feet From Pumping Well

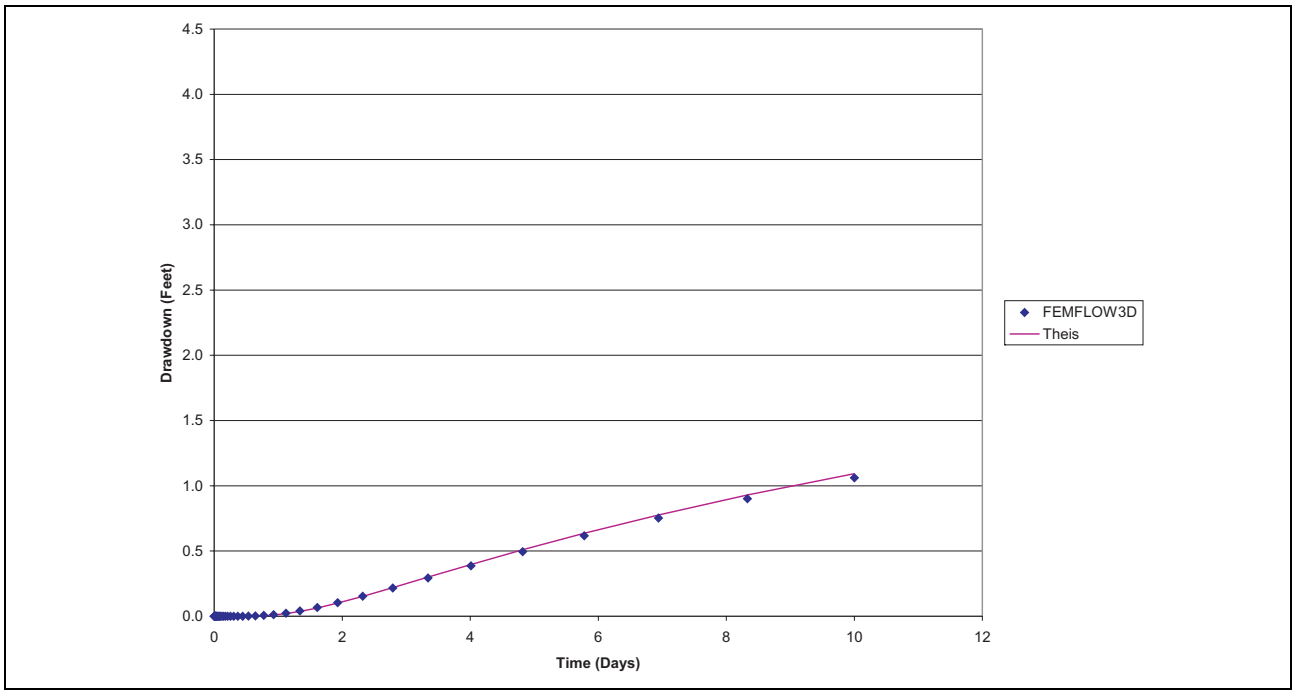

Figure 4-4
Comparison of FEMFLOW3D Simulated Drawdowns
With Theis Solution at a Distance of 800 Feet From Pumping Well

- Aquifer is confined,
- Aquifer is of constant thickness,
- Aquifer is homogeneous but anisotropic in transmissivity,
- Principal components of transmissivity are aligned symmetrically with the *x*-*y* coordinate axes,
- Hydraulic head initially is uniform throughout the aquifer,
- Well fully penetrates the aquifer,
- Well has negligible diameter, and
- Well is pumping at a constant rate.

The solution has the following form

$$s = \frac{Q}{4\pi(T_{xx}T_{yy})^{1/2}}W(u) \qquad (4\text{-}3)$$

where

s = the drawdown in the aquifer at the specified time and distance from the well [L],
Q = the pumping rate [L^3t^{-1}],
T_{xx} = the principal component of the transmissivity tensor along the *x*-axis [L^2t^{-1}]
T_{yy} = the principal component of the transmissivity tensor along the *y*-axis [L^2t^{-1}],
$W()$ = the well function [L^0], and
u = a parameter [L^0].

The parameter u has the form

$$u = \frac{S}{4t}\left(\frac{T_{xx}y^2 + T_{yy}x^2}{(T_{xx}T_{yy})}\right) \qquad (4\text{-}4)$$

where

t = the time since the start of pumping [t], and
S = the storage coefficient for the aquifer [L^0].

4.3.2 Model Simulation

As with the Theis problem, the Papadopulos problem was simulated with FEMFLOW3D in a transient-state over 10 days and 40 time steps. The simulation was divided into a single stress period, with all 40 time steps occurring within the single stress period. Within each stress period, time-steps were accelerated by a factor of 1.2. The initial time step for the simulation was 0.00136 days.

The finite-element mesh used for the simulation is illustrated in Figure 4-5. The mesh is a slab-shaped mesh that is 5,167.4 ft by 5,167.4 ft in area and 100 ft thick. The mesh is not coincident

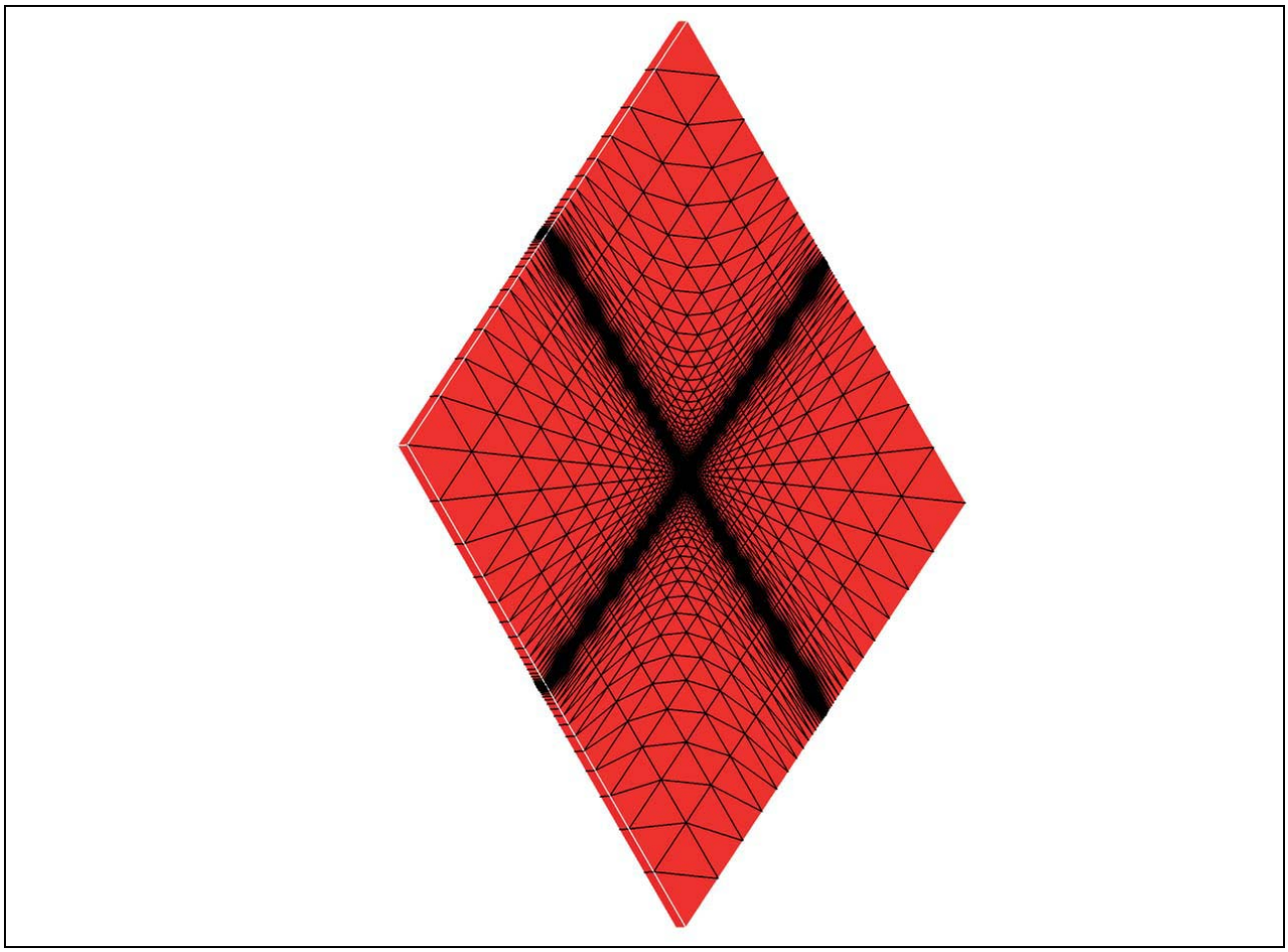

Figure 4-5
Finite-Element Mesh Used for Papadopulos Model Simulation

with the *x*-*y*-*z* coordinate system. Rather, the mesh is rotated horizontally and vertically, and twisted. Specifically, the mesh is rotated horizontally in the *x*-*y* coordinate plane 60 degrees in the counter-clockwise direction from the *x*-coordinate axis, rotated vertically in the plane perpendicular to the *x*-*y* plane 30 degrees in the counter-clockwise direction from the *x*-*y* coordinate plane, and twisted 45 degrees (which is the counter-clockwise angle in the plane perpendicular to the *x*-principal axis of the hydraulic conductivity tensor from the intersection with the *x*-*y* coordinate plane to the *y*-principal axis of the hydraulic-conductivity tensor).

The pumping well is located in the center of the slab-shaped mesh. The single pumping well is assumed to have an infinitesimal diameter, and the screened interval is assumed to fully penetrate the aquifer. The grid-spacing is symmetric in the radial direction, with the first node at 1.1 feet from the well, and increases in the radial direction by a factor of 1.3 with increasing distance from the well. The finite-element mesh contains a total of 5,000 wedge-shaped elements and 5,202 nodes. The hydraulic parameters assigned to the mesh are listed in Table 4-2, along with descriptions of the initial and boundary conditions.

Table 4-2
Parameters for the Papadopulos Problem

Parameter	Value
Hydraulic Conductivity (K_x, K_y, K_z)	50 ft/d, 50 ft/d, 50 ft/d
Storage Coefficient (S)	0.01 ft^0
Directional Parameters (α_1, α_2, α_3)	-60.0 degrees, -30.0 degrees, -45.0 degrees
Pumping Rate of Well (Q)	-100,000 ft^3/d

4.3.3 Results

Three observation wells were placed in the finite-element mesh, designated the South, East, and Southeast wells, and located, respectively, at approximately 184 ft, 409 ft, and 448 ft from the pumping well. FEMFLOW3D's output files provided hydrographs for these wells over the simulation period. These hydrographs were translated into drawdowns in each observation well. The simulated drawdowns were then plotted on a graph along with the analytical solution for the drawdown calculated using the same parameters as those used in the FEMFLOW3D simulation. As shown on Figures 4-6, 4-7, and 4-8, the FEMFLOW3D simulated drawdowns replicate the analytical solution for a range of distances and times.

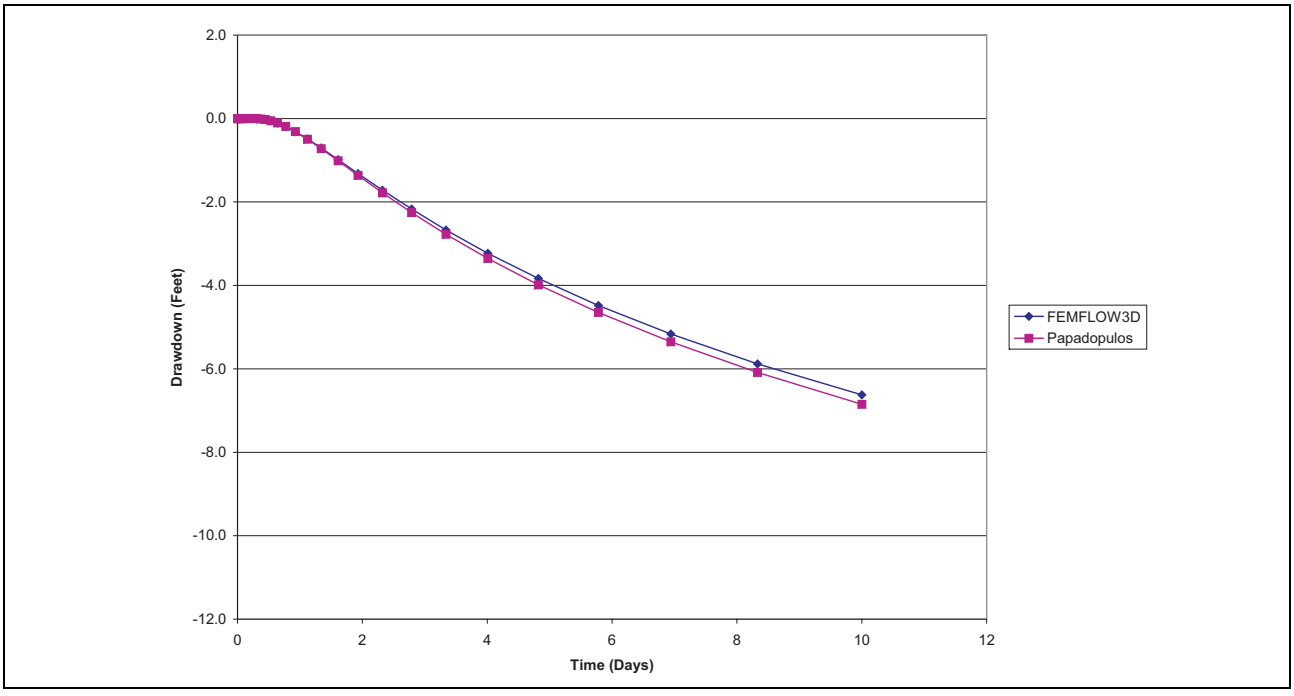

Figure 4-6
Comparison of FEMFLOW3D Simulated Drawdowns
With Papadopulos Solution at a Distance of 184 Feet From Pumping Well

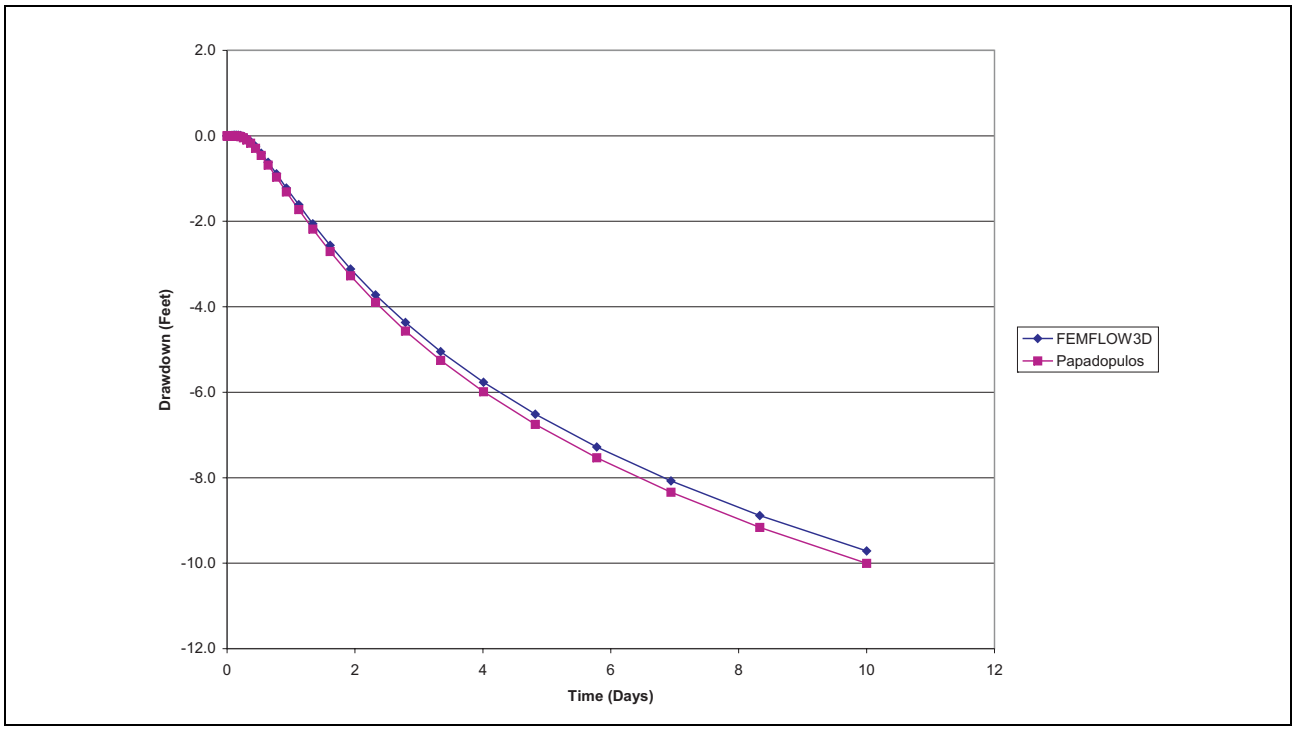

Figure 4-7
Comparison of FEMFLOW3D Simulated Drawdowns
With Papadopulos Solution at a Distance of 409 Feet From Pumping Well

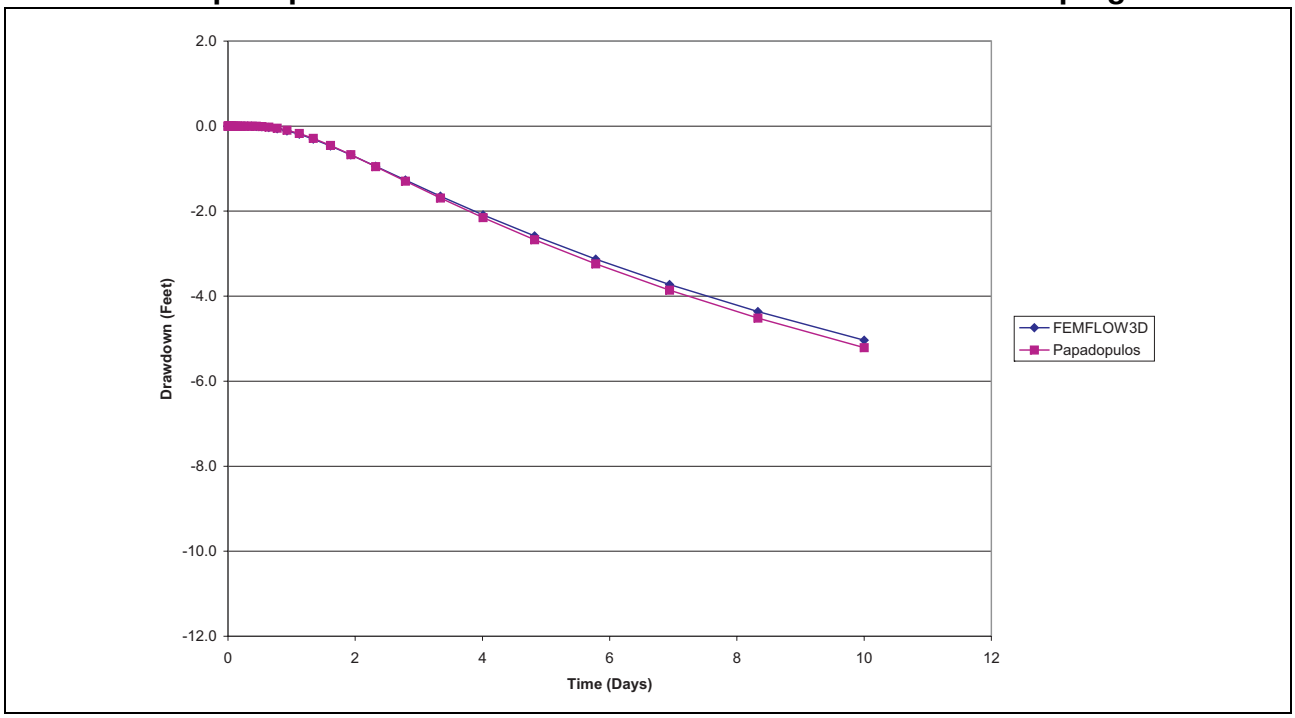

Figure 4-8
Comparison of FEMFLOW3D Simulated Drawdowns
With Papadopulos Solution at a Distance of 448 Feet From Pumping Well

4.4 The Neuman Problem

4.4.1 Problem Description

The Neuman Problem (Neuman, 1974) examines transient, unconfined flow to a well. This problem further modifies the ideal conditions of the Theis Problem by examining the drawdowns induced by a partially penetrating well in an unconfined aquifer. The Neuman problem is based on the assumptions that the:

- Aquifer is horizontal,
- Aquifer is infinite in lateral extent,
- Aquifer is unconfined,
- Aquifer is of constant thickness,
- Aquifer thickness does not change with time,
- Hydraulic head initially is uniform throughout the aquifer,
- Pumping well partially penetrates the aquifer,
- Observation wells partially penetrate the aquifer,
- Well has negligible diameter, and
- Well is pumping at a constant rate.

The solution has the following form.

$$s = \frac{Q}{4\pi KB} W(\sigma, \beta, z_D, l_D, d_D, t_S) \quad (4\text{-}5)$$

where

s = the drawdown in the aquifer at the specified time and distance from the well [L],
Q = the pumping rate [L^3t^{-1}],
K = the radial hydraulic conductivity of the aquifer [Lt^{-1}],
B = the aquifer thickness [L],
$W()$ = the well function [dimensionless],

and where the dimensionless parameters of the well function $W()$ are

$$\sigma = \frac{S_S}{S_Y} \quad (4\text{-}6)$$

$$\beta = \frac{K_Z}{K_r}\frac{r^2}{B^2} \quad (4\text{-}7)$$

$$z_D = \frac{z}{r} \quad (4\text{-}8)$$

$$l_D = \frac{l}{B} \tag{4-9}$$

$$d_D = \frac{d}{B} \tag{4-10}$$

and

$$t_S = \frac{KB_t}{S_S r^2} \tag{4-11}$$

where

S_S = the specific storage of the aquifer [L^{-1}],
S_Y = the specific yield [L^0],
K_Z = the vertical hydraulic conductivity [Lt^{-1}],
K_r = the radial hydraulic conductivity [Lt^{-1}],
r = the radial distance from the well to the observation point [L],
z = the height above the bottom of the aquifer to the observation point [L],
l = the distance from the top of the aquifer to the bottom of the pumping well perforations [L],
d = the distance from the top of the aquifer to the top of the pumping well perforations [L], and
t = the time since the start of pumping [t].

4.4.2 Model Simulation

The Neuman problem was simulated with FEMFLOW3D in a transient-state over 10 days and 40 time steps. The simulation was divided into a single stress period, with all 40 time steps occurring within the single stress period. Within each stress period, time-steps were accelerated by a factor of 1.2. The initial time step for the simulation was 0.00136 days.

The finite-element mesh used for the simulation is illustrated in Figure 4-9. The mesh is radially symmetric and represents an 18-degree wedge-shaped groundwater system with a single pumping well at the narrowest edge of the wedge. The radial length of the mesh is approximately 10,337 ft, which is sufficient to avoid adverse boundary effects. The grid-spacing in the radial direction begins at 8.6 ft from the well to the next node column, and increases in the radial direction by a factor of 1.1 with increasing distance from the well. The vertical thickness of the mesh is 200 feet, and was discretized into 10 feet intervals. The wedge-shaped face of the mesh is parallel with the *x*-*y* coordinate plane, with the line between the center of the narrowest edge of the wedge and the center of the widest edge of the wedge lying along the *x*-coordinate axis. The quadrilateral face of the finite-element mesh lies parallel to the *z*-coordinate axis. The screened interval of the pumping well lies between 110 ft and 200 ft below the surface of the finite-element mesh. The finite-element mesh contains a total of 3,920 wedge-shaped elements and 3,150 nodes. The hydraulic parameters assigned to the mesh are listed in Table 4-3, along with descriptions of the initial and boundary conditions.

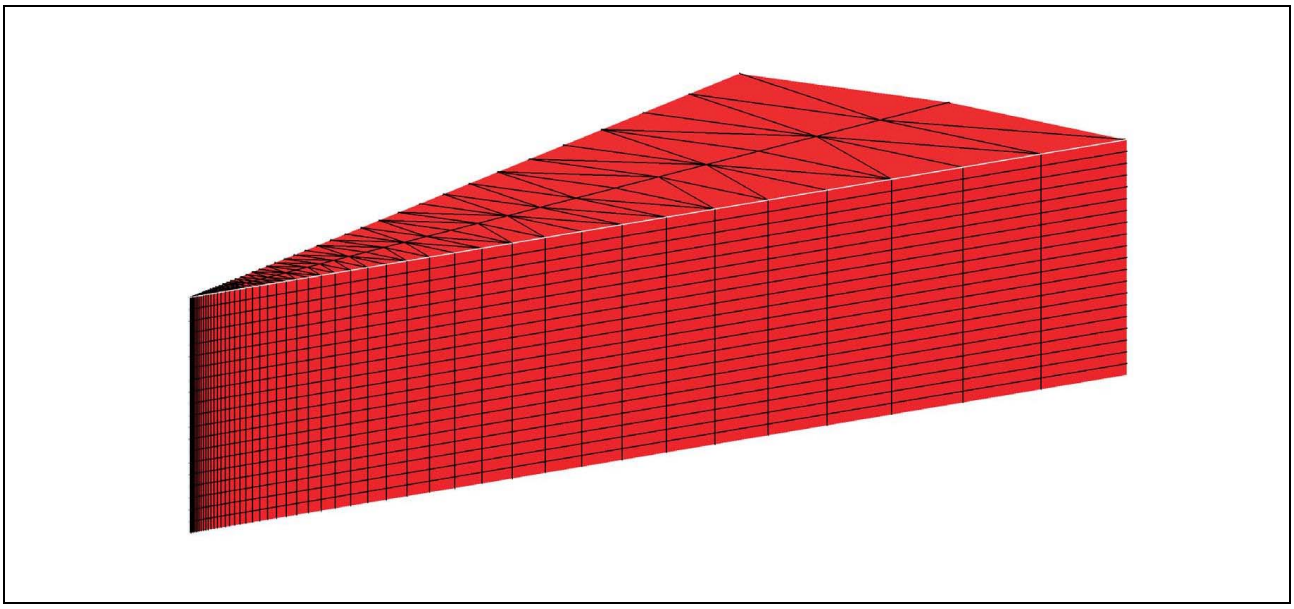

Figure 4-9
Finite-Element Mesh Used for Neuman Model Simulation

Table 4-3
Parameters for the Neuman Problem

Parameter	Value
Hydraulic Conductivity (K_x, K_y, K_z)	50 ft/d, 50 ft/d, 50 ft/d
Specific Storage (S)	0.00001/ft
Specific Yield (S_y)	0.20 ft^0
Pumping Rate of Well (Q)	400 ft^3/d

4.4.3 Results

Nine observation wells were placed in the finite-element mesh. These were divided into three clusters located at approximately 200 ft and 400 ft from the pumping well. Within each cluster of three observation wells, one observed groundwater flow at 150 ft below the surface (the deep well), the second observed groundwater flow at 100 ft below the surface (the middle well), and the third observed groundwater flow at 50 ft below the surface (the shallow well). FEMFLOW3D's output files provided hydrographs for these wells over the simulation period. These hydrographs were translated into drawdowns in each observation well. The simulated drawdowns were then plotted on a graph along with the analytical solution for the drawdown, which was calculated using the software WTAQ. WTAQ (Barlow and Moench, 1999) is a computer-based modeling program that uses a partial analytical solution to calculate drawdowns in an aquifer due to partially penetrating wells. As shown in Figures 4-10 through 4-15, the FEMFLOW3D simulated drawdowns very closely replicate the analytical solution calculated by WTAQ for a range of distances, depths, and times.

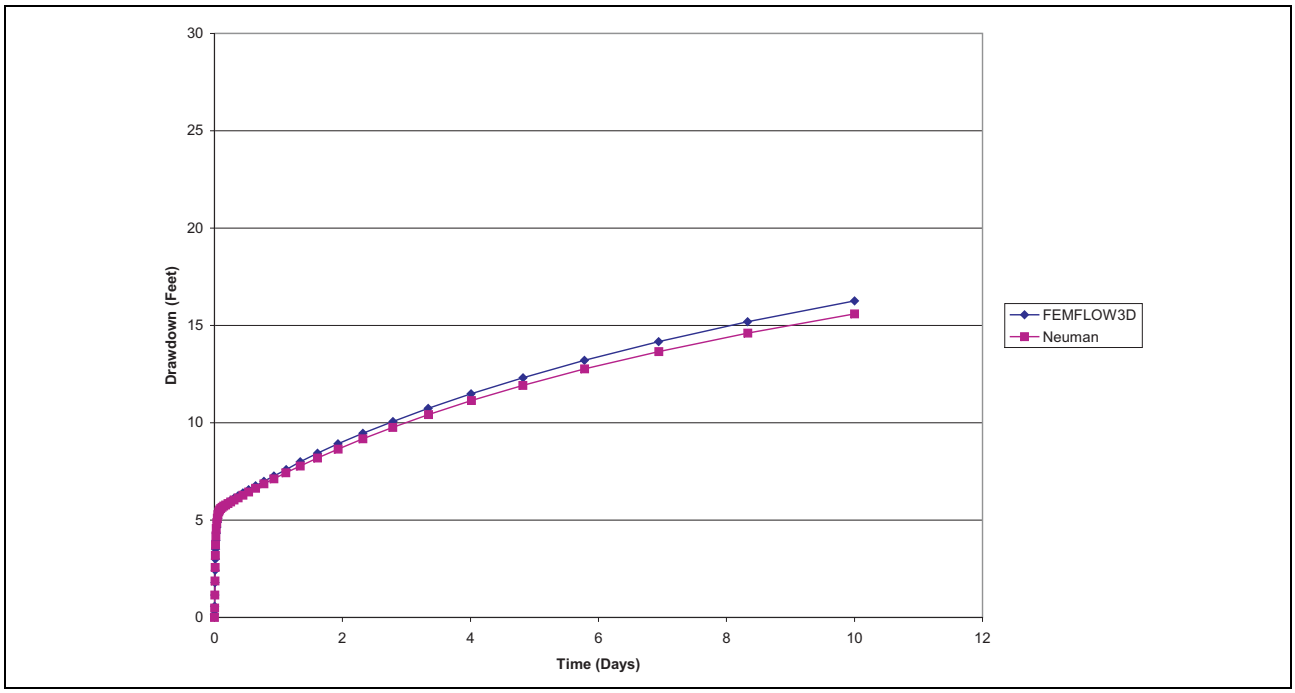

Figure 4-10
Comparison of FEMFLOW3D Simulated Drawdowns With Neuman Solution for Shallow Well at a Distance of 200 Feet From Pumping Well

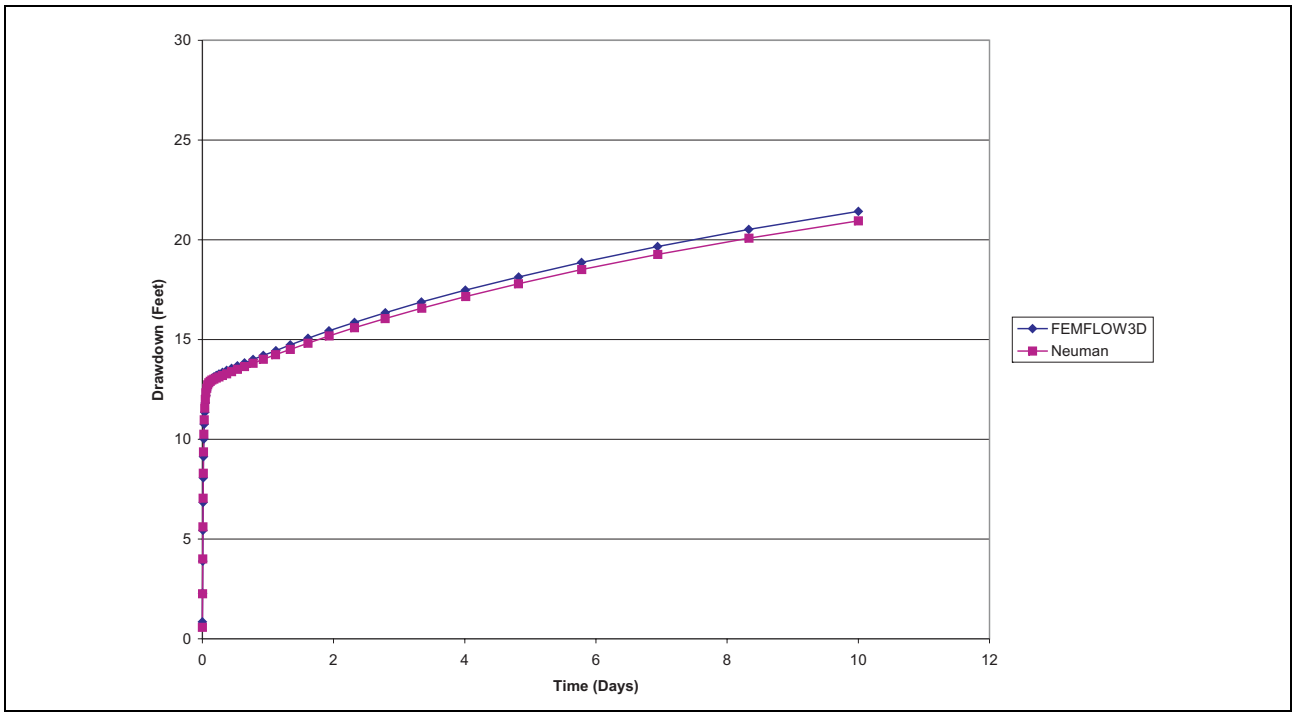

Figure 4-11
Comparison of FEMFLOW3D Simulated Drawdowns With Neuman Solution for Middle Well at a Distance of 200 Feet From Pumping Well

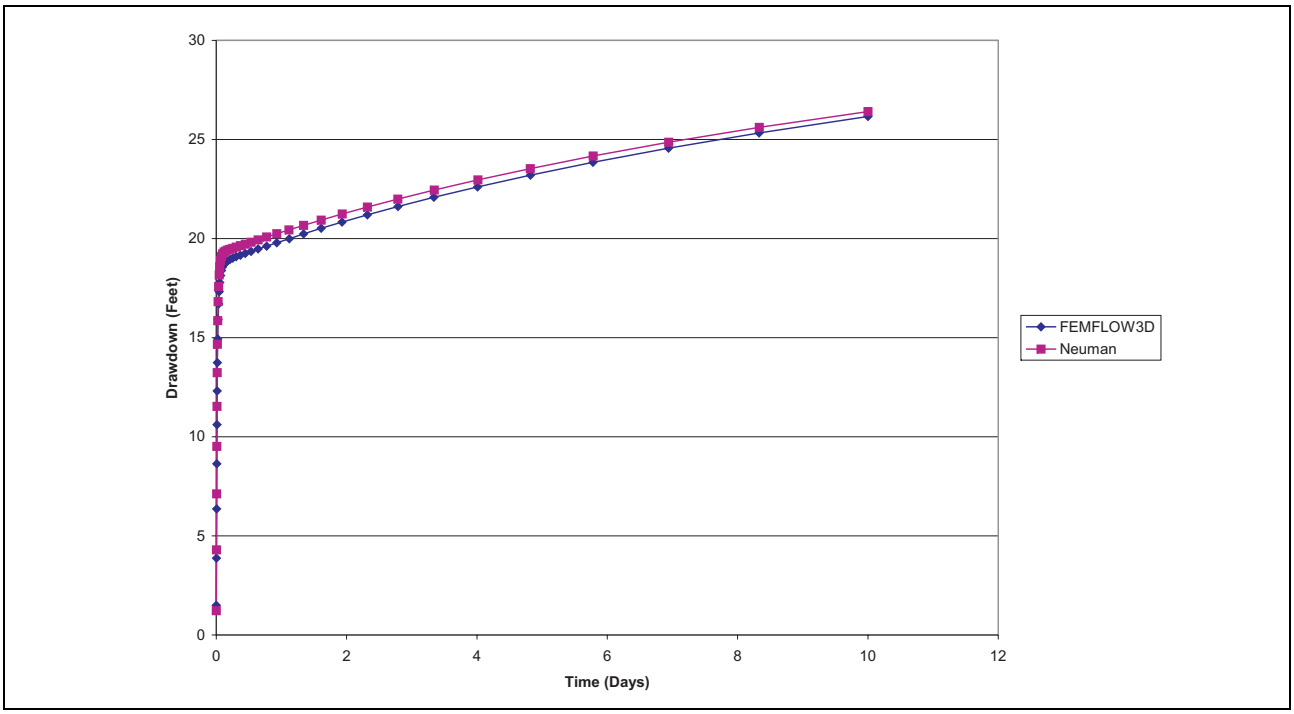

Figure 4-12
Comparison of FEMFLOW3D Simulated Drawdowns With Neuman Solution for Deep Well at a Distance of 200 Feet From Pumping Well

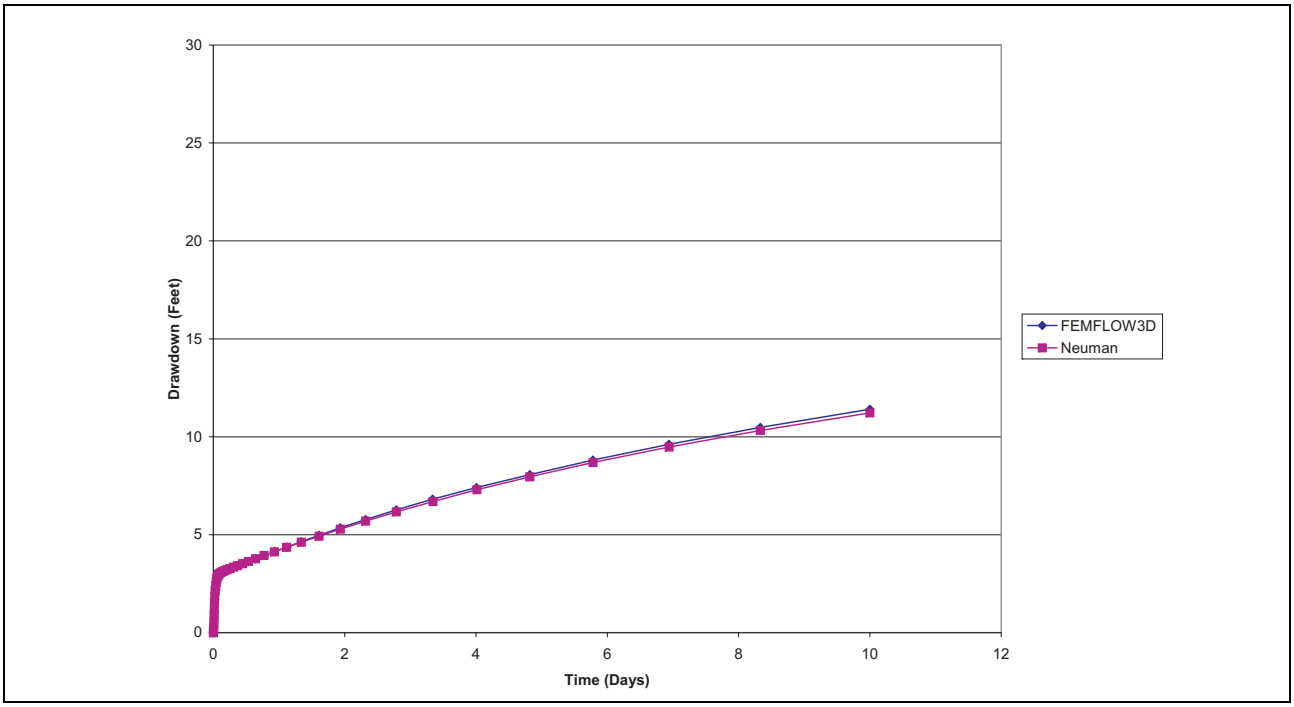

Figure 4-13
Comparison of FEMFLOW3D Simulated Drawdowns With Neuman Solution for Shallow Well at a Distance of 400 Feet From Pumping Well

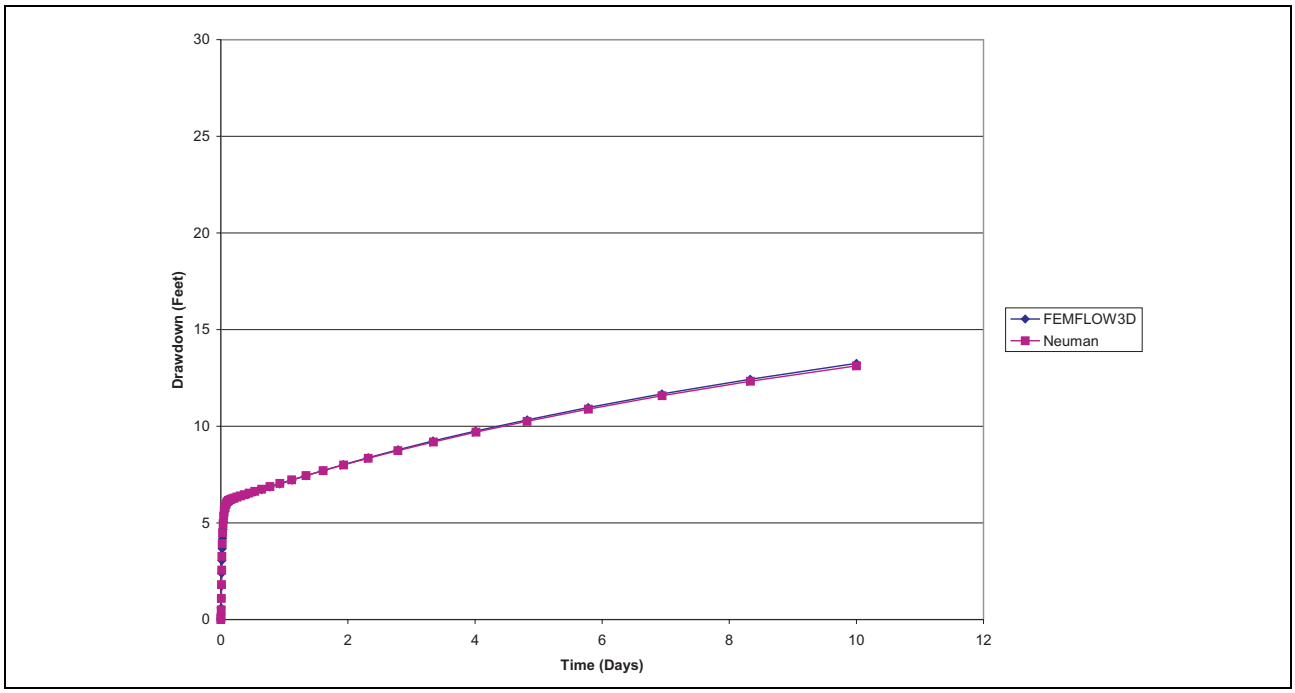

Figure 4-14
Comparison of FEMFLOW3D Simulated Drawdowns With Neuman Solution for Middle Well at a Distance of 400 Feet From Pumping Well

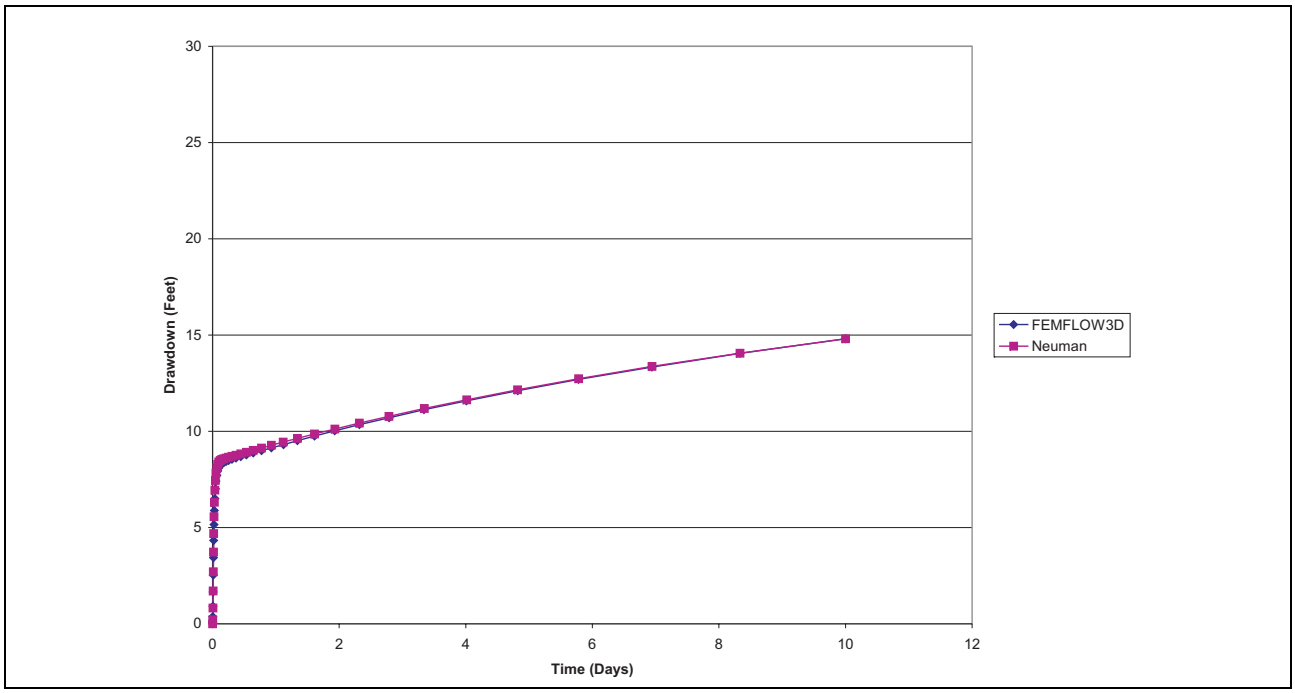

Figure 4-15
Comparison of FEMFLOW3D Simulated Drawdowns With Neuman Solution for Deep Well at a Distance of 400 Feet From Pumping Well

This Page Intentionally Left Blank

5.0 REFERENCES

Barlow, P.M., and Moench, A.F., 1999, WTAQ – A computer program for calculating drawdowns and estimating hydraulic properties for confined and water-table aquifers: U.S. Geological Survey Water-Resources Investigations Report 99-4225, 74 p.

Durbin, T.J., and Berenbrock, C., 1985, Three-dimensional simulation of free-surface aquifers by the finite-element method: U.S. Geological Survey Water-Supply Paper 2270, pp. 51-67.

Durbin, T.J., and Bond, L.D., 1998, FEMFLOW3D – A finite-element program for the simulation of three-dimensional aquifers: U.S. Geological Survey Open-File Report 97-810, 338 p.

Hageman, L.A., and Young, D.M., 1981, Applied iterative methods, Academic Press, New York, NY.

Hager, W.W., 1988, Applied numerical linear algebra: Prentice Hall, Englewood Cliffs, New Jersey, 424 p.

Haverkamp, R., Vauclin, M., Wierenga, P.J., and Vachuad, G., 1977, A comparison of numerical simulations for one-dimensional infiltration: Soil Society of America Journal, vol. 41, pp 285-294.

Hayakorn, P.S., and Pinder, G.F., 1983, Computation methods in subsurface flow: Academic Press, New York, 473 p.

Kincaid, D.R., and Young, D.M., 1980, Adapting iterative algorithms developed for symmetric systems to nonsymmetric systems: Center for Numerical Analysis Report 161, University of Texas, Austin, TX.

Kincaid, D.R., Respess, J.R., Young, D.M., and Grimes, R.G., 1982, Algorithm 586 – ITPACK 2C, A FORTRAN package for solving large sparse systems by adaptive accelerated iterative methods: Transactions Mathematical Software, vol. 8, pp. 302-322.

Mehl, S.W. and Hill M.C., 2001, MODFLOW-2000, The USGS Modular Ground-water Model -- User's Guide to the LINK-AMG (LMG) PACKage for Solving Matrix Equations Using an Algebraic Equation Multigrid Solver: U.S. Geological Survey Open-File Report 01-177, pp. 33.

Neuman, S.P., 1974, Effects of partial penetration on flow in unconfined aquifers considering delayed aquifer response: Water Resources Research, vol. 10, no. 2, pp. 303-312.

Papadopulos, I.S., 1965, Nonsteady flow to a well in an infinite anisotropic aquifer: Proceeding of Dubrovnik Symposium on the Hydrology of Fractured Rocks, International Association of Scientific Hydrology, Dubrovnik, Yugoslavia, pp. 21-31.

Pinder, G.F., and Gray, W.G., 1977, Finite element simulation in surface and subsurface hydrology: Academic Press, New York, 396 p.

Ruge, J.K., and Stüben, K., 1987, Algebraic Multigrid, *in* McCormick, S.F., ed., Multigrid Methods: Society for Industrial and Applied Mathematics, Philadelphia, pp. 73-130.

Theis, C.V., 1935, The relation between the lowering of the piezometric surface and the rate and duration of discharge from a well using ground-water storage: Transactions American Geophysical Union, no. 16, pp. 519-524.

Voss, C.I., and Provost, A.M., 2003, SUTRA – A model for saturated-unsaturated variable-density groundwater flow with solute and energy transport: U.S. Geological Survey Water-Resources Investigations Report 02-4231, 250 p.

Young, D.M., 1971, Iterative solutions of large linear systems: Academic Press, New York, 436 p.

Young, D.M., and Kincaid, D.R., 1980, The ITPACK package for large sparse linear systems: Center for Numerical Analysis Report 160, University of Texas, Austin, 186 p.

Zienkiewicz, O.C., 1988, The finite element method, Volume 1, Basic formulation and linear problems: McGraw Hill, New York, 648 p.

Appendix A

Fortran Source Code

(provided on the CD-ROM)

Appendix B

Model Documentation and Source Code Review

Model Code Validation - Comparison of Results Between FEMFLOW3D and MODFLOW